Maciej Roman Ruciński

BSc Geology

Novel placodont material and paleoenvironment analysis of Triassic deposits of Rocha da Pena (Algarve, southern Portugal)

Dissertação para obtenção do Grau de Mestre em

Paleontologia

Orientador:Doutor Octávio João Madeira Mateus, Professor Associado com agregação, Faculdade de Ciências e Tecnologia da Universidade Nova de Lisboa

November 2020

Novel placodont material and paleoenvironment analysis of Triassic deposits of Rocha da Pena(Algarve, southern Portugal)

Maciej Roman Ruciński

BSc Geology

Dissertação para obtenção do Grau de Mestre em Paleontologia

Novembro 2020

Orientador: Doutor Octávio João Madeira Mateus, Professor Associado com agregação, Faculdade de Ciências e Tecnologia da Universidade Nova de Lisboa

Novel placodont material and paleoenvironment analysis of Triassic deposits of Rocha da
Pena (Algarve, southern Portugal)

Abstract

The Triassic deposits of the Algarve region have been known for almost 200 years with the first vertebrate fossil descriptions published in 1976 by Palain and in 1977 by Russell and Russell. It was followed by the discovery of the monospecific bonebed in Rocha da Pena. The bonebed bears numerous temnospondyl remains, which in 2015 were assigned to a novel species *Metoposaurus algarvensis*. The occurrence of that taxon suggested a chronostratigraphic range between Carnian and middle Norian. During the following fieldwork, the first Portuguese placodont material was recovered. Based on osteoderm morphology was assigned to genus *Henodus*, which previously was exclusively known from lower Carnian deposits in Lustnau in southern Germany. Since then new Portuguese fossil material has been recovered including an isolated, nearly complete skull, which is described herein. Based on several features (flat and broad skull with short and broad rostrum composed of maxillae and premaxillae, rectangular shape of the skull, toothless maxillae substituted by longitudinally extending curved groove and non-contacting palatines), the specimen is assigned to the genus *Henodus,* confirming the occurrence of this taxon in Portugal. This extends its paleogeographic range up till western Laurasia. The occurrence of this taxon in Rocha da Pena may indicate either age of lower Carnian for the local deposits or an extended chronostratigraphic distribution of *Henodus*. The described specimen comes from a fossiliferous layer that contains isolated remains of placodonts (most probably *Henodus*), actinopterygian fishes, and the first occurrence of hybodont sharks in the Triassic deposits of Portugal. The gathered sedimentological data-enabled interpretation of the paleoenvironment of the studied sections. The studied deposits can most likely be attributed to a marginal environment, with the transition from playa to near-shore or shallow lagoon.

Keywords: Triassic, *Henodus,* placodonts, Rocha da Pena, playa environment, marginal environment

Resumo

Os depósitos triásicos do Algarve são conhecidos há quase 200 anos com as primeiras descrições de fósseis de vertebrados publicadas em 1976 por Palain e em 1977 por Russell e Russell. Seguiu-se a descoberta de uma cadada de ossos, monoespecífica, na Rocha da Pena, que apresenta inúmeros vestígios de temnospôndilos, que em 2015 foram atribuídos a uma nova espécie *Metoposaurus algarvensis.* A ocorrência desse táxon sugeriu uma idade entre Carnian e Norian médio. Durante as escavações seguintes, o primeiro material de placodonte português foi recuperado e com base na morfologia da osteoderme foi atribuído ao género *Henodus*, que anteriormente era conhecido exclusivamente de depósitos carnianos inferiores em Lustnau no sul da Alemanha. Desde então, novo material fóssil foi recuperado, incluindo um crânio quase completo isolado, que é descrito aqui. Com base em várias características (crânio plano e largo com rostro curto e largo composto de maxilares e pré-maxilares, forma retangular do crânio, maxilas desdentadas substituídas por sulco curvo que se prolonga longitudinalmente e palatinos sem contato), o espécime é classificado como género *Henodus*, confirmando a ocorrência deste táxon em Portugal. Isso estende seu alcance paleogeográfico até o oeste da Laurásia. A ocorrência deste táxon na Rocha da Pena pode indicar uma idade de baixo Carnian para os depósitos locais ou uma distribuição estratigráfica estendida de *Henodus*. O espécime descrito provém de uma camada fossilífera que contém restos isolados de placodontes (muito provavelmente *Henodus*), peixes actinopterígios e a primeira ocorrência de tubarões hibodontiformes nos depósitos triásicos de Portugal. Os dados sedimentológicos permitiram a interpretação do paleoambiente das seções estudadas como um ambiente marginal mais provável, com transição de playa para próximo à costa ou ambiente de lagoa rasa.

Table of Contents

Table of figures

Table index

Anatomical abbreviations

Bo - bassioccipital

F-frontal

J – juga

M - maxilla

O – occipital

P - parietal

Pl- palatine

Pt – pterygoid

Q – quadrate

Qj – quadratojugal

Sq- squamosal

T – temporal fenestrae

V-vomer

Institutional abbreviations

Faculdade de Ciências e Tecnologia da Universidade Nova de Lisboa (FCT/UNL)

Municipal de Loulé (ML)

1. Introduction

Examination of the fossil record is essential for the understanding of the evolutionary history of life. It also provides information on ecosystem dynamics in relation to the changing environment. Fossils give a unique insight into macroevolutionary and ecological processes which would not be possible to be observed otherwise. The Upper Triassic deposits of southern Portugal possess a large potential to contribute in this regard and provide new data about vertebrate assemblage, from the time of profound biotic changes, which were also followed by mass extinction at the end of Triassic.

1.1 The Triassic period - vertebrate fauna and biotic events

The Triassic, the first period of the Mesozoic era, was a profound time for life on Earth. On one hand, marked by the largest extinction in the history of the Earth, taking place at the end of the Permian 252 Ma. On the other hand, it was also characterized by extremely dynamic radiation and the variability of newly formed evolutionary clades (Sues and Fraser, 2010; Brayard et al., 2017). On land, Paleozoic survivors such as therapsids and temnospondyls coexisted with newly evolved groups of archosaur reptiles such as aetosaurs, phytosaurs, rauisuchians, crocodylomorphs, dinosaurs and pterosaurs. It was during that time, when many of the currently known vertebrate clades appeared, such as turtles, lepidosaurs, crown amphibians (Lissamphibia) and mammals (Sues and Fraser, 2010).

The Triassic succession of terrestrial fauna has been divided into three episodes (Romer, 1966; Sues and Fraser, 2010):

1. Early Triassic (252 Ma – 247 Ma; Induan and Olenekian), marked by slow biotic recovery and widespread occurrence of disaster taxa e.g. *Lystrosaurus.* Therapsids (cynodonts, therocephalians and dicynodonts), rhynchosaurs and temnospondyls were a dominant component of terrestrial communities. Archosaurs evolved at that time (this is still under debate, with a possible first representative appearing at the end of the Permian).

2. Middle Triassic (247 – 237 Ma; Anisian and Ladinian), when cynodonts, dicynodonts, and rhynchosaurs predominated, while archosaurs highly diversified and had started to take over many of the terrestrial communities. Temnospondyls still comprised an important and diverse part of the terrestrial fauna.

3. Late Triassic (237 – 201 Ma; Carnian, Norian and Rhaetian), when dinosaurs gradually started to predominate, with the decline of other groups of archosaurs and therapsids. Temnospondyls occurred prolifically (but in low diversity) in early-middle Late Triassic (Carnian-Norian) but suffered a profound decline by the end of the Late Triassic (Late Norian - Rhaetian). Synapsids radiated, resulting in the appearance of various lineages of mammaliforms (including crown Mammalia).

Particularly interesting is the transition to the last of these successions in the Late Triassic. Many hypotheses have already been raised on this subject, some of which assumed relatively slow and gradual changes in faunal composition (e.g. Romer, 1960). However, subsequent research on this subject suggested a completely different scenario, according to which the fauna transition took place very quickly in the context of geological time and is associated with the Carnian Pluvial Event

(hereafter CPE).This event marked the climate change event taking place in the middle Carnian around 234 and 232 Ma ago (Dal Corso et al., 2020). The causation of that event remains unsettled with few hypotheses being under discussion. The prevailing one links the occurrence of CPE with the high activity of the Wrangellia large igneous province at the area of modern North-western North America, which was estimated to produce at least 1 million km³ of basalts (Grenne et al., 2010). Such large emissions of volcanic material are thought to have contributed to the sudden humidification of the climate. This environmental change included a shift in the flora composition with conifers becoming its dominant part. This ultimately led to faunal turnover involving terrestrial vertebrates(Tanner, 2018; Benton et al., 2018).

Particularly discussed in the matter of the above-mentioned transition is the rise of dinosaurs, of which the oldest undisputed material is known from Carnian deposits of South America (Benton et al., 2018). It is assumed that new adaptations like bipedal movement (Charig, 1984), or the appearance of a respiratory system similar to that of today's birds might have been essential for dinosaurs' evolutionary success. In conditions with significantly reduced atmospheric oxygen and increased carbon dioxide content during the Late Triassic, those features might had given an advantage over the other archosaurs, leading to their rapid spread and diversification. More recent studies proposed the CPE as the main cause of the rising predominance of dinosaurs. As a result of environmental instability, other groups of archosaurs started to decline, enabling dinosaurs to take over some of the niches (eg. Benton et al., 2018).

The Triassic was also a profoundly significant period for marine communities, which saw a nearly complete change in faunal composition and ecological structure. In the aftermath of the P-T extinction, during which most of the vertebrate marine taxa got extinct, ecological niches were left vacant. That enabled new fauna radiation in the Early Triassic. However, there are two competing hypotheses concerning the character and dynamics of the biota recovery. The older one assumes, the relatively stagnant stage at the beginning of the Early Triassic and gradual, prolonged rebuilding of the ecosystems, which accelerated in the late Early and early Middle Triassic (Chen and Benton, 2012; Benton et al., 2013). That was proposed to be caused by repeated significant environmental disturbances, which were taking place until 5-6 Myr after P-T (Chen and Benton, 2012; Benton et al., 2013). On the other hand, the second hypothesis claims that recovery was rapid, with the appearance of multilevel trophic webs already at the beginning of the Early Triassic with the actinopterygian fishes and trematosaurid temnospondyls as apex predators (Scheyer et al., 2014). The marine communities underwent almost complete faunal turnover, which resulted in new lineages taking over the dominance in the seas and the appearance of taxa that started to fill new niches, which had not been present during the Paleozoic (Benton at al., 2013). That includes the marine reptiles, which underwent their first major radiation, which was followed by the appearance of taxa such as thalattosaurs, ichthyopterygians and sauropterygians including nothosaurs, pachypleurosaurs, pistosaurs and placodonts (Rieppel, 2000; Benton et al., 2013). Some of the archosaurs also, at least partially, adapted to the marine environment e.g. Tanystropheids (e.g. Renesto, 2005). Fishes, especially actinopterygians, also radiated, although some of the Paleozoic representatives persisted throughout the Triassic or even whole Mesozoic e.g. hybodontid sharks or coelacanths (e.g. Benton, 2015).

Another large abrupt change in the marine ecosystem occurred during the previously mentioned CPE, which due to global warming, ocean acidification and the spreading of anoxic conditions, altered the marine communities, particularly impacting crinoids, bryozoans, ammonoids and conodonts (e.g. Preto, 2019). One of the most notable consequences of that event was the first massive appearance of scleractinian corals and calcareous nannoplankton (e.g. Preto, 2019). However,

it is not certain how these changes impacted most of the marine vertebrates, as their record in Upper Triassic seems to be deficient (especially in Rhaetian). That impedes any detailed interpretation of impact not only of CPE but also other events like Late Norian faunal turnover or Triassic-Jurassic extinction, on marine vertebrates (Renesto and Vecchia, 2018). Nevertheless, based on the present known fossil record, it can be assumed that the decline and extinction of numerous clades of the marine reptiles occurred throughout the whole Late Triassic, starting with the disappearance of some taxa, especially those which lived in near-shore habitats, at the Ladinian-Carnian boundary (e.g. Pachypleurosaurians and most of nothosauroid taxa). That was correlated with frequently occurring regressions, resulting in shallow-marine habitat loss, which was essential for many of the marine reptiles at that time (Renesto and Vecchia, 2018). Probably by the time of the middle Norian most of Sauropterygians and Tanystropheids got extinct or significantly declined, including substantial impoverishment of placodonts (Renesto and Vecchia, 2018). In contrast, pelagic animals such as ichthyosaurs diversified and some of them reached astonishing sizes, like Shonisaurus reaching 21 meters, becoming the largest marine reptile in history. Open marine pistosaurid sauropterygians like plesiosaurs also persisted, however, their fossil record is scant (Renesto and Vecchia, 2018).

The last episode of the Triassic period was marked by mass extinction and disappearance (e.g. conodonts, various archosaurs like aetosaurs or phytosaurs) or impoverishment (e.g. bivalves, ammonoids) of numerous taxa. Nevertheless, the big severity of the extinction has been questioned. Instead the significantly prolonged timing of extinction was suggested based on the lack of fossil record of many groups already in Norian or Rhaetian (Lucas and Tanner, 2018). That according to some authors may imply multiple extinctions at the time of Late Triassic, which were smaller in scale and temporarily dispersed (Lucas and Tanner, 2018). The causation of the End Triassic Event also remains under debate with the main hypothesis suggesting the formation of the Central Atlantic Magmatic Province (e.g. Marcoliet al., 1999; Davies et al., 2017), or the impact of an extraterrestrial object (e.g. Olsen et al., 1987), and possibly the composition of both (Tanner et al., 2004), as the main mechanism responsible for the extinction.

1.2 Paleogeography and climate

Throughout the Triassic period, all continents were connected, forming the Pangea supercontinent (Fig. 1). As a result of the opening of the Atlantic during the Late Triassic, Pangea was divided into northern part - Laurasia (which consisted of modern areas of Europe, Asia, North America and Greenland) and southern - Gondwana (composed of today South America, Africa, Antarctica, Australia and India). Nevertheless, both units, for most of the Triassic, were partially separated by the Tethys ocean, which cut from the east into the supercontinent. The rest of the land was surrounded by the large Panthalassa ocean.

Such a paleogeographic system, with no barrier for the flow of currents between the equator and regions located at higher latitudes, induced a much warmer climate at higher latitudes, which may be indicated by the lack of evidence of the existence of ice caps at that time (Frakes et al., 1992). However, the geological and palynological record indicates that a much warmer climate did not only apply to the above-mentioned regions but also the entire globe (Selwood and Valdes, 2006). This is demonstrated by the layers of carbonates, evaporites and red mudstones (so-called red beds) found in multiple places around the world, as well as the occurrence of thermophilic flora ranging from low to high paleogeographic latitudes (up to 70-85° N) (Kidder and Worsley 2004; Fraser and Sues, 2010; Tanner, 2018). The existence of such a large continent also impacted the system of air exchange between land and oceans. Huge pressure differences due to the heating of landmasses in the summer and its cooling in winter, caused the climate in a significant part of Pangea, to be characterized by extreme seasonality (Yan and Zhao, 2002). That might have prompted the occurrence of the mega-monsoons (Wilson et al., 1994), which especially affected regions located near the Tethys ocean, such as the eastern part of Laurasia, which corresponds to modern Europe.

Even though the climate diversity between regions during Triassic was much less pronounced than today, significant variations have been noted, depending on the latitudes. This mainly concerns the Late Triassic, as prior Triassic epochs were characterized by a more homogeneous climate. In general, the high and medium latitudes were more humid and temperate than the subtropical regions, which were drier and more seasonally affected (Sellwood and Valdes, 2006). There are also differences between the western and eastern parts of the Pangea, due to the proximity of Tethys to the eastern edge of the continent and the lack of an Atlantic providing ocean heat exchange (Fraser and Sues, 2010). However, the above-mentioned climatic features changed quite dynamically over time (Ahlberg et al., 2002). That was probably caused by the northward movement of the Pangea, which led to the change of climate belts in particular regions and the climate drying within many of them (Parrish et al., 1986), which was briefly interrupted by the occurrence of the CPE. The record of these changes, which apogee was in Carnian, is recorded at many sites in Eastern North America (Newark Supergroup) and South America (e.g. Los Colorados formation in Argentina or Catturita in Brazil; Fraser and Sues, 2010. In Rhaetian, the climate became more humid and moderate, and the deposition of red beds was replaced by kaolinite, coal and paleosoils formation (Tanner, 2018). This indicates a transition from a dry environment with periodically occurring rivers and lakes wich were predominant during late Carnian and Norian, to a wet environment with predominant fluvial and lacustrine environments with abundant vegetation during Rhaetian. In the southern edge of Gondwana, the chronology is reversed: at the beginning of the Carnian the climate was humid and temperate (e.g. Ischigualasto Formation in Argentina), while at the end of the Carnian and the beginning of the Norian it became significantly drier (record e.g. in Los Colorados Formation in Argentina; Curtin and Parrish 1999).
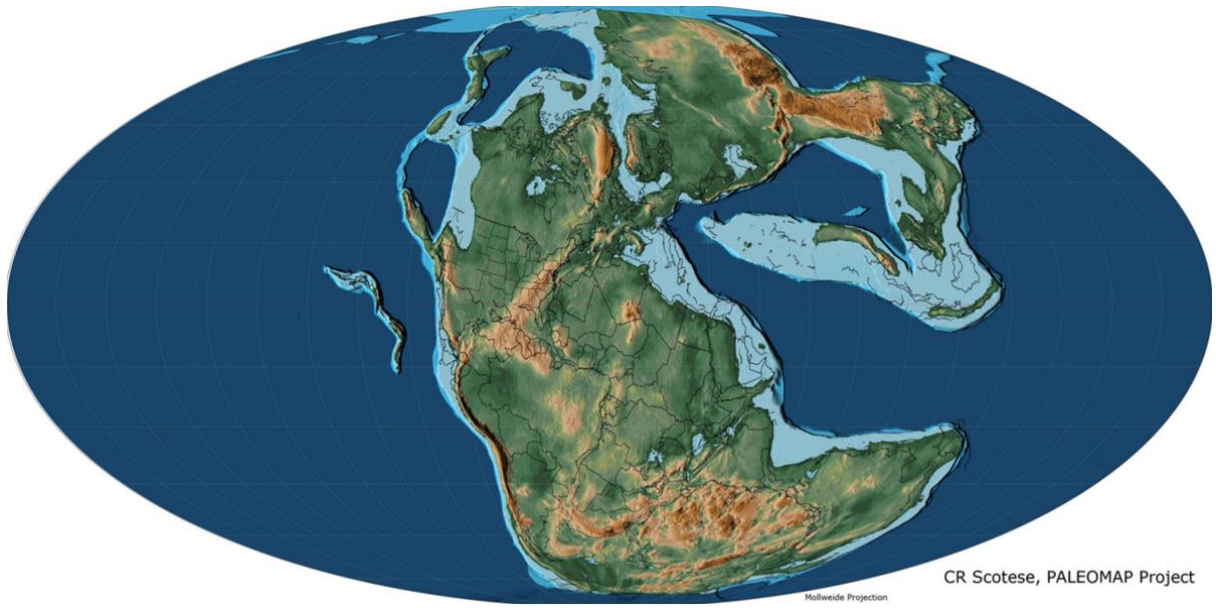
Fig. 1 Paleogeographic map of the world in the Late Triassic (Carnian). Map from Scotese (2014).

1.3 Algarve Basin

Algarve Basin encompasses the meso-cenozoic sediments deposited in the southern part of Portugal (Fig. 2). It extends for around 140 km, between Cabo de São Vicente at the western coast of Portugal and Guadiana river at the east, at the Spanish border (Terrinha et al., 2006). The basement of the basin constitutes part of the South Portuguese Zone and comprises sedimentary, metamorphic and igneous rocks, which are Neoproterozoic to Carboniferous in age (Pereira *et al.*, 2016). The top of the basement is built of Carboniferous (Visean to Moscovian) flysch deposits (graywacke), which were deformed and metamorphosed during the Variscian orogeny (Terrinha *et al.*, 2006; Pereira et al., 2016). The folded rocks of the basement are overlaid by (probably lower) Triassic deposits (Fig. 3) (Arenitos de Silves), implying the angular unconformity and hiatus of around 70 Myr (Terrinha *et al.*, 2006).
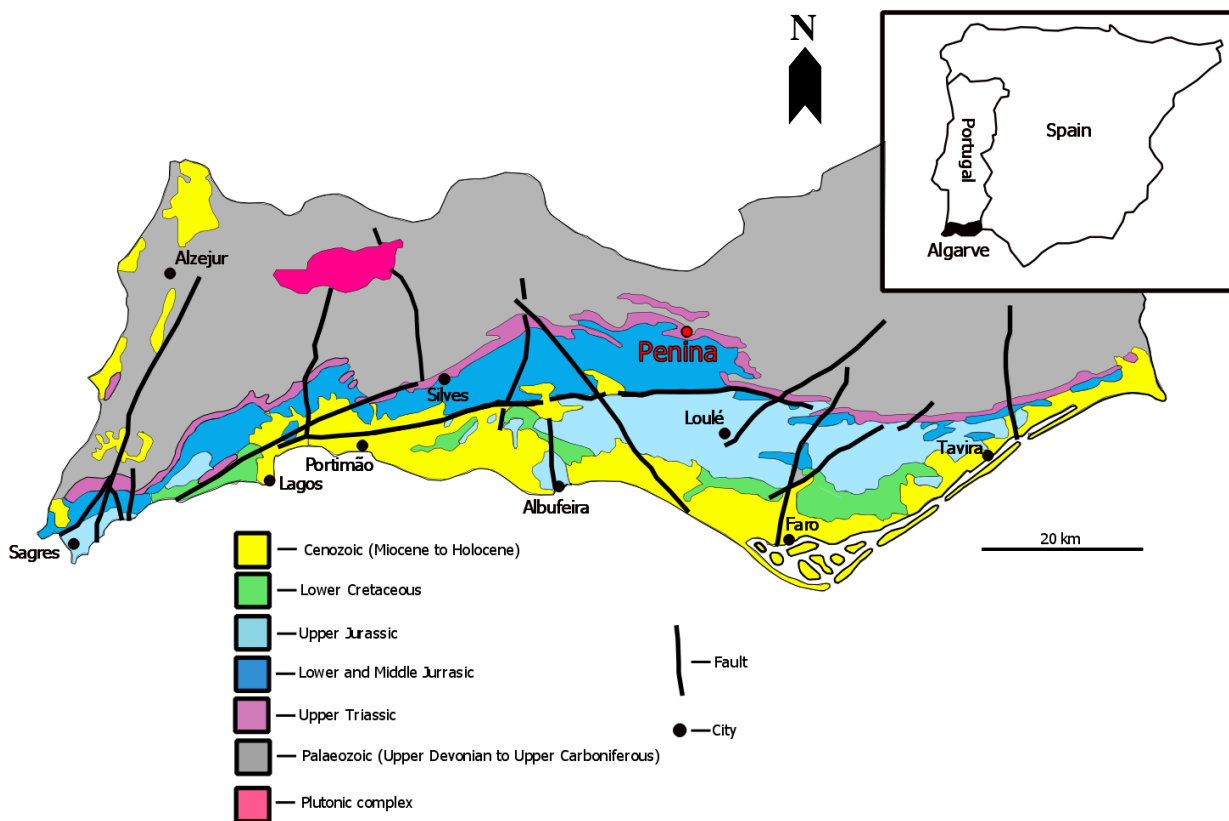
Fig. 2.Geological map of Algarve Basin (Adapted from Geological Map of Portugal, 1:500 000 SGP, 1992).

The Algarve Basin owns its origin to divergent movements occurring during the opening of the Atlantic Ocean in the Late Triassic - Early Jurassic. This event also initiated the breakup of Pangea, what eventually led to the formation of the oceanic crust between Algarve and North Africa (Terrinha et al., 2006). During most of the Triassic, the terrestrial sedimentation preponderated, with a transition to shallow marine intercalations in the Late Triassic. This resulted in the creation of various

facies composed of sandstone, red beds (claystones /mudstones), evaporites and volcanic rocks (Fig. 4) (Rocha, 1976; Terrinha et al., 2006), with the latter being associated with the Central Atlantic magmatic province. The ending of Late Triassic and the beginning of Early Jurassic were marked by the marine transgression and deposition of mainly massive, fine crystalline dolomitic limestones and dolomites (Rocha, 1976; Terrinha et al., 2006) as well as basalts associated with CAMP. These units are followed by dolomitic limestone containing numerous chert nodules (lower Pliensbachian), massive limestone (upper Pliensbachian) and marly limestones (Toarcian).

The Middle Jurrasic was a time of significant land level fluctuations causing the increase of facies variability and their areal constriction due to regional land emersions. Nevertheless, marine facies were at that time dominant, which is manifested by fossiliferous (Bajocian) and later marly (Bathonian) and turbiditic limestones (Callovian) (Terrinha *et al.*, 2006). During the Upper Jurrasic substantial regional uplift (at the western sub-basin) and subsidence (in eastern sub-basin) took place, leading to the extremely differentiated thickness of deposits among the sub-basins varying between 200 and 1600 meters (Terrinha *et al.*, 2006). In the Cretaceous, the sedimentation within the basin was more homogenous, with the carbonate facies being the most common and Cenomanian rocks being the youngest from that period. Those deposits are overlaid by Miocene rocks, indicating yet another hiatus of around 70 Myr or even bigger in few areas, where Neogenic deposits overly older Mesozoic or even Paleozoic strata. The Neogenic (Miocene and Pliocene) rocks have been divided into two main sequences both bearing numerous macro and microfossils: (1) carbonated sequences comprised of carbonates or carbonated siliciclastic rocks mostly outcropping in the western part of the basin and (2) arenitic sequence consisting siliciclastic rocks of different sizes varying between fine sandstones to conglomerates mostly outcropping in the eastern part of the basin (Terrinha *et al.*, 2006) All of the Mesozoic and Neogenic strata have been deformed, resulting in the formation of a monocline, with strata inclined to the south (Terrinha *et al.*, 2006).
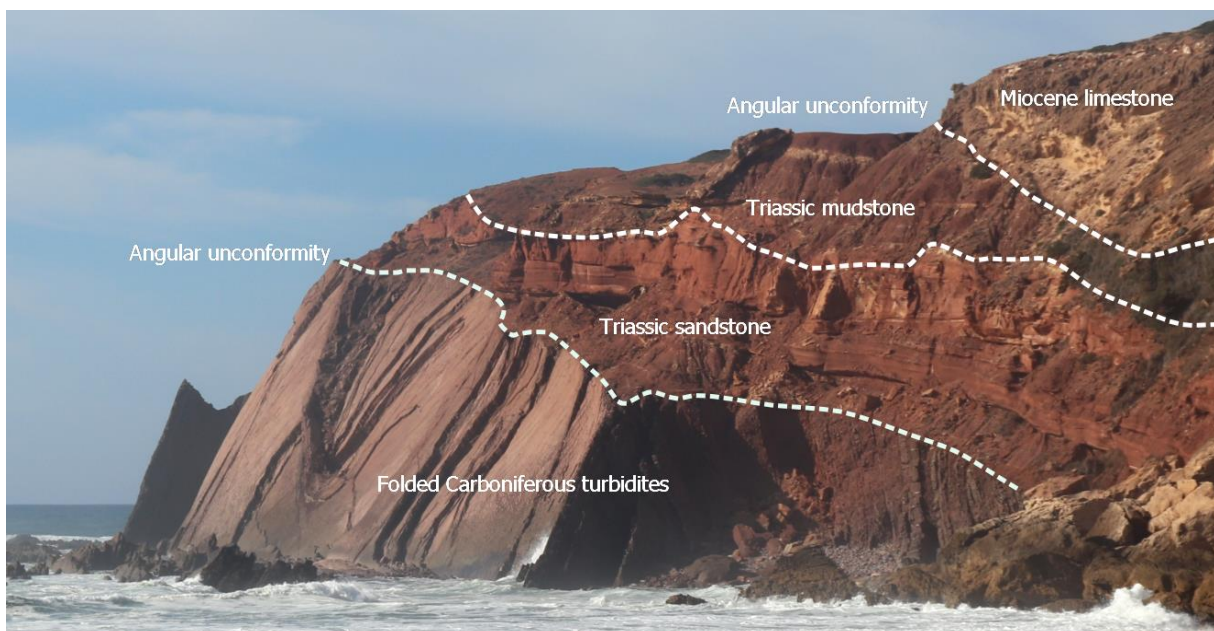
Fig 3. Outcrop at Telheiras Beach. The folded Carboniferous basement visible at the base of the outcrop. The basement is overlaid by Triassic sandstones and mudstones, and Miocene limestone indicating two angular unconformities.

1.4 "Grés de Silves" Formation

The Upper Triassic rocks in the Algarve region are attributed to the "Grés de Silves" Formation (Fig.5), which was first described by Paul Choffat in 1887. However, the division of the particular units within the formation and their dating have been longly debated, resulting in multiple different interpretations (Teixeira, 1942; Da Costa, 1944; Pratsch 1958; Palain, 1968; 1976). According to those works the chronostratigraphic ranges from probable Lower Triassic till Sinemurian. The so far most accepted is an interpretation of Palain (1976), who determined the Formation age as ranging between Keuper (Upper Triassic) and Sinemurian, and divided the Grés de Silves Formation into 4 units:

- Unit AA - Encompass up to 100 meters thick, discontinuous sandstone member composed of reddish sandstone interbedded with mudstone, siltstone, and conglomerate (Palain 1976; Pereira et al., 2016).
- Unit AB1 - Comprised of 10 to 150 m thick sequence of parallel or cross-bedded fine to coarse sandstone, locally intersected by paleochannels filled with polygenic, moderately to a poorly sorted conglomerate with iron oxide and carbonate cement (Palain 1976; Pereira et al., 2016).
- Unit AB2 - Made of 50 to 180 m thick sequence of mudstone (mainly reddish and greenish) interbedded with siltstone and dolomite with locally occurring fine sandstones and evaporites (Palain 1976; Pereira et al., 2016). The Metoposaurus bonebed was attributed to the upper part of that unit, indicating Carnian- middle Norian age (Brusatte et al., 2015).
- Unit AB3 - Constitute the Volcanic-Sedimentary Complex composed of carbonate (including dolomite and pelitic dolomite as well as volcanic (basalts) and volcaniclastic rocks (tuff) (Palain 1976; Pereira et al., 2016). The unit is Hettangian in age.
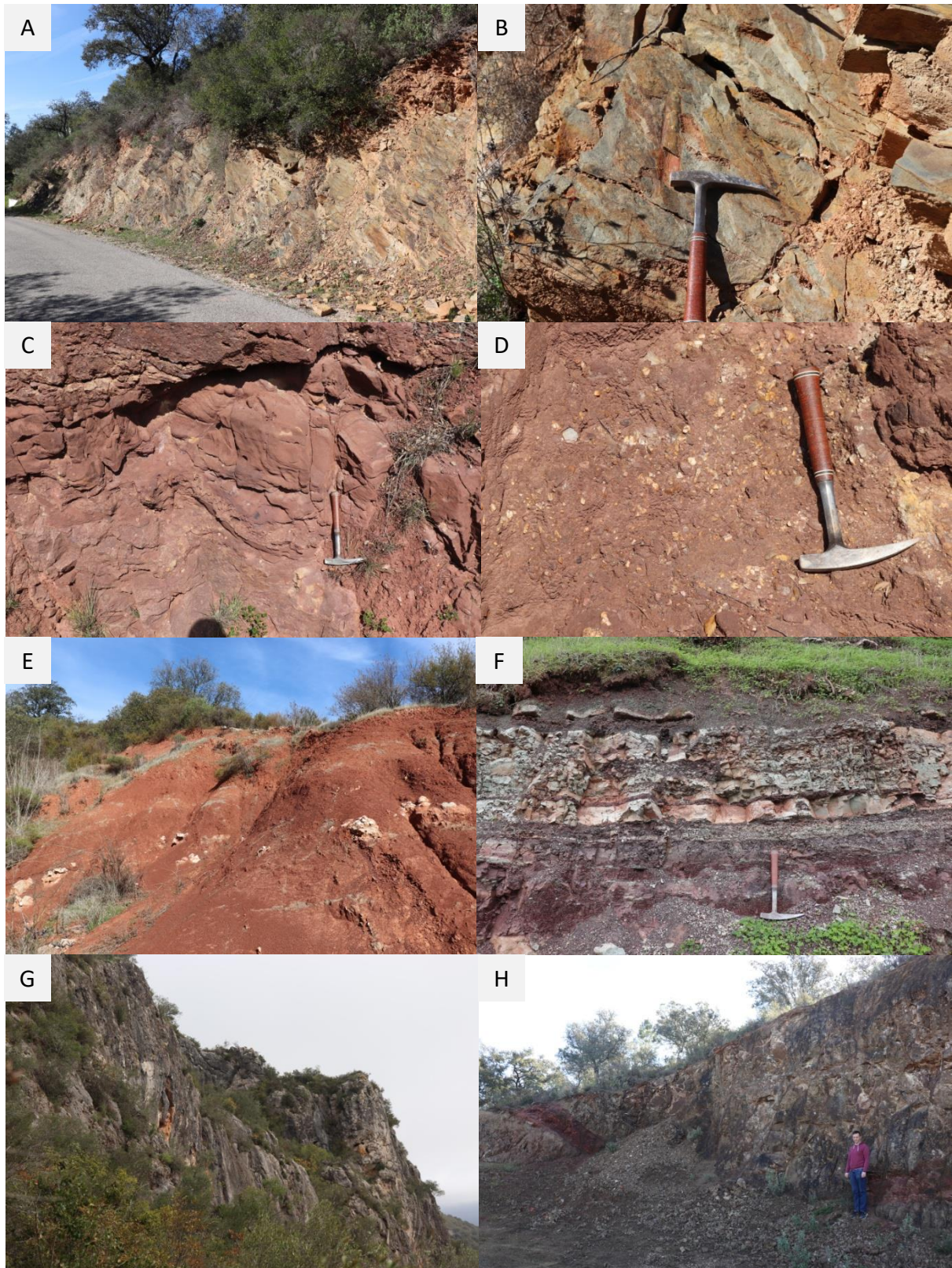
Fig. 4. Diverse lithologies present in the area of Loulé mucipality and Rocha da Pena. **A**. Inclined strata of the Carboniferous turbidites. **B.** Carboniferous turbidites with fragment of *Sigillaria* stem.**C.** Late Triassic sandstones and conglomerates of the AB1 unit. **D.** Late Triassic conglomerate of AB1 unit. **E.** Late Triassic red mudstones with gypsum nodules of the AB2 unit. **F.**The Upper Triassic mudstone-carbonate complex of the AB2 unit. **G.** Early Jurrasic dolomite of the AB3 unit. **H.** Late Triasssic/Early Jurrasic basalts with volcanic intrusions possibly associated with Central Antlantic Province.

9
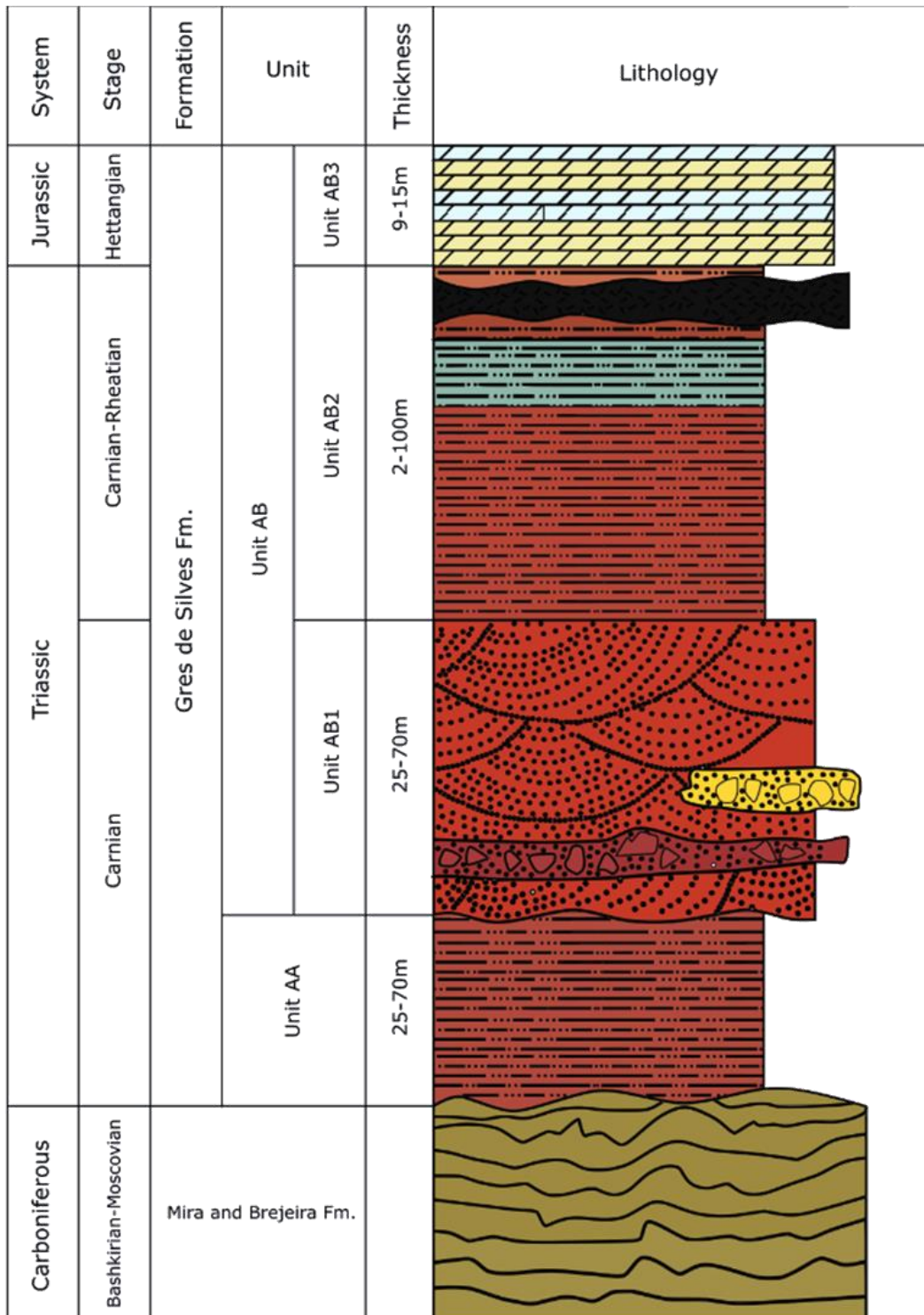
Fig. 5. Schematic stratigraphy of the Paleozoic and Lower Mesozoic part of the Algarve Basin (adapted from Palain, 1976; Manuppella, 1988; Brusatte et al., 2015)

1.5 Placodonts - taxonomy and evolutionary history

Taxonomy

Sauropterygia is a clade of extinct aquatic sauropsids of problematic phylogenic position. which has been considered, depending on the analysis, to be the most closely related to turtles (Motani, 1998), archosauromorphs (Lee, 2013), lepidosaurs (Lee, 2013), constitute the far outgroup of archosauromorphs and lepidosauromorphs (Neenan et al., 2013; Scheyer, 2017), or being polytomous with the latter taxa (Scheyer, 2017). The clade appeared in the Early Triassic, as an aftermath of reptile radiation after the P-T extinction and survived around 180 million years till the Late Cretaceous. Sauropterygia includes nothosaurs, pachypleurosaurs, plesiosaurs (which form a clade of Eusauropterygia) and placodonts.

Placodontia Cope, 1871is an extinct monophyletic taxon (at the range of an order), which includes *Placodontoidea* "unarmored" placodonts and the Cyamodontoidea "armored" placodonts (Fig. 6) (Rieppel, 2000). Placodonts were medium-sized marine reptiles, which can be characterized by the following set of features: (1) three or less premaxillary teeth; (2) maxillary, palatine, and posterior dentary teeth flat, rounded toothplates; (3) diastema separating premaxillary from maxillary teeth present; (4) palatines meet in ventromedial suture (reversed in *Henodus*); (5) pterygoids shorter than palatines; (6) pterygoid flanges prominent, longitudinally oriented; (7) coracoid of rounded contours; (8) ventromedial gastral rib element straight; (9) and osteoderms present (not in *Paraplacodus*) (Rieppel, 2000).

The evolutionary history of placodonts

The origins of placodonts and obtainment of their characteristic features remain largely unresolved, due to a very scant fossil record of "transitional" forms. However, a good glimpse in the first steps of their evolution is possible owing to the remains of a stem placodontid (Placodontiformes), *Palatodonta bleekeri*, uncovered in early Anisian deposits of Winterswijk, in the Netherlands (Neenan et al., 2013). The notable feature of that taxon are the row of conical palatine teeth constituting rather a plesiomorphic feature, characteristic for more basal diapsids, and blunt, peg-like premaxillary teeth, which resemble the chisel-shaped premaxillary teeth of the later placodont forms. That suggests the transitional character of these features and implies conversion from a carnivorous diet probably focused on soft prey to durophagous feeding in Placodontia. Another present feature in *Palatodonta* which connects it to placodont lineage is L-shaped jugal (Neenan et al., 2013). The so far recorded exclusive occurrence of the most basal representative of Placodontiformes in Europe indicates the western Tethys as a place of the origin of the Placodonts (Neenan et al., 2013).

Paraplacodus, uncovered in late Ladinian - early Anisian deposits of southern Alps (Diedrich and Gradinaru, 2013), is considered to be the most basal placodont, being also the first representative of Placodontoidea (Nennan et al., 2013). It is characterized by elongated, pointed and anteriorly orientated premaxillary and posterior maxillary teeth as well as slightly irregular, massive, and rounded tooth plates on mandible, maxilla, and palatine, suggesting the acquisition of a durophagous diet, which is characteristic for most of the representatives of Placodontia (excluding *Henodus*) (Rieppel, 2000; Scheyer et al., 2012). This tooth morphology is assumed to be helpful in the

detachment of mollusks from the sediment by using premaxillary teeth and crushing their shells by maxillary, mandible and palatine teeth (e.g. Rieppel, 2002; Scheyer et al. 2012).

Starting from the early Anisian new genus of a placodont - *Placodus* - thrived in the European epicontinental sea of the Germanic Basin, which covered the area of modern Germany and parts of France, Netherlands and Poland (Diedrich, 2010). This taxon was mainly characterized by reduction of teeth count comparing to *Paraplacodus*, enlargement of the palatine teeth, elongation of orbits, loss of temporal fossa and closure of the cheek region by secondarily developed and expanded temporal arch, which includes enlarged and extended jugal. (Rieppel, 1995; 2000). *Placodus* also developed a pachyostotic skeleton, which is characteristic for most of the subsequent placodont taxa. The thickened and robust skeleton most likely served as ballast, helping in locomotion and feeding at the bottom of the sea (Rieppel, 2000).

During the early Middle Triassic, another group of placodonts evolved - Cyamodontidae. They can be easily distinguished by their fused osteoderms forming a carapace (the dorsal shield) and in some species a plastron (ventral shield) (Rieppel, 2000). Due to the occurrence of those shell elements, they may superficially resemble turtles, however, the anatomy and origin of the shell are utterly different. The turtle shell is an outcome of the fusion of ribs (creating carapace),gastralia and clavicles (forming plastron) (Schoch and Sues, 2019). Whereas placodont shields are formed by fused osteoderms which are dermal bones (Rieppel, 2000). Their skull also underwent significant changes, which is especially evident in pronouncedly enlarged temporal fossae, elongated temporal arch and broad exclusion of postfrontal from temporal fossae (Rieppel, 2000). Further specialization in durophagous feeding is marked by a considerable enlargement of palatine teeth, general reduction of tooth count, and very prominent coronoid process (Rieppel, 2000). The enlarged tooth plates and reduced number of teeth probably enabled more even distribution of stresses and stains throughout the skull (Scheyer et al., 2012), whereas the large coronoid process expanded the area for mussel attachment (adductors), what could increase the bite power. Cyamodontid placodonts can be also characterized by the trend of elongation of premaxillary rostrum (snout) through time (Rieppel, 2000), with basal forms (e.g. *Cyamodus*) having short and rounded one and more derived forms possessing long, narrow and edentulous snout.

The most basal Cyamodontid placodont is a *Cyamodus*, which is known from Anisian and Ladinian deposits of Germanic Basin, as well as western (southern Alps) and eastern Tethys (south-western China) (e.g. Rieppel, 2000; Diedrich, 2011; Wang et al., 2019). It developed a set of features, novel for placodonts at that time, including an extensive carapace composed of fused, mostly irregular osteoderms creating two separate shields that covered the dorsal parts of the trunk and pelvic region (Diedrich, 2011; Scheyer et al., 2014). Moreover, its dorsal vertebrae lost their spinous processes whereas transverse processes became largely elongated and curved, which probably enabled the closer association between vertebrae and carapace, providing the better support of the latter (Diedrich, 2011). The skull also acquired morphological features, characteristic for most of the Cyamodontid placodonts, which were mentioned in the previous paragraph. Cyamodus diverged within the area of Eastern Tethys giving rise to *Sinocyamodus,* of which remains were uncovered in Carnian deposits of China (Wang et al., 2018). Other Middle Triassic Cyamodontid placodont record includes *Glyphoderma* (Zhao et al., 2008) and *Psephosauriscus* (Rieppel, 2002).

In the Upper Triassic deposits, placodont material is represented by few Cyamodontoid placodonts, including *Placochelys, Psepchochelys*,*Psephosaurus*, *Psephoderma, Macroplacus and Protenodontosaurus*(e.g. Rieppel, 2000;2001;2002b). All of these taxa were characterised by distinctly elongated narrow rostrums and oval carapaces composed of smooth as well as keeled hexagonal

osteoderms (Rieppel, 2000; 2002b). However, at that time also a new form of cyamodontoid placodonts evolved, the Henodontoids, so far represented only by two known taxa: *Parahenodus atancensis*(de Miguel Chaves et al., 2018) and *Henodus chelyops*(Huene, 1936). *Parahenodus* remains were uncovered in Carnian-Norian (presumably marine) deposits of central Spain and may represent the transition from more basal forms to highly derived *Henodus* (de Miguel Chaves et al., 2018). That is mainly manifested by reduction of the dentition to only two palatine teeth, acquirement of a flattened skull and expansion of a parietal resulting in the reduction of upper temporal fossae. However, it also retained some of the plesiomorphic features like open temporal fossae (closed or vestigial in *Henodus*), more posterior position of orbits in comparison to *Henodus*, and anteriorly tapering skull (de Miguel Chaves et al., 2018).

Starting from the Carnian, placodonts suffered a profound decline, with only 2 taxa surviving till Rheatian: *Macroplacus* and *Psedhoderma* (Norden et al., 2015). It was probably due to widely occurring regressions causing the shallow marine habitat loss, which ultimately could cause the placodont extinction at the end of the Rhaetian, with one of the youngest representatives of that clade found in England (Norden et al., 2015).
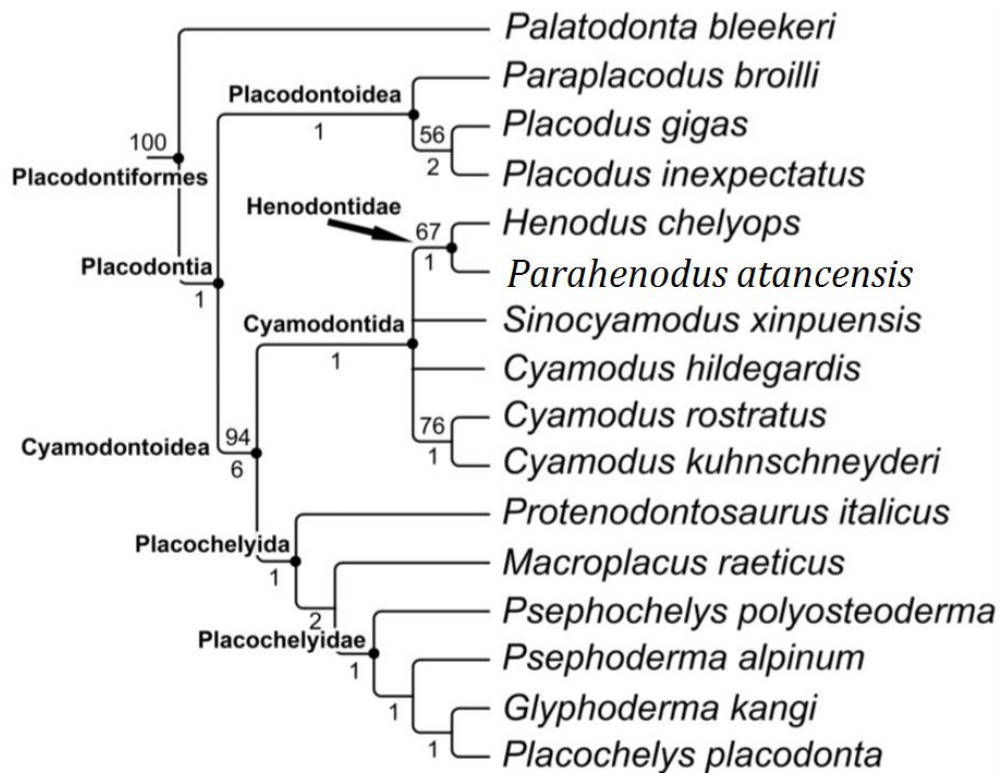
Fig. 6. Strict consensus tree of Placodontia. Adopted from de Miguel Chaves (2018).

1.6 *Henodus* - overview

Henodus is a genus of cyamodontoid placodont, exclusively known from Goldersbach near Tübingen-Lustnau situated in southwestern Germany. It was first described by Friederich von Huene in 1936 (Fig. 7), mainly based on two almost complete skeletons and an isolated skull. That was followed by the description of a third partial specimen in 1938. To this day only eight specimens of that genus have been recovered (Werneburg and Böhme, 2017) all representing one species – *H. chelyops*. In subsequent years, descriptions of osteology, palaeoecology, and palaeobiology of *H. chelyops* were included, in usually overview articles concerning multiple placodontid taxa.
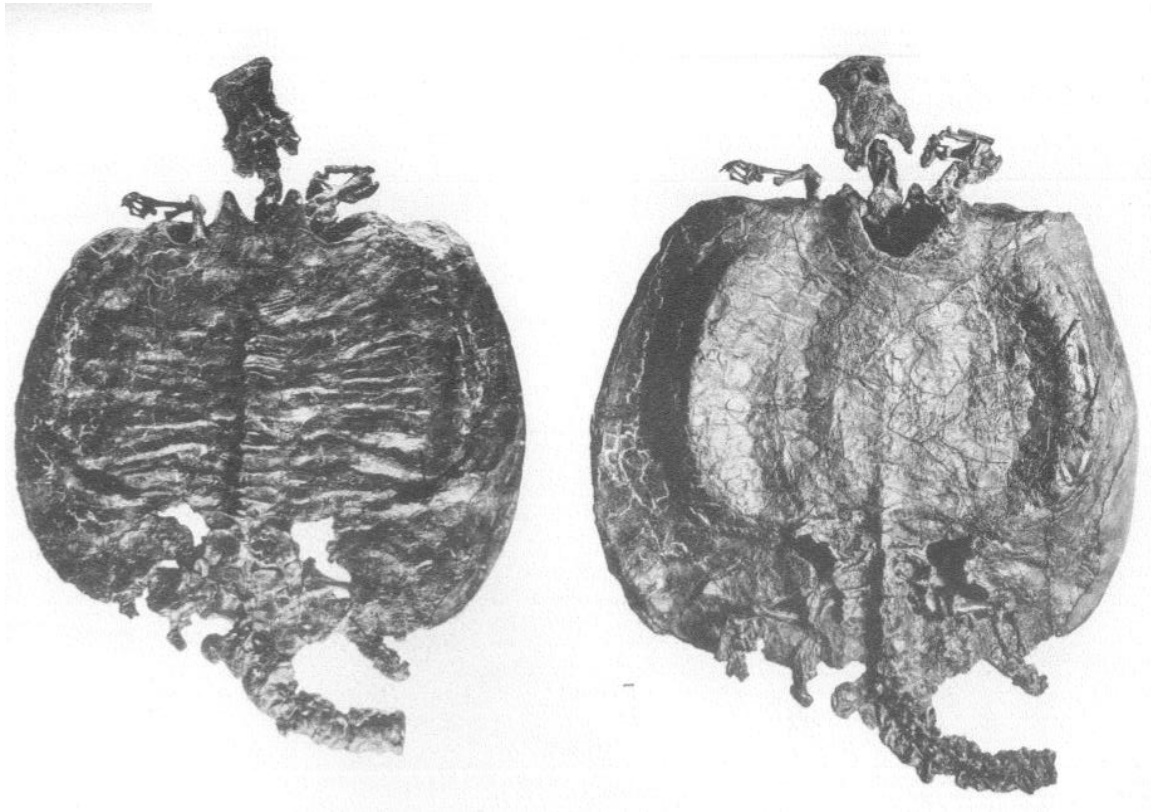
Fig. 7.*Henodus chelyops*skeleton (specimen 1) in ventral (left image) and dorsal view (right image). Adopted from von Huene (1936).

Henodus is a prominently taxon characterised by numerous autapomorphies, significantly disparate in many morphological aspects from other placodonts. That pertains mainly to the skull, which underwent many modifications. It is most clearly manifested by shape modification to rectangular outline and reduction of tooth count just to one small tooth on each of the paired palatines (Rieppel, 2000). The latter do not contact each other, being separated by broad vomers and pterygoids (Rieppel, 2000). Skull of *Henodus* also lost the temporal fossae, probably in the result of lateral enlargement of a parietal, which obtained a characteristic fan-like shape (Rieppel, 2000; 2001). The anterior portion of the skull became steeply inclined ventrally with orbits oriented anteriorly. Quite peculiar is the morphology of the maxillae and premaxillae which form a very short but quite broad rostrum. The anterior part of rostrum terminates ventrally with a cutting edge, which possesses a row of denticles (Rieppel, 2000). On the ventral side of the maxillae, the curved grooves extend

longitudinally, which were hypothesized to bear the baleen-like structure (Huene, 1936; Rieppel 2000). Quite distinctive is the unproportionally massive mandible in relation to the skull. It possesses a relatively low coronoid process, which is much smaller compared to other cyamodontoid placodonts (Rieppel, 2001).

The low coronoid process together with highly reduced dentition and modified rostrum suggest distinct feeding behavior of *Henodus* from other placodonts, which was in lesser degree durophagous (Rieppel, 2002). Based on myological reconstruction, which indicated dual jaw adductor system unique in Placodontia, as well as jaw apparatus morphology, Rieppel (2002) concluded that despite the reduced biting power, the jaws of *Henodus* were able to be opened quite rapidly. That could possibly enable suction feeding, with supposed baleen structure possibly acting as a sieve. For that reason it was considered to be an omnivore, conceivably feeding on both plants and small invertebrates using its palatine teeth for an additional size reduction of the food. Other authors portrayed *Henodus* as a herbivore (Reif and Stein, 1999), that - consistent with their interpretation - could have used the rostrum's cutting edge to scrape and cut plant material (Rieppel, 2002). If the interpretation is correct, that would make *Henodus* one of the oldest known herbivorous marine reptiles (Chun et al., 2016).

Henodus can be also distinguished by possessing one of the most robust carapace within Placodontia, which is composed of few osteoderm morphotypes. The most diagnostic one includes transversally elongated hexagon-shaped osteoderms, which form a medial part of a carapace (Huene, 1936). The more lateral ones, creating the margins of the shield, are more irregular and scalene. However, they usually maintain a hexagonal-like shape. Most of the *Henodus* osteoderms are flat, with a smooth surface, lacking any ornamentation or keels, with exception of keeled and slightly dorsally curved osteoderms covering the area of the C-shaped carapace ridges. The carapace has a reniform shape, is around 2 times wider than long, and poses two distinct notches at the proximal and distal edges, which consisted the opening for a neck and a tail respectively. Carapace also poses two pronounced C-shaped ridges located near the lateral margins of the shield, parallel to its edges. They are extending through most of the carapace length.

Besides the carapace, the postcranial skeleton of *Henodus* has not been considered diagnostic. It posses many features shared with other cyamontodid placodonts like pachyostotic ribs or rather simple morphologically, amphiceouls vertebra. Limb bones are very short and gracile in respect to the animal's body, suggesting rather restricted utility in locomotion (Rieppel, 2002)

Deposits in which *Henodus* remains were found are assigned to the uppermost Gipskeuper of Lower Carnian Grabfeld formation. Sediments (shales, nodular gypsum, salt, and pedogenic deposits) of the formation are interpreted to be deposited in the succession of sabkha, playa and salina systems (Shukla et al., 2010). However, the occurrence of thin dolomite beds indicates a temporary marine influence. The first *Henodus* remains were noted by Huene to be found in dolomite concretions placed within gypsum marls (Huene, 1936). Those deposits were interpreted to represent the marginal marine environment (Chun et al., 2016), thus suggesting the shallow marine or possibly brackish habitat of *Henodus*.

Fig. 8. Skeleton of *Henodus chelyops* and its life reconstruction. Photograph of the skeleton of *H. chelyops* found in Goldersbach, southwestern Germany. Specimen was recovered from dolomite concretions of Lower Carnian Grabfeld formation. B. Life reconstruction of *H. chelyops* by Jakub Kowalski and Piotr Janecki.

1.7 Late Triassic vertebrates and palaeoenvironment of Algarve - state of the art

The Triassic deposits of Algarve have been known for almost 200 years (Bonnet, 1846). Despite that, the first vertebrates descriptions were published by Palain (1976) and Russell and Russell (1977), which concerned the fragmented cranial material identified as belonging to *Stegocephalia*. The temnospondyl bonebed near Roch da Pena was discovered by Schroter in 1981 and described in an unpublished thesis. Witzman and Gassner (2008) published the first article depicting material from that site, which included vertebra centra, fragments of cranial and clavicle remains assigned to metoposaurid and mastodontosaurid temnospondyls. In subsequent years the bonebed was relocated and excavated by an international team of scientists including Octávio Mateus, Steven Brusatte, Richard Butler and Sébastien Steyer. Those works resulted in the first description of the bonebed (Steyer et al., 2011). The first Late Triassic phytosaur from the Iberian Peninsula was recovered with material comprising hemimandibula and isolated teeth features (Mateus et al., 2014). The Algarve phytosaur was suggested to be the basal representative of that group, based on the plesiomorphic mandibular features (Mateus et al., 2014). Nevertheless, the most significant was the discovery of numerous Metoposaurs remains, which enabled the description of a new species, *M. algarvensis* (Brusatte et al., 2015). This finding also enriched knowledge about the paleogeography of metoposarid temnospondyls and took notice of the creation of *Metoposaurus* bonebeds.

In many of the previously mentioned works concerning stratigraphy of Gres de Silves formation, the paleoenvironmental interpretations were made. Thence, the units AA and AB1 were construed as a terrestrial, alluvial deposits formed in semi-arid climate (Palain 1976; 1979; Pereira et al., 2016). AB 2 sequence was interpreted by Palain (1976) as a coastal plain with small alluvial deposition. Azerêdo et al. (2003) suggested the marine influence in the AB2 sequence based on dolomite and euryhaline fauna occurrence and implied the shallow-marine or coastal lagoon environment. Schroter (1981) proposed the deltaic environment, which was later dismissed by Witzmann and Gassner (2008). The last volcano-sedimentary unit (AB3) is thought to be created mostly in the marine environment and associated with the first phase of rifting (Azerêdo et al. 2003). In addition to those works, the geochemical analysis were published, construing the "evaporitic transitional environment" based on high contents of Mg, dolomite, hematite and illite (Trindade et al., 2010).

1.8 Objectives

This study aims to describe the new vertebrate material from Rocha da Pena, with a focus on placodont fossils and provide paleoenvironmental and taphonomic interpretations of newly discovered fossiliferous bed.

The work includes:

- Osteological description and taxonomic identification of a newly acquired vertebrate material from Rocha da Pena with focus on the '*Henodus*' skull
- Phylogenetic analysis based on the '*Henodus*' skull
- Provision of new stratigraphic logs of the uncharted part of the Rocha da Pena outcrops
- Paleoenvironment interpretation based on sedimentological features.

2. Materials and methods

The newly obtained collection from Penina is comprised of 42 specimens. which are housed at Departamento de Ciências da Terra of Faculdade de Ciências e Tecnologia of Universidade Nova de Lisboa. Henodus skull - ML. A9182 was found by Luis Graça in isolated block coming from layer 9. Specimen ML. A9182 is housed in Museu Municipal de Loulé.

Most of the presented fossil samples were collected during personal fieldtrips. Most of those fossils were collected from the isolated blocks coming from Layer 9. Few specimens were excavated directly from the layer using geological hammer and chisel. The obtained specimens were preliminary described, packed into bags and protected by bubble wrap. SpecimenML. A9182 and other newly obtained specimens were prepared in Dinopark Lourinhã and at Departamento de Ciências da Terra of Faculdade de Ciências e Tecnologia of Universidade Nova de Lisboa using air scribes of different sizes and tongsten pen. In case of few specimens, the dissoluted10 % chloric acid (HCl) was used in aim to dissolute the carbonated parts of rock covering fossils (performed at Departamento de Ciências da Terra of Faculdade de Ciências e Tecnologia of Universidade Nova de Lisboa). The chloric acid was applied by a brush on the rock to assure the small amount of acid being delivered in the specific places of the rock. In case of appearing breakages the 5% and 50% Paraloid B-72 diluted in acetone was used as consolidant and glue. Big cracks occurring in fossils were filled with 50% and approximately 70% Paraloid B-72.

The phylogenetic tree was performed in TNT (version 1.5, Nov. 2018). The traditional search was applied, employing branch swapping (TBR) options.All the character states have the same weight. Based on the obtained data, a consensus tree was created. In the next step CI, RI and RC were calculated. Next, bremer support and bootstrap (number of replicates: 1000) decay values were calculated to assess the robustness of support for each node. After obtainment of the basic information about a tree (topology, length, statistics, Bremer and bootstrap values) synapomorphies were mapped and listed. Afterward, they were analyzed in the context of recognition of autapomorphies by mapping the characters.

3. Geographical and geological setting of Rocha da Pena

The geological and paleontological study was performed at the outcrops located near Penina, municipality of Loulé (Fig. 9). The investigated outcrops belong to the upper part of the AB2 unit of Grés de Silves Formation (Brusatte et al., 2015). The studied profiles are exposed at the north-eastern slope of longitudinally extended hill facing Rocha de Pena to the north (Fig. 10). Three sections has been investigated. Distance between the most outermost sections is approximately 400m (Fig.11). Due to the restricted avaibility of performing fieldwork during the time of the research only two sections has been investigated in detailed. Section 3 lacks precise measurments therefore is not presented herein. Based on the preliminary observations the sequence and sedimentological character of the layers in the section 3 is almost the same as in Section 1, suggesting distinct lateral extension of strata.
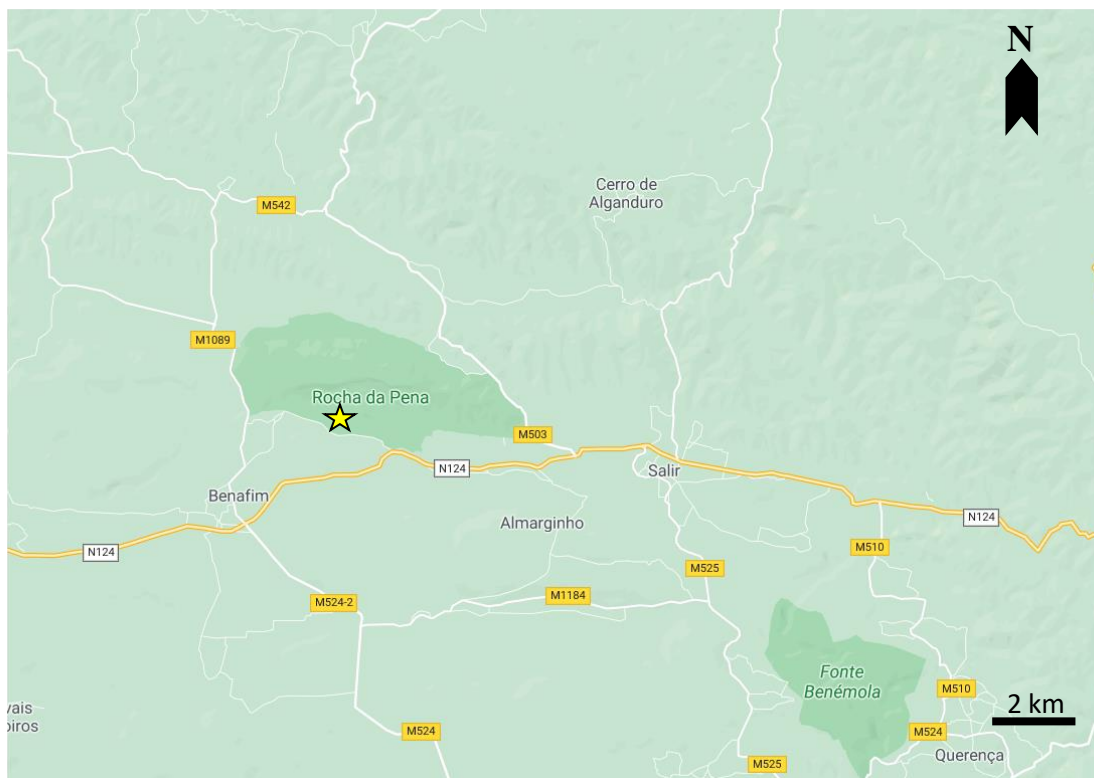
Fig.9 Map of the northern part of Loule municipality showing areas of Rocha da Pena. Site investigated marked by yellow star.
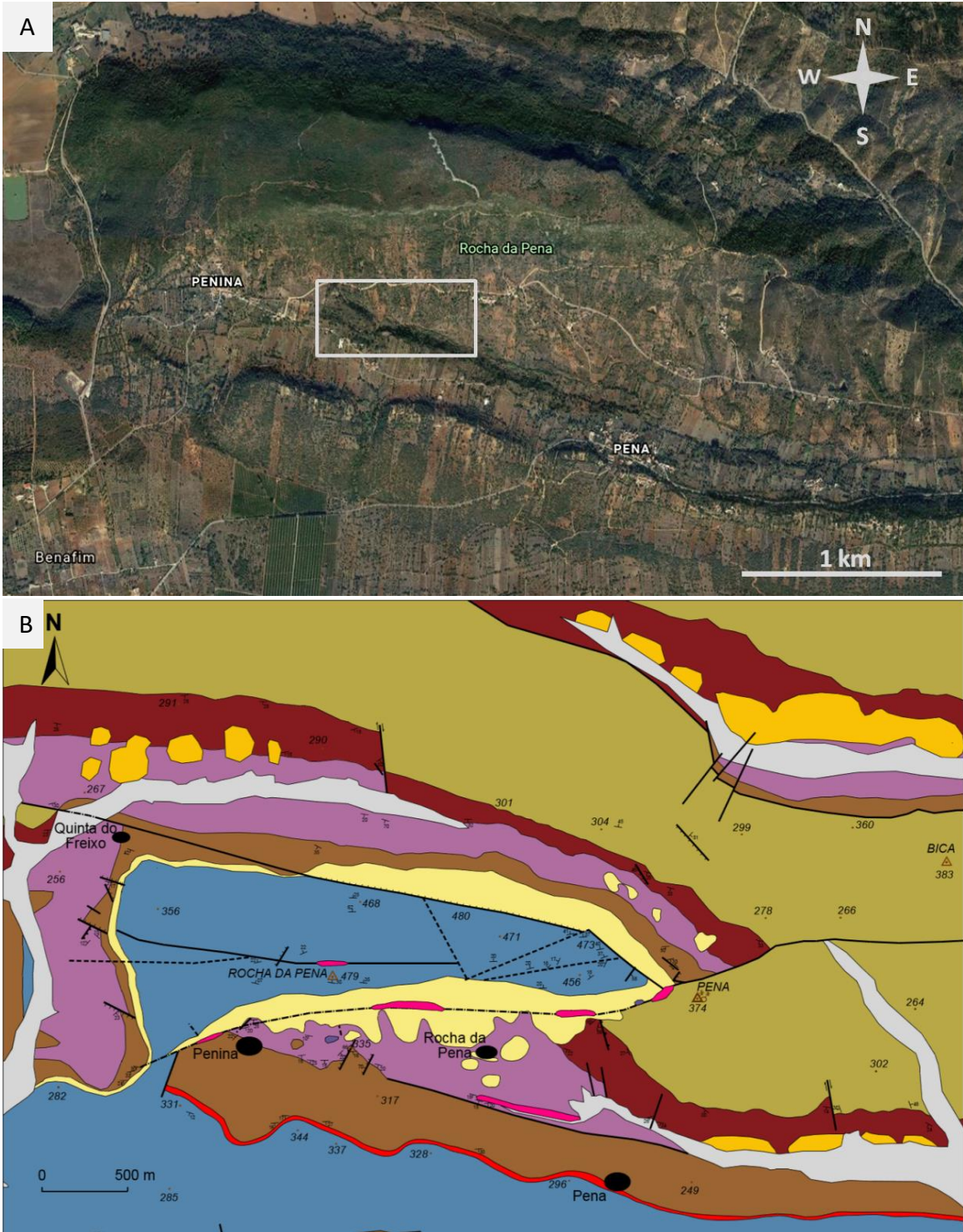
Fig. 10. The investigated area. A. The Google earth view at the studied area. B. Geological map of the Rocha da Pena (adapted from Lopes, 2006)
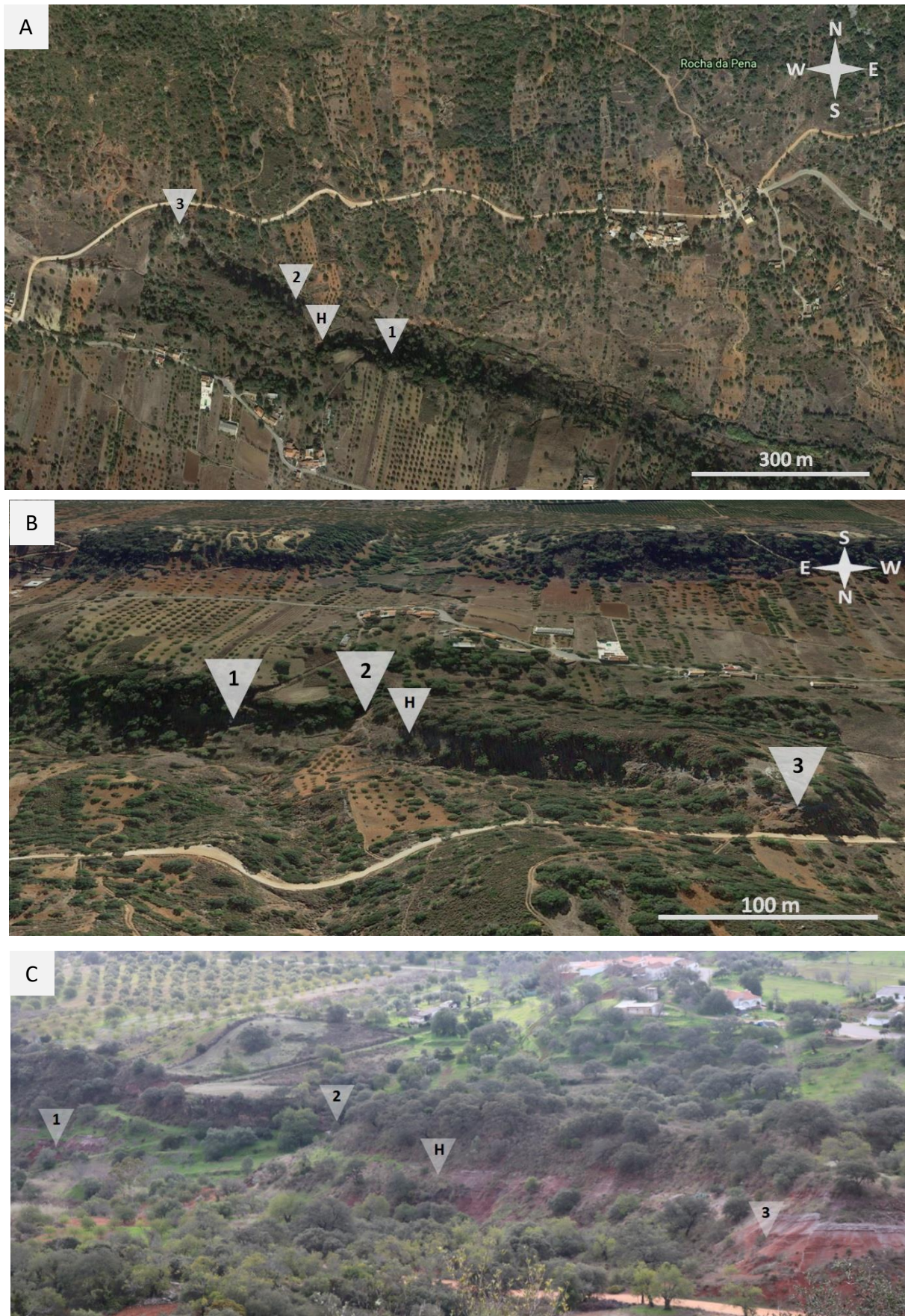
Fig. 11. Google Earth view from the studied outcrop with indication of the positions of the studied sections (indicated by numbers) and place, where *Henodus* skull was found (H).

Section 1

N 37º 14' 58.489''; W 8º 6' 33.668''

Section 1 is the easternmost investigated part of the outcrop. It is the lowermost of the investigated profiles. It contains over nine meters of sediments of various lithologies (Figs.12,13).

Fig. 12.Photos of the outcrop atSection 1 at Rocha da Pena.

Fig. 13. The geological profile from the easternmost investigated section of the outcrop – Section 1.

Bed	Description	Photograpy
1	Dark red, massive claystone, marbly with three light blue/green laterally continuous intercalations. Common microcracks and slickensided surfaces cemented by beige secondary carbonate/evaporite. Common bluish grey colour mottling Conchoidal cleavage. Thickness: 160 cm	
2	Dark red/brown marbly claystone with rare pale blue color mottling. Massive, blocky cleavage, structureless. Thickness: 150 cm	
3	Dark purple massive claystone) with irregular, light blue carbonate nodules mainly oriented vertically. Blocky cleavage Thickness: 30 – 40 cm	

4	Dark red/dark purple massive claystone with rare pale blue color mottling, blocky cleavage, structureless. Thickness: 30 cm	
5	Light blue massive carbonate with irregularly distributed carbonated massive purple mudstone at the top. Occasionally desiccation cracks at the top of the layer. Thickness: 10 – 15 cm	
6a	Dark red/dark purple massive claystone with pale blue/grey color mottling; blocky cleavage, structureless. In the middle of the layer, lens-shaped intercalation is composed of light blue carbonate with dark and pink spots. Thickness: 50 cm	

6b	Intercalation with the claystone, composed of light blue, massive carbonate with dark and pink spots. Thickness: 0 – 15 cm	
7	Beige massive carbonate with rare patches of light green and dark mudstone, occuring mainly near the top. Blocky clevage (more evident at the base) to massive mainly homogenous structure at the top. Common geodes, filling the irregular and usually large (> 5 cm) pores/fractures. Top surfaces often undulating due to occurance of dome-shaped protrusions. At the top gypsum dessert rose-like structures. Thickness: 10-20 cn	
8	Very light blue, massive claystone with dark spots. Small scale blocky clevage, structureless. Near the base, dark purple, laterally continuous 5 cm thick intercalation of claystone. Thickness: 50 cm	

9	Light green/blue, massive carbonated claystone with irregularly distributed patches of light green or dark brown spots of non-carbonated claystone. Very common pores (including geodes) ranging from very small to middle sizes (>1 mm - 5 cm), mostly filled with crystals. At the top common dessert rose like structures, more rarely desiccation cracks. Common isolated and usually incomplete bone elements. Thickness: 5-10 cm	
10 a	Dark purple, massive, marbly claystone with grey and dark green color mottling. Small scale blocky cleavage, structureless. Common microfaults with beige carbonated sediment infilling. Around 40 cm from the base a white, 4 cm thick, massive limestone intercalation. Thickness: 250 cm	
10 b	White/pale green, massive limestone intercalation. Thickness: 4 cm	

| 11 | White to light red massive structureless siltstone. | |

Section2

N 37º 14' 58.449''; W 8º 6' 33.658''

Section 2 includes 3 rock exposers located within 10 meters between each other. The lowest one includes layers which can be correlated with the uppermost part of section 1. Section 2 include mudstones, carbonates, siltstones and silty sandstones (Figs 14,15).

Fig. 14.Photographs of the outcrop within the area of the section 2. A. The lower part of the section with mudstones, siltstones and carbonates. B. The middle part of the section with mudstones, siltstones and carbonates. C. The upper part of the section with silty sandstone and fine sandstone.
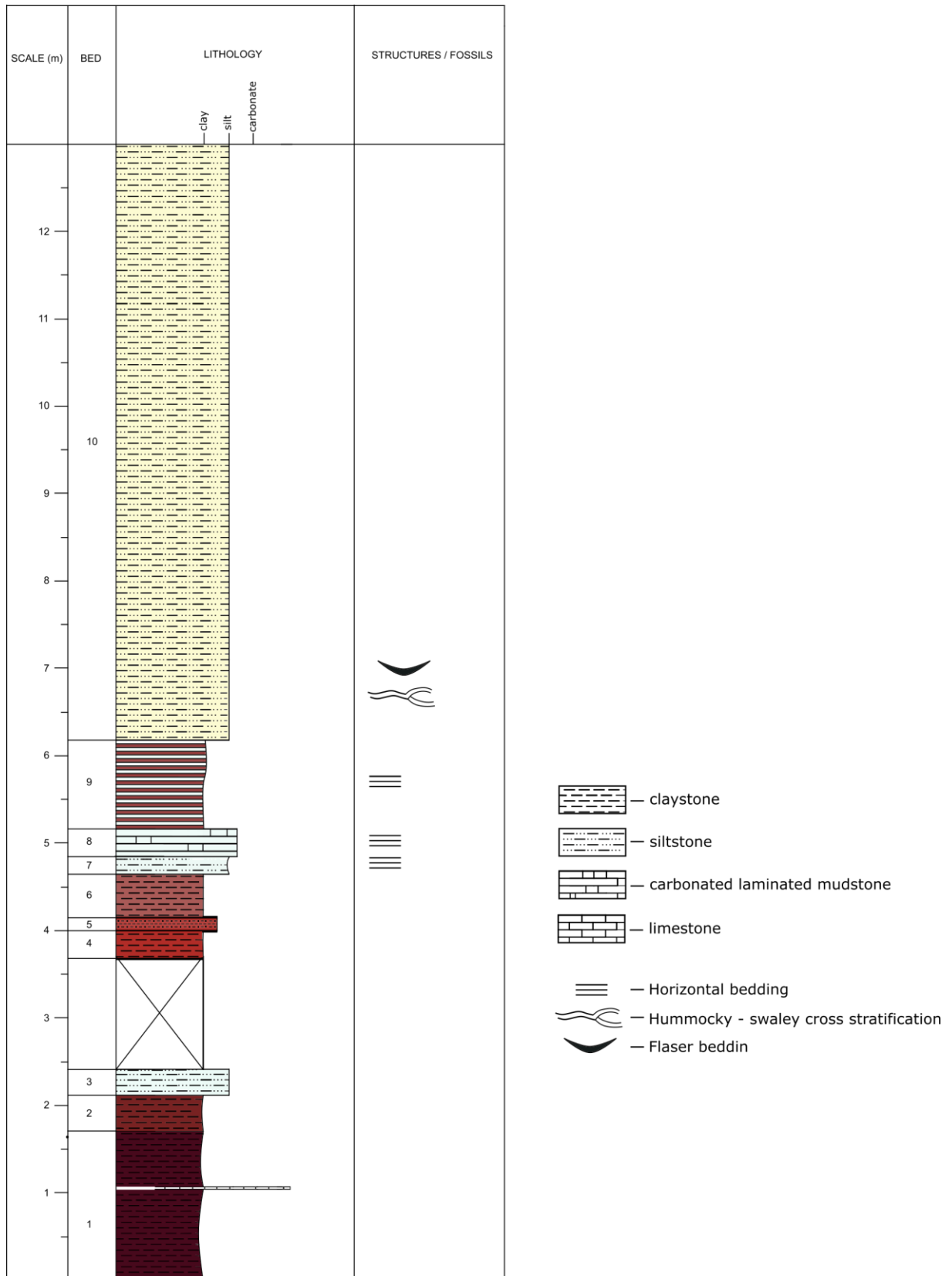
Fig. 15. The geological profile from the easternmost investigated section of the outcrop – Section 1.

Bed	Description	Photography
1a	Dark purple, massive, marbly claystone with light blue spots.Small scale blocky cleavage. Common slickenside surfaces cemented by secondary carbonate. Around 40 cm from the base a white, 4 cm thick, massive limestone intercalation. Thickness: 240 cm	
1b	White, massive limestone intercalation. Thickness: 4 cm	
2	Brown/red massive claystone. Marbly with light blue spots, especially at the middle and top part of the layer. Upward decrease of the scale of blocky cleavage. Thickness: 70 cm	

3	White to light blue massive, marbly siltstone with red spots. Thickness: 40 cm	
4	Red massive claystone with blocky cleavage. Thickness: 30 cm	
5	White/light blue laminated silty mudstone with red and dark lamina. Thickness: 15 cm	

6	Red massive claystone, blocky cleavage with angular to subangular, interlocking blocks Thickness: 50 cm	
7	White to light blue silt with red and black spots. Thickness: 20 cm	
8	Light blue laminated carbonate. Thickness: 30 cm	

9	Shale with red, light blue and dark lamina. Thickness: 110 cm	
10	White to beige sandy siltstone. Near the base cross bedding. Thickness: Ca. 700 cm	
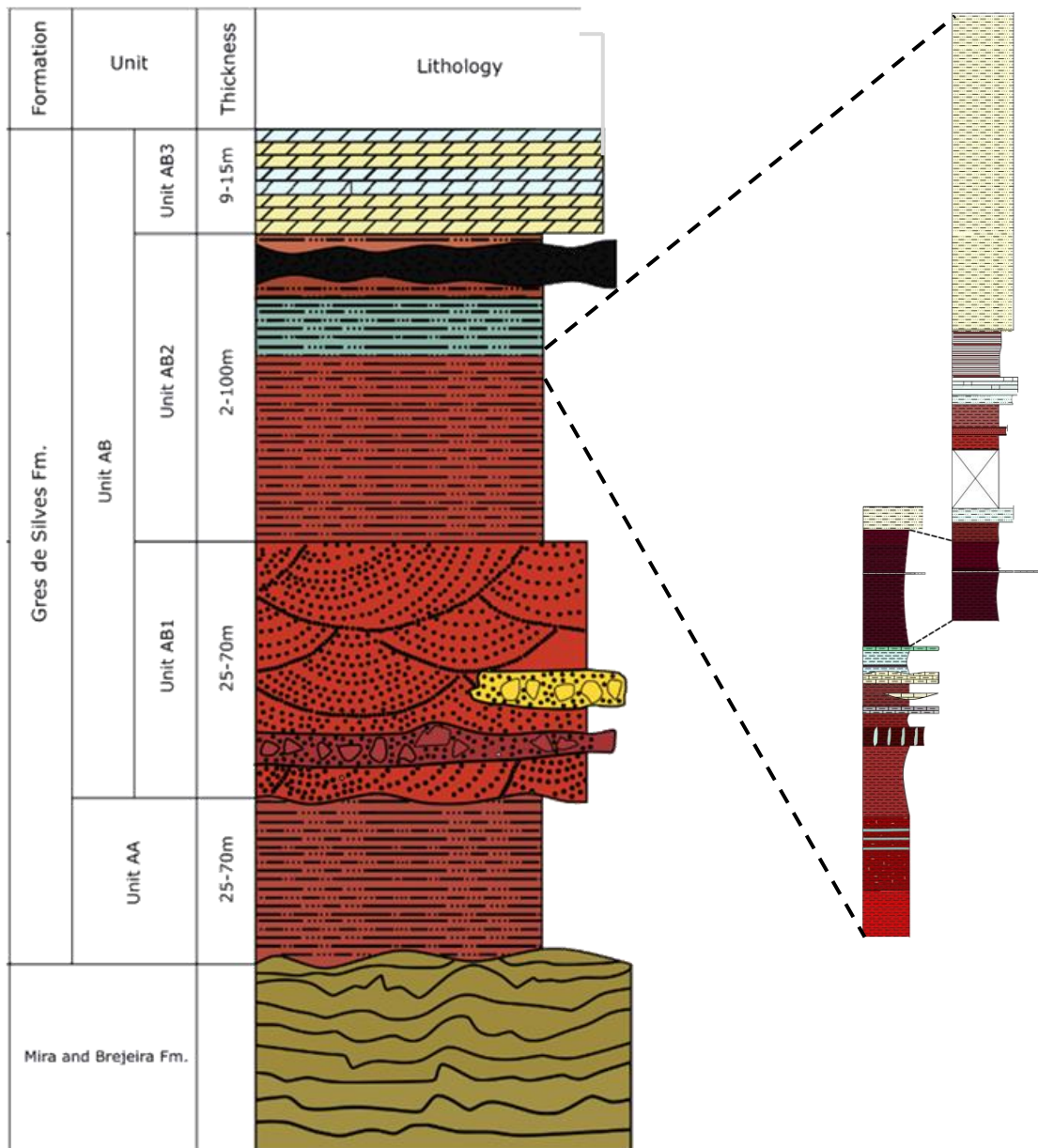
Fig. 16 Schematic stratigraphy of the Paleozoic and Lower Mesozoic part of the Algarve Basin (adapted from Palain, 1976; Manuppella, 1988; Brusatte et al., 2015) with tentative assignation of section investigated to upper part of Unit AB2.

4. Facies and interpretation of the deposition environment

4. 1. Blocky claystone (layers: S1L1; S1L2; S1L3; S1L6a; S1L10a; S2L1)

Blocky claystone facies constitute layers of massive claystone with blocky cleavage. They are dispersed across most of the thickness of the section and are separated from each other by layers of carbonates and carbonated mudstones. Almost all layers exposed in Section 1, also occurs in Section 3 (with exception of S1L3), which suggests a distinct lateral extension of those layers. Most of the layers are characterized by various degrees of color mottling (Fig. 17). It might be caused by marmorization, a phenomenon based on pedogenic processes and water movement through soil causing an irregular distribution of iron oxide, hydroxide and/or carbonate (Tucker, 2001). Besides shared properties, each of the layers is of a different color and presents slightly different sedimentological features.

S1L1

Dark red to brown, massive claystone, with three light blue/greenish laterally continuous intercalations. Microcracks and slickensides surfaces occur commonly. They are usually straight and elongated and filled with secondary precipitated carbonate or evaporates. Similar structures are noted to occur in various types of paleosoils (e.g. Retallack, 1988; Muller et al., 2004; Milroy et al., 2019). Their origin might be due to the clay properties which include high plasticity and hydrophilic nature, causing swelling in wet conditions and shrinking in arid conditions. Due to the sediment movement, stress can be generated causing the creation of slickenside surfaces and microscale displacement of the soil. The best circumstances for the occurrence of such conditions occur in a highly seasonal climate which characterises modern tropical and subtropical regions (Soil Survey Staff, 2006; Milroy et al., 2019). The prevalent red/brown color of the clay may indicate the deposition under the arid climate and oxidizing environment resulting in weathering of ferromagnesian minerals (Milroy et al., 2019). Color mottling can be caused by redoximorphic conditions which occur during the early diagenesis stage or pedomorphosis. The occurrence of pale blue intercalations might be the result of lasting of prolonged humid conditions which could have lead to a higher water table and decrease in oxidizing conditions. Based on the occurrence of the described features this layer may be interpreted as early-stage paleosoil.

S1L2

Dark red/purple marbly claystone with rare pale blue color mottling. Color mottling is much less developed comparing to S1L1, restricted only to small irregular spots. Microcracks and slickenside surfaces occur but are rare and of a small size. The smaller scale of those features may indicate deposition under more arid and less variable conditions comparing to S1L1 or/and smaller impact of diagenesis/pedomorphosis.

S1L3

Dark purple massive claystone with blocky cleavage. Differing from the other layers by darker color, lack of evident slickensided surfaces and occurrence of irregular, light blue, massive carbonate nodules mainly oriented vertically. Based on the elongated shape of nodules and their vertical orientation, it can be presumed that they are rhizoconcretions created due to the pedogenic accumulation of carbonate around roots (Klappa, 1980; Milroy et al., 2019). However to confirm this tentative interpretation investigation, the microfabric analysis is needed. The dark purple color suggests either more reducing conditions comparing to underlying layers or/and increased organic content.

S1L6a

The layer includes dark red/dark purple massive claystone with pale blue/grey color mottling. The dark purple color suggests reducing environment and possible enrichment in organic matter (Tucker, 2001).

S1L10a

Dark purple, massive, marbly claystone with grey and olive color mottling. The dark purple color suggests a more reducing environment and possible enrichment in organic matter (Tucker, 2001). The olive color mottling can be the result of the reduction of iron by migrating groundwaters or from the local occurrence of organic matter (Tucker, 2001). Microcracks and slickenside surfaces occur quite commonly and some of them are relatively large reaching over 1 m in length (Fig. 17). They are usually straight and elongated and filled with secondary precipitated carbonate or evaporates.
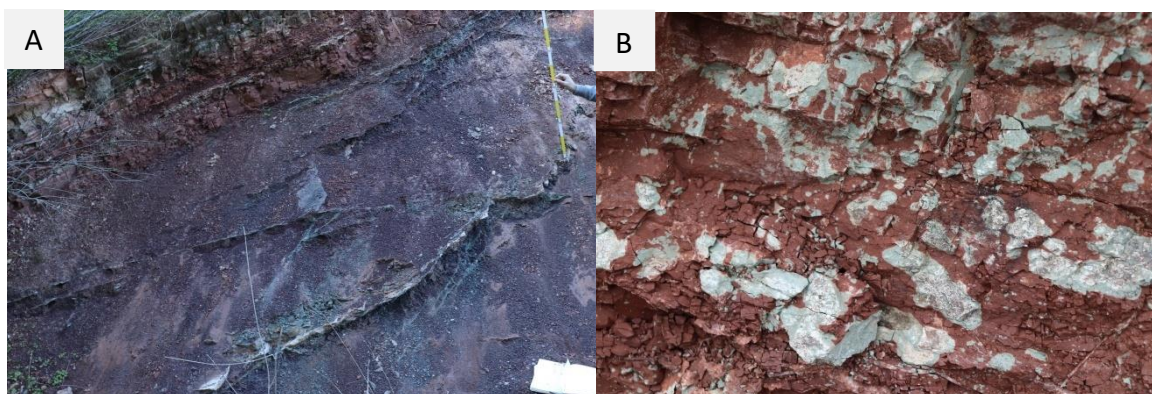
Fig. 17.Photographs of mudstone facies A. Mudstones with slickenside surfaces and cracks, filled with carbonates and evaporites. B. Mudstone displaying colour mottling.

4.2 Laminated silty mudstone facies (layers: S2L5; S2L7; S2L9)

Laminated silty mudstones are solely exposed in Section 2, which represents the upper part of the investigated sequence. The laminated silty mudstones comprise planar millimeter-thick repeatedly interlayered laminated pale grey-blue, red and dark laminae of silty mudstone (Fig. 18). The pale grey/blue laminae are usually the thickest ones (from 2 mm up to around 10 mm). The red lamina are almost always thinner with a thickness generally ranging between 1-3 mm. Despite the prevalent planar geometry, they are sometimes slightly undulated. The dark laminae are the finest are usually less than 1 mm thick. They are often strongly undulated and lack lateral continuity. Red laminae seem to be composed of mainly very fine clay-sized grains (very smooth surface with separate grains, impossible to detect with the naked eye). The pale grey-blue laminae also contain silt-size grains. The dark laminae contain a larger quantity of siltstone-size grains. The geometry of lamination is not consistent within the layers, with some sections comprised of horizontal or sub-horizontal laminae and others with mostly undulated laminae. However, the physical extension of the occurrence of this sedimentological feature remains unknown due to the largely weathered nature of surfaces of the investigated layers, which impedes precise observation. The described facies is displayed by 3 layers which differ by texture and degree of consolidation. **The S2L5** consists of well-consolidated silty mudstones, which weathers into faintly marked conchoidally fractured blocks. The laminae within the layer are often strongly undulated. **S2L7** is composed of poorly consolidated silty mud. **S2L9** can be defined as a slate. It is very well consolidated and exhibits a moderate degree of fisselity. Laminae within this layer are mostly horizontal or subhorizontal with some sections displaying undulated laminae.

The occurrence of finely laminated sediments indicates deposition on low gradient surfaces and a low-energy deposition environment. Sections with horizontal mostly undisturbed laminae suggest an absence or at least a low abundance of bottom-dwelling organisms. That on the other hand may indicate an oxygen-depleted environment (Talbot and Allen, 1996). Sections with undulated laminae indicate the environment with higher energy depositional setting. The repeated occurrence of three distinctly different laminae allows the classification of those sediments as heterolithes, and rhythmites.To decipher the mechanism leading to rhytmic deposition of those sediments, more precise investigation is needed, including the fabric and mineralogical composition analysis. Rhythmites or in general finely laminated sediments are thought to be the most common in restricted environments, especially in lacustrine settings(Talbot and Allen, 1996). However, they may also be deposited in the tidal environment such as tidal flats within coastal, deltaic or estuarine environments (Davis and Dalrymple, 2012).
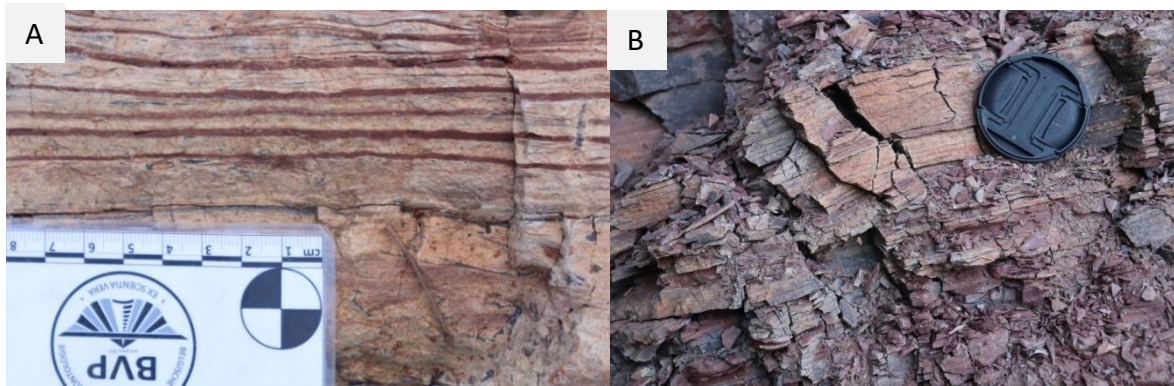
Fig.18. Photographs of laminated siltstone facies.A,B. Laminated siltstone with distinct beige, red and dark laminae.

4.3. Calcareous mudstone/ limestone facies (S1L5; S1L6b; S1L7; S1L9; S1L10b = S2L1b, S2L8)

Within the investigated section carbonate sediments are common and occure in a great variety of textures. All of them are relatively thin, ranging between 4 and about 30 cm of thickness. Almost all layers are exposed in both Section 1 and Section 2 (with exception of S1L6b), which suggest a distinct lateral extension. The investigated layers vary in terms of the texture and composition of the carbonate.

S1L5

Pale blue massive carbonate with irregularly distributed carbonated massive purple mudstone mainly occurring at the top of the layer (Fig. 19). Occasionally syneresis cracks occur at the top of the layer (Fig. 19). Syneresis cracks are shrinkage cracks, but in contrast to desiccation cracks, they form in subaqueous conditions in the process of sediment dewatering in the results of eg. salinity changes. They also have simpler shapes comparing to desiccation cracks, like incomplete polygons, spindle or V-shapes. Faintly marked polygonal cracks, as well as spindle-shaped, V-shaped or straight cracks, had been observed.

The occurrence of a massive carbonate layer suggests the temporary existence of the water body, within which carbonate precipitated. The common occurrence of purple mudstone within the upper parts of the layer may suggest the increased influx of siliciclastic sediment or/and decreased carbonate precipitation rate. Syneresis cracks indicate the shallow water depositional environment.

S1L7

Beige massive carbonate with rare lenses of light green and dark mudstone, occurring mainly near the top of the layer (Fig. 19). Conchoidal cleavage (more evident at the base) to massive structure

at the top. Common geodes, filling the irregular and usually large (> 5 cm) pores/fractures. Geodes are often filled with gypsum crystals. Top surfaces often undulating with commonly occurring dome-shaped structures, protruding up to around 20 cm comparing to the surrounding surface of the layer. They are usually composed of massive limestone. Pores and fractures quite common. Conchidal cleavage locally does not occur or is subtly marked. At the top of the layer, centimeter-sized gypsum dessert rose-like structures, occur mainly at the surface of the domes (Fig. 19).

The occurrence of around 10-20 cm thick carbonate layer suggests the temporary existence of the water body, within which carbonate precipitated. The varying thickness may be the result of an irregularity of the depositional surface. The common occurrence of mudstone within the upper parts of the layer may suggest the increased terrigenous influx of sediment or decrease in salinity which could have caused the water undersaturation with calcium carbonate and decreasing carbonate precipitation rate. The occurrence of desert rose-like structures implies a high evaporation rate and probably disappearance/withdrawal of the water body. Notable are the dome-shaped protrusions which usually have more massive structure than the surrounding sediment. They also seem to be relatively regular and rounded. Possibly, they may represent a microbialite structure– the leiolite, which is a type of a structureless thrombolite lacking lamination and posses aphanitic mesostructure (Riding, 2011). Like stromatolites and remaining types of thrombolites, leolites are the product of bacteria-induced precipitation of carbonate. The proposed interpretation is however tentative and needs revision by thin section investigation, which could possibly reveal cryptic microbial texture characteristics for leolites (Cordie, 2019). Worth noting is that the proposed interpretation could help to explain a very high porosity of the rock, as a microbialite structures are often characterised by large porosity (Cordie, 2019).

S1L9

Pale green, massive carbonated claystone with irregularly distributed spots of light green or dark brown spots of non-carbonated claystone. Sometimes the dark claystone forms a few millimeters wide vertical veins, stretching throughout the whole thickness of the layer (Fig. 19). This feature has been observed only in the westernmost part of the exposure of the layer. The matrix contains rounded few millimeter-sized carbonate grains as well as pink grains of unidentified origin. Very common pores ranging from very small to middle sizes (>1 mm - 5 cm), mostly filled with euhedral gypsum crystals (Fig. 19).At the top common gypsum dessert rose-like structures. More rare are polygonal desiccation cracks, which usually reach around 15-20 cm of maximal extension (Fig. 19). Common isolated and usually fragmented bone elements.

Based on the irregular distribution of carbonate within the layer and the occurrence of non-carbonated patches of mudstone, it can be deduced that the carbonate is secondary and precipitated after the deposition of mudstone. The pale green color of the mudstone may suggest the deposition under subaqueous reducing conditions (Tucker, 2001). The occurrence of carbonate grains, carbonate cement and locally occurring vertical veins of dark claystone, suggest that primarily deposited mudstone underwent distinct diagenetic processes, possibly related with early-stage paedomorphosis. The occurring dessert rose-like structures and desiccation cracks imply high evaporation and (at least local and temporary) disappearance of the water body. Thus the layer could have been exposed for the aerial condition leading to early-stage pedomorphosis. Layer contains numerous bone fragments (part of them assigned to aquatic *Henodus*), fish scales and a hybodont shark spine. The recovered fauna is another indication for sediment deposition in the aquatic environment.
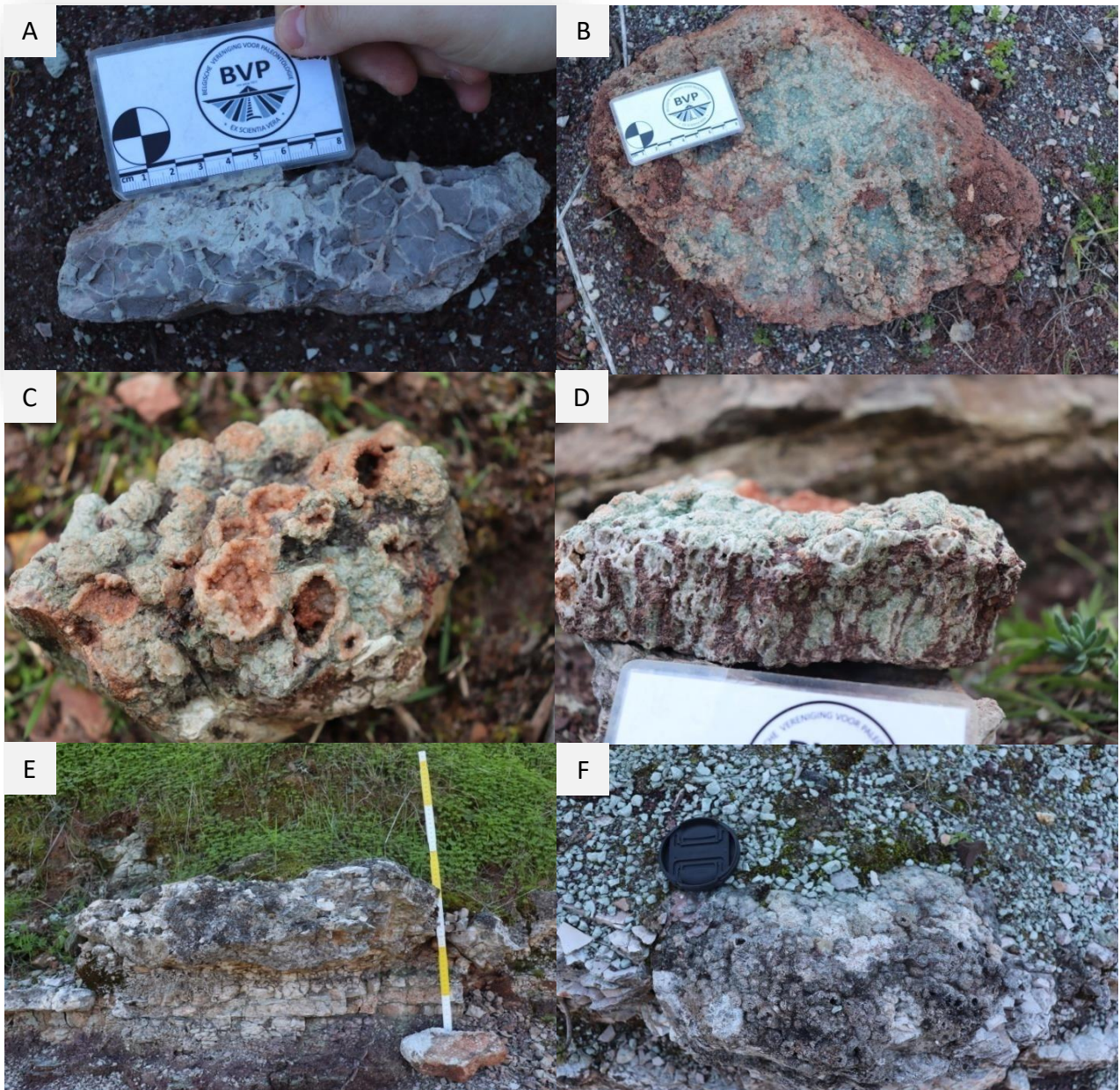
Fig. 19.Photographs of carbonated mudstone and carbonate facies. A. Carbonated mudstone with synersis cracks. B. Carbonated mudstone with desiccation cracks. C. Carbonated mudstone with diplaying geodes with calcite crirstals. D. Carbonated mudstone with vertical structures filled with mudstone. E. Carbonate forming dome-shaped structure resembling a thrombolitic structure. F. Top of the dome-shaped carbonate structure, covered with desert rose gypsum crystals.

4.4. Siltstone-silty sandstone facies.

Siltstones and silty sandstones are exposed in each of the studied sections. Siltstones are usually massive, lacking any evident sedimentological structures. They are usually white,light brown to light grey.

The silty sandstone body is exposed in the central area of the investigated outcrop. Sandy siltstone is white, beige to light brown. Grains are well-sorted and mainly composed of quartz. At top increased content of feldspars. Near the base cross-stratification occurs, closely resembling hummocky-swaley cross-stratification (Fig. 20A) as suggested by the occurrence of: convex upward hummocks, concave swales and extensive low angle curved lamina intersections (Nichols, 2012). Isolated blocks with Flasser bedding (Fig. 20B) plausibly coming from the upper part of the layer were observed. Flasser bedding is composed of light brown to beige siltstones and the wavy parting of black mudstone.

Hummocky-swaley cross-stratifications is a seafloor sedimentological structure built by rounded mounds of sand (Nichols, 2012). Its origin is related to the oscillatory movement of sediment due to the combined action of waves and currents, which usually is related to storms (Nichols, 2012). The occurrence of Hummocky-swaley cross-stratification is thought to be restricted to the offshore zone within the depth range of storm-affected waters, usually ranging from 20 to 50 meters (Nichols, 2012).
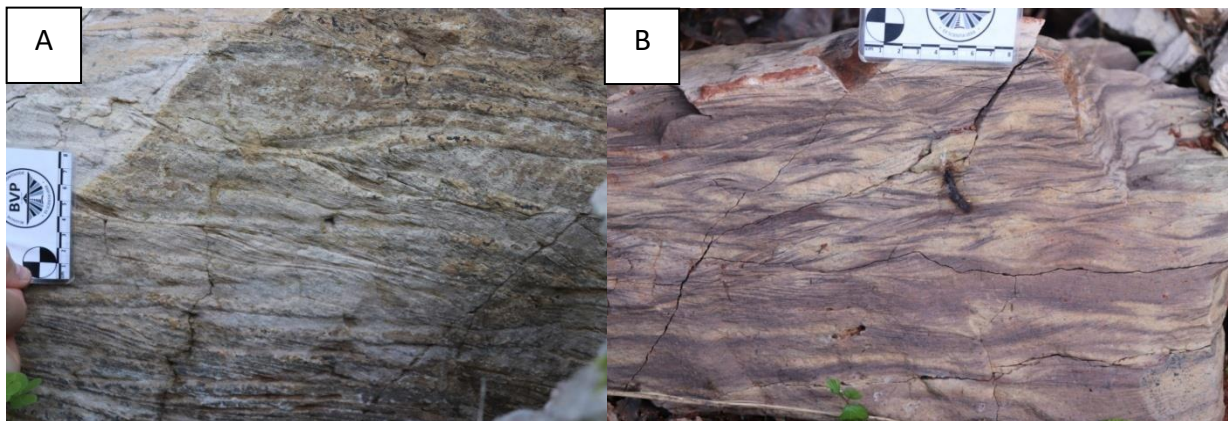
Fig. 20.Photographs of silty sandstone facies A. Silty sandstone with Hummocky-swaley cross-bedding. B. Silty sandstone with Flasser bedding.

4.5 Paleoenvironmental interpretation

The investigated rock sequence containing mixed siliciclastic and carbonate material implies a changing environment with predominant low energy depositional setting. The lowermost outcropping layers, which are exposed near the southern slope of Rocha da Pena, are mainly composed of red blocky mudstone containing numerous *Metoposaurus* remains. The occurrence of red beds, *Metoposaurus* and phytosaur remains are characteristic for many localities identified as floodplain (playa) environment (e.g. Lucas et al., 2010; 2016; Szulc et al., 2015; Chakravorti and Sengupta, 2018). Playa environment can be described as a highly seasonally affected floodplain with periodically forming ephemeral lakes, ponds, and mounds (eg. Nichols, 2012; Szulc et al., 2015).

The lowermost investigated layers within the studied sections are similar to *Metoposaurus*-bearing sediments and are predominantly composed of red to brown mudstones. Those sediments display paedogenetic features (slickenside structures, color mottling, carbonate nodules) implying the deposition in terrestrial floodplain setting under the seasonal and arid climate (Fig. 21). The depositional conditions were therefore overall similar to underlying *Metoposaurus*-bearing beds but likely characterised by conditions of increased water fluctuations within the sediment, as suggested by larger lithological variability and more evident early-stage paedogenetic features. Similar sedimentological features and their transition were observed e.g. in Upper Triassic deposits of Mercia Mudstone Group in England and Chinle formation in USA (Muller et al., 2004; Milroy et al., 2019). In such a scenario, the terrain would be seasonally flooded, resulting in the formation of ephemeral lakes and pounds. The mud would deposit from suspension. During the drier period,water bodies would evaporate exposing the sediments for aerial conditions leading to weathering and formation of early-stage paleosoils. There was probably some variations in those cycles as layers exhibit a various degree of formation of pedogenic features.

The complex of calcareous mudstones, mudstones, siltstones and limestones, suggest large fluctuations of water content and depositional conditions. The complex displays some of the characteristics of a seasonally affected lacustrine environment. It is suggested by the occurrence of multicolored mudstones displaying features related to temporal aerial exposure, which are rhythmically intercalated with carbonated mudstones or carbonates. The various colors of mudstone can indicate the fluctuations of the water table. That could correspond to cyclical flooding, formation of ephemeral lakes or pounds and deposition of the mud from suspension. That would be followed by evaporation of water and formation of carbonate, carbonate cement and evaporites. Such depositional cycles are well recorded in the Upper Triassic geological record, for example in the Germanic Basin (e.g. Bahr et al., 2019). The mudstone-carbonate complex, however, also displays features suggesting marine influence. Lacustrine and shallow lagoon sediments are often hard to distinguish from each other, as they may be deposited under similar depositional conditions, namely low energy deposition

in the restricted environment (Nichols, 2012). This fact impedes the precise and definitive interpretation of the studied sediments. However few features are linking the mudstone-carbonate complex with the marine-influenced environment. The occurrence of *Henodus* remains, may suggest the proximity to the sea, as this taxon is thought to occupy the shallow marine or lagoon environment (eg. Reif and Stein, 1999; Rieppel, 2000). Other known placodonts are exclusively known from marine deposits (Rieppel, 2000; Neenan et al., 2015). The large porosity of calcareous mudstone layers with pores sometimes forming elongated hollow tubes (resembling the fenestral type of porosity), filled with commonly occurring gypsum crystals, evaporitic recrystallizations within the fractures and patches of calcitic cement are thought to often occur in Sabkha-related and intertidal mudflats (Warren, 2006; Nichols, 2012). The occurrence of possibly microbialitic structures would also comply with coastal Sabkha or lagoon interpretations, as they are noted to preferably occur in hypersaline and coastal environments characterised by an arid climate (Dupraz et al., 2011). However microbialitic structures are also known from saline and even freshwater lakes formed in a continental setting (Dupraz et al., 2016) and thus give no definitive indication of a specific environment. Based on those characteristics, the definitive assessment of the depositional environment of the mudstone-carbonate complex is impeded. However few interpretations might be considered: an arid floodplain with ephemeral lakes, coastal Sabkha-like plain with ephermal brackish/saline lakes or coastal area of a shallow lagoon. Based on the previously mentioned characteristics, I consider the coastal mudflat and lagoon interpretations as the most plausible. Regardless of the detailed interpretation, the mudstone-carbonate complex is construed as a proximal deposit of a restricted standing water body, subjected to temporal evaporations or withdrawals coupled with subaerial or aerial exposure leading to the development of early paleosoils features.

The complex composed of mudstone and laminated siltstones was deposited in the low energy depositional setting. The gathered evidence is not conclusive for one specific interpretation, however, few scenarios could be suggested. Mudstones and laminated strata are known to be deposited mainly in the restricted environment in both marine and terrestrial settings, but they may also occure in tide influenced environment (Talbot and Allen, 1996). The intercalations of mudstones with laminated siltstones may suggest the rhythmical shifts in the depositional environment, possibly related to the depth of the water body. As the underlying layers are interpreted as possibly marginal deposits related to coastal plain or shallow lagoon, it is likely that the mudstone-laminated siltstone complex may represent a tidal mudflat environment. However, the lacustrine origin of those deposits can not be completely dismissed.

Features displayed by the sandy siltstone layer also provide inconclusive shreds of evidence for its origin. However few observations may stand for the interpretation of marine deposition. A silty sandstone body is characterised by the occurrence of HCS and SCS, which are thought to mainly form in a shallow marine environment and are often considered as its indicator (e.g Tucker, 2001; Nichols,

2012). However, it should be taken into account that there are also rare records of HCS in proximal lacustrine deposits (eg. Basilici, 1997). The large thickness of over 7 meters of the layer also more strongly implies the marine deposition rather than the lacustrine related sedimentation. In the case of lacustrine deposits, over a few meters thick sandstone layers not intercalated by lamina or layers of different lithology are considered to be quite rare (Zieliński, 2007). According to the marine interpretation of those deposits, they would represent a transgressive episode. Deltaic deposition can be also considered due to the type of sediments and grain maturity. However, in the investigated section none of the characteristic features of delta, related to its progradational character, have not been noticed. Due to those observations, I consider the shallow marine deposition of the sandy siltstone layer, as the most coherent with the gathered data. Nevertheless, this interpretation requires further investigation.

The preceding geological studies of Gres de Silves formation implied the coastal plain (Palain, 1976) or shallow marine and/or coastal lagoon (Azerêdo et al., 2003) environments for AB 2 unit. However, those interpretations were based on macro-scale geological studies lacking layer-scale interpretations. Nevertheless, as the studied deposits are attributed to the upper part of the AB2 unit, the suggested paleoenvironment assessments are consistent with interpretations presented in those works.

Some of the more detailed paleogeographic reconstructions provided for the Iberian area during the Late Triassic depict the Algarve Basin as located in proximity to the eastern branch of the Neotethys formed in the Maghrebian-Gibraltar rift (Pereira et al., 2016; Orti et al., 2017). Therefore, the provided interpretation of part of the Rocha da Pena rock section as a marginal environment with marine influence concurs with the paleogeographic setting.

According to those reconstructions, the Algarve area would be located at low latitude ca. 20° N, within the tropic zone. During the Late Triassic, the area of the Laurasian southern margin is thought to be characterised by an overall quite arid and largely seasonally affected monsoonal climate. Such climatic conditions are well represented in the studied deposits of Rocha da Pena. The high aridity and seasonality of the climate during the Late Triassic in the area of Algarve Basin can be inferred on the basis of:the prevailing red color of mudstones suggesting oxidizing conditions, common paedogentic features, abundant evaporites, rhythmical deposition of mudstones and carbonated layers.

A — Playa environment. Arid, seasonal climat

Ephemeral playa lake
Floodplain mudlfalt
Unit AB 2
Unit AB 1
Paedogenetic processes
Water table fluctualtions
Paedogenetic processes
River channels
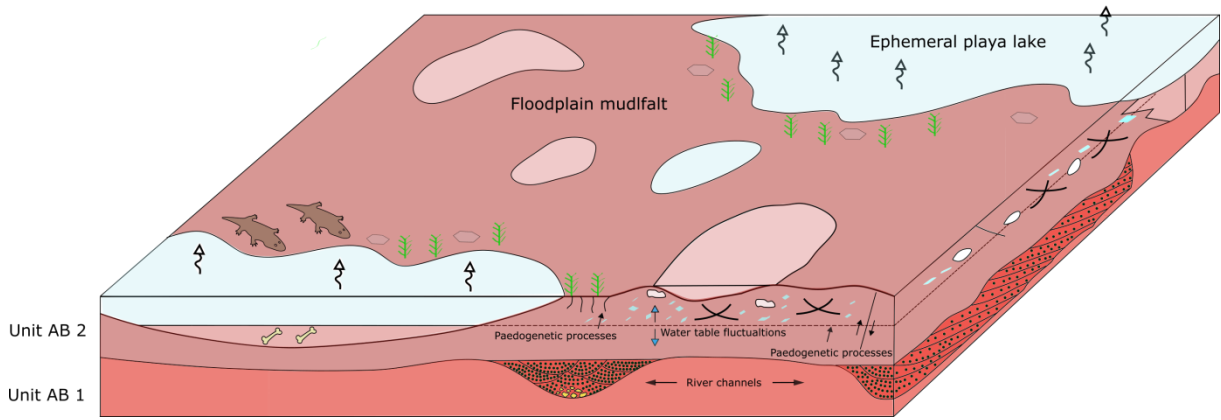
B — Marginal environment - Mudflat/shallow lagoon. Arid, seasonal climat

Formation of evaporites and carbonates
Muddy barrier
Mudflat/Sabkha
Lagoon
Shallow sea
Tidal/seasonal changes
Muddy barrier
Unit AB 2
Unit AB 1
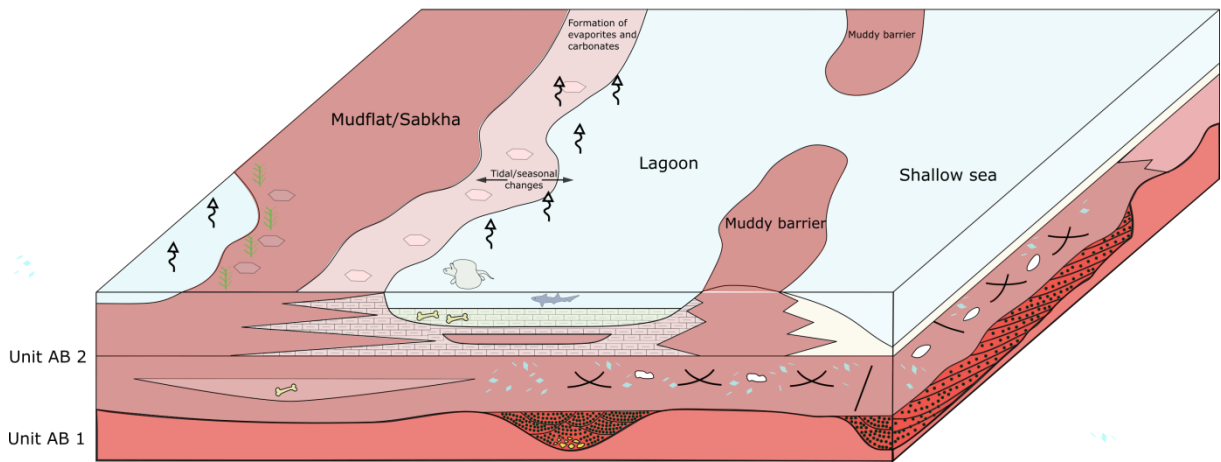
C   Coastal/shallow marine environment.

Legend

Fig. 21.Schematic environmental reconstruction of the Upper Triassic of Algarve showing changes in depositional settings. (A) Playa environment (B) Coastal./lagoon environment (C) Shallow sea environment.

5. Systematic Paleontology

SAUROPTERYGIA Owen, 1860

PLACODONTIFORMES Neenan et al., 2013

PLACODONTIA Cope, 1871

CYAMODONTOIDEA Nopcsa, 1923

CYAMODONTIDA Nopcsa, 1923

HENODONTIDAE Huene, 1936

HENODUS sp. Huene, 1936

Etymology: *Henodus* – in Latin ''single tooth''

Horizon and age: Grés de Silves Formation, AB2 unit, Layer 9; Upper Triassic; Carnian to Norian

Locality: Rocha da Pena, Algarve, southern Portugal

Material: nearly complete skull, possibly up to eight osteoderms

5.1 ML. A9182 - skull description

ML. A9182 is a partial skull, lacking the posterior and part of the lateral area including the occipital region, a large part of squamosals and parietal. Originally the skull was embedded within the carbonated mudstone block and associated with the osteoderm. It exhibits a rather poor state of preservation resulting from the taphonomic alterations. It is broad, dorsoventrally flattened and measures 10.3 cm of length anteroposteriorly. It is the widest at the anterior margin of the skull, reaching a width of 8.1cm, and narrows posteriorly until it reaches the narrowest point of 4,8 cm of width, at the midpoint of the preserved cranium. Posterior to the midpoint of the skull, the posterior half broadens, resulting in an hourglass-like shape in ventral view. However, much of the skull table is highly taphonomically affected, especially its anterior half. The distortion is evident by the numerous cracks and fragmented nature of the preserved cranial elements, several of which are displaced. The long, few millimeters thick crack extends obliquely throughout the whole skull, from the left anterolateral margin of the maxilla up till the narrowest area of the cranium. The area extending anterolaterally from the margin of the crack is characterized by a larger degree of bone fragmentation and distortion than the posterior part, which includes almost complete bones exposing original or only slightly changed morphology. These conditions hamper the precise identification of most of the bone borders within the skull table and margins of the orbits. In lateral view, the dorsal margin of the preserved skull is irregular but overall convex. The exposed posterior half of the skull table presents a shallow dorsal extension, with the posterior margin being subtly inclined anterodorsally, and then abruptly dipping anteroventrally. This upraised portion of the skull table constitutes the highest point

of the cranium (2,5 cm). Most of the ventral surface of the skull is sub-horizontal, only with the lateral process being inclined ventrolaterally.

The anterior-most part of the preserved skull is composed of paired **maxillae** which constitute the anterolateral and anterior margins of the preserved cranium. The **premaxillae** are lacking, which originally would have extended anteriorly to the **maxillae**. The premaxillae probably slightly terminated posteriorly and were incising between the maxillae in the medial area of cranium, possibly contacting medial borders of maxillae and anterior margin of vomers. **The left maxilla** is complete, whereas the right one lacks a large part of its posteroventral portion. In dorsal view the left maxilla expands only on the anterior part of the skull, being posteriorly and medially constricted by the jugal at the level of the anterior margin of the orbit. Beneath the contact with jugal, the maxilla terminates ventromedially and form the lateral margin of the ventral side of the rostrum, expanding longitudinally till the narrowest point of the skull. In the ventral view, the maxilla is distinctly curved laterally, resulting in the concave character of the lateral margins of the rostrum. In ventral view, the maxilla is J-shaped, being laterally curved, narrow in the posterior part, slightly broadening anteriorly and significantly expanding transversely in its anterior part at the level of internal nares. The medial portion of the anterior part of the maxilla extends medially, where it contacts the middle part of the lateral border of internal nares. At the right cranium margin, a similar condition is not visible due to the bone breakage and covering sediment. Close to the right lateral margin of the bone, curved, having a half-moon shape, deep and wide U-shaped in cross-section, groove stretches throughout the almost whole length of the maxilla, slightly broadening posteriorly. It is laterally and medially constricted by ridges extending parallel in regard to the groove. The lateral ridge is slightly more pronounced than the medial one, and dorsally terminates with a smooth, rounded surface. At the left maxilla, only the anterior part of the groove is preserved. This groove differs from the one located at the right maxilla by being more constricted and straight. Medially and in the area of anterior medial termination also distally, maxillae are confined by palatines.

The **vomers** extend at the anteriormost area of the medial part of the cranium. The anterior and anterolateral margins define the medial and posterior borders of the internal nares. There is a short irregular incision at the anterior margin of the vomers, probably resulting from the lack of not preserved part of the premaxillae, which probably would have contacted the vomer in this region. The central area of the vomers is slightly depressed. At the level of the posterior internal nares' margins, the vomer expands laterally slightly beyond the level of the lateral margin of internal nares, where they contact the anteromedial border of palatines. Posteriorly, the left lateral side of the vomer contacts the palatine, which originally probably had been covered by the pterygoid. In the medial and right lateral area the vomer contacts the anterior margin of pterygoids.

Paired **palatines** stretching longitudinally near the later margins of the skull are separated by vomers in their anteriormost portion and pterygoids in their middle and posterior parts. The right palatine is almost completely preserved, whereas the left one lacks a big posterior portion. The

preserved parts of palatines have an overall rectangular outline being also slightly laterally curved. They stretch in parallel in regard to maxillae. The anterior margin contacts the posterolateral margin of the internal nares and posterolateral margin of vomers. At the lateral margins, palatines contact maxillae and are separated from them by the subtle rounded ridge. Palatines' posterior-medial borders are confined by the vomer and in their posterior more part by pterygoids, which originally probably contacted the posterior margins of palatines. The posteriormost part of the right palatine at the level of the most narrow area of the skull includes an oval carbonate geode, most probably created during the diagenesis. In *H. chelyops* small oval teeth were located (one per each of the palatines) in a similar position, which is at the level of the posterior maxilla's margin and the most narrow area of the skull. Therefore it is possible that the mentioned geode resulted from the crystal infilling of alveoli after the detached tooth. In the case of the right palatine, this area is badly preserved. The palatines' surface is irregularly covered with small, millimeter-sized, shallow irregular polyhedral pits.

Pterygoids are quite poorly preserved, with only small isolated fragments preserved hampering any detailed description. The preserved fragments of pterygoids are irregular and dispersed within the central area of the cranium. Small elongated pterygoid fragments terminate anteriorly covering parts of distal extensions of vomers. Based on the preserved elements it can be deduced that pterygoids covered the medial section of the middle and posterior parts of the ventral side of the skull, anteriorly contacting vomers, and laterally palatines.

The lateral margin of the skull is defined by a complex of bones, most probably including **maxilla, jugal, squamosal, quadratojugal and quadrate**, which are preserved only at the right margin of the skull (with exception of the maxilla which is also preserved at the left margin). However, the interpretation of bone extensions and sutures is highly impeded due to bone preservation and multiple cracks. Nevertheless, few general features can be noticed. All of these bones form a uniform element extending almost up till the posterior margin of the preserved part of the skull. This element is broad but slender, dorsoventrally flattened and slightly ventrally inclined. In the posterior part, the triangular-shaped process terminates ventrolaterally, reaching the right maxilla's maximum lateral extension. The medial margin within the anterior part of the bone complex constitutes the lateral margin of the orbit. The medial margin within the area of the ventrolateral process constitutes the lateral margin of an opening which possibly could be a temporal fenestra or its vestigial remnant.

Most of the skull table is substantially cracked and some of its parts are displaced. However few incomplete elements can be identified. The posterior area of the skull is upraised and slightly dorsally inclined. It is presumably composed of **fragmented parietal and squamosal**. The preserved area has a rectangular outline with posterolateral termination of the part of the squamosal. The preserved part of the **parieta**l is broad and has an irregular outline. At the level of the anterior margin, the preserved fragment of the parietal is the narrowest. Posteriorly parietal broadens and extend posteriorly with undulated but overall straight lateral margins. The parietal expands laterally at its distal area, approximately at the level of the posterior margin of the opening. which is only visible

at the preserved left margin of the bone. The parietal constitute most of the posterior margin of the preserved part of the skull. To the left lateral margin of the distal part of the parietal, a fragment of a squamosal extends, but at the more ventrally oriented plain in regard to parietal. Anteriorly, the parietal fragment contacts the area of highly fragmented bones, which possibly constituted parts of **the postorbital, postfrontal and frontal**. At the level of the anterior margin of that area the preserved part of the skull table abruptly inclines ventrally. It includes a fragment of the possibly posterior part of the paired **frontal.** The fragment is longer than wide and narrows anteriorly. Anteriorly and laterally the fragments of the frontals contact the area covered with highly fragmented bones. The surface covered with those bones diverges almost at the level of the anterolateral margin of the orbit, giving the Y-like shape to this association of bone fragments. This bone association extends anteriorly till it contacts maxillae and premaxillae, near the anterior margin of the skull. Based on the observations of the specimen it is impossible to assess with any appropriate dose of certainty which bones are included in this accumulation. However, while comparing the specimen to *H. chelyops*, it can be assumed that the area extending throughout the right margin was probably composed of the maxilla (at the anterior portion) and jugal (at posterior part). More medial and the anterior area can be possibly covered by fragments of the postorbital, frontal and prefrontal. At the anteromedial area of the skull, a fragment of the **vomer** is exposed. It is rectangular, with slightly irregular but mostly straight margins. Its medial part is cut by a longitudinally extending shallow furrow.

ML. A9182 – associated osteoderm description

Nearly complete hexagonal osteoderm with maximal width of 2,2 cm. The osteoderm edges are damaged and cracked. The surface of the osteoderm is flat and smooth lacking any ornamentation.
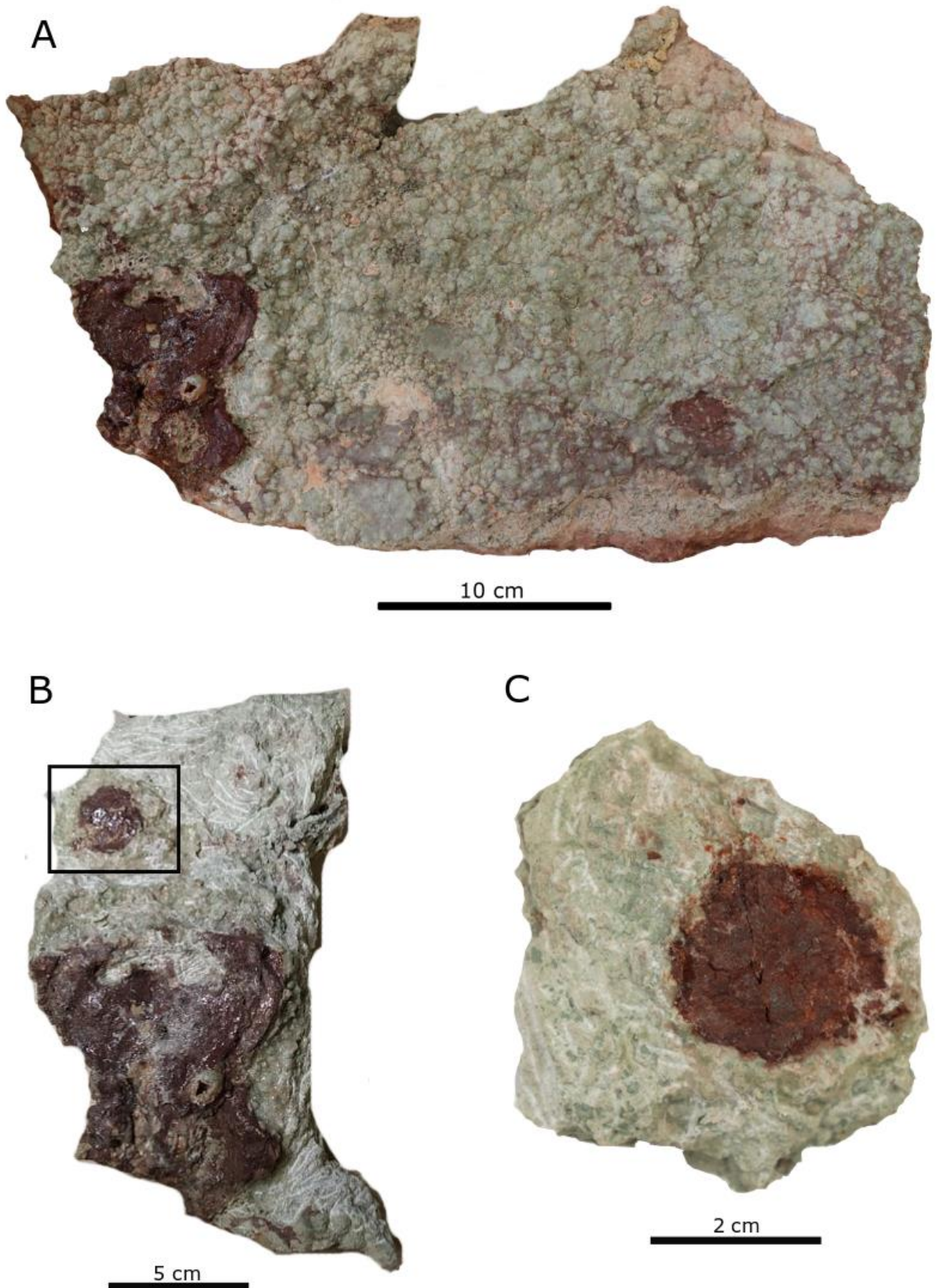
Fig. 22. Skull ML. A9182 – *Henodus sp*., embedded in carbonated mudstone block from Rocha da Pena . A. Carbonated block with ML. A9182 in ventral view. B. The carbonated block after the early preparation and uncovered associated osteoderm marked in the rectangle. C. An osteoderm associated with the ML. A9182 skull.
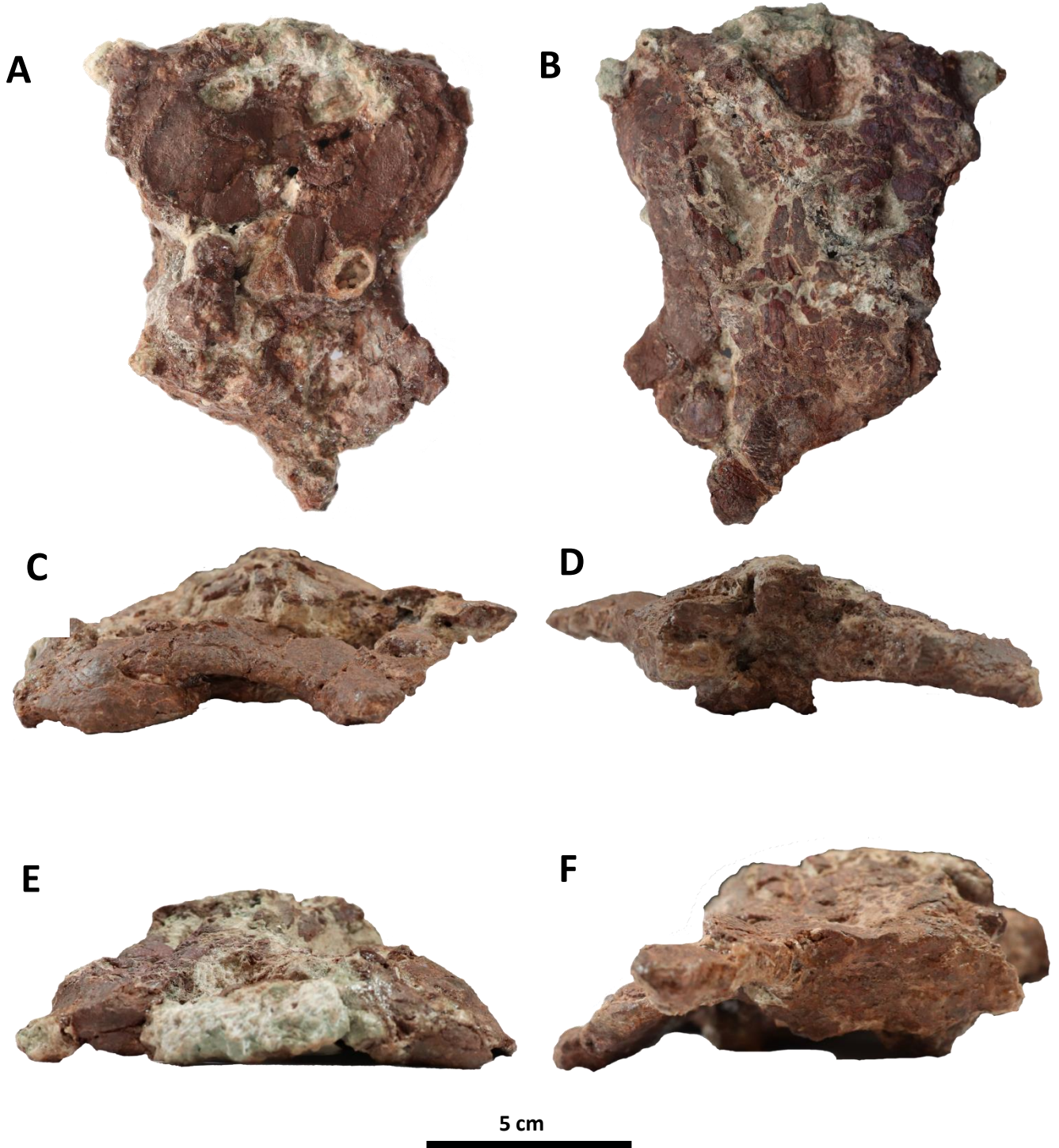
Fig. 23.Skull ML. A9182. – *Henodus sp.* from Rocha da Pena. A. Ventral view. B. Dorsal view. C. Left lateral view. D. Right lateral view, E. Frontal view. F. Cranial view.

Fig. 24.Skull ML. A9182 – *Henodus sp*. from Rocha da Pena in ventral view.
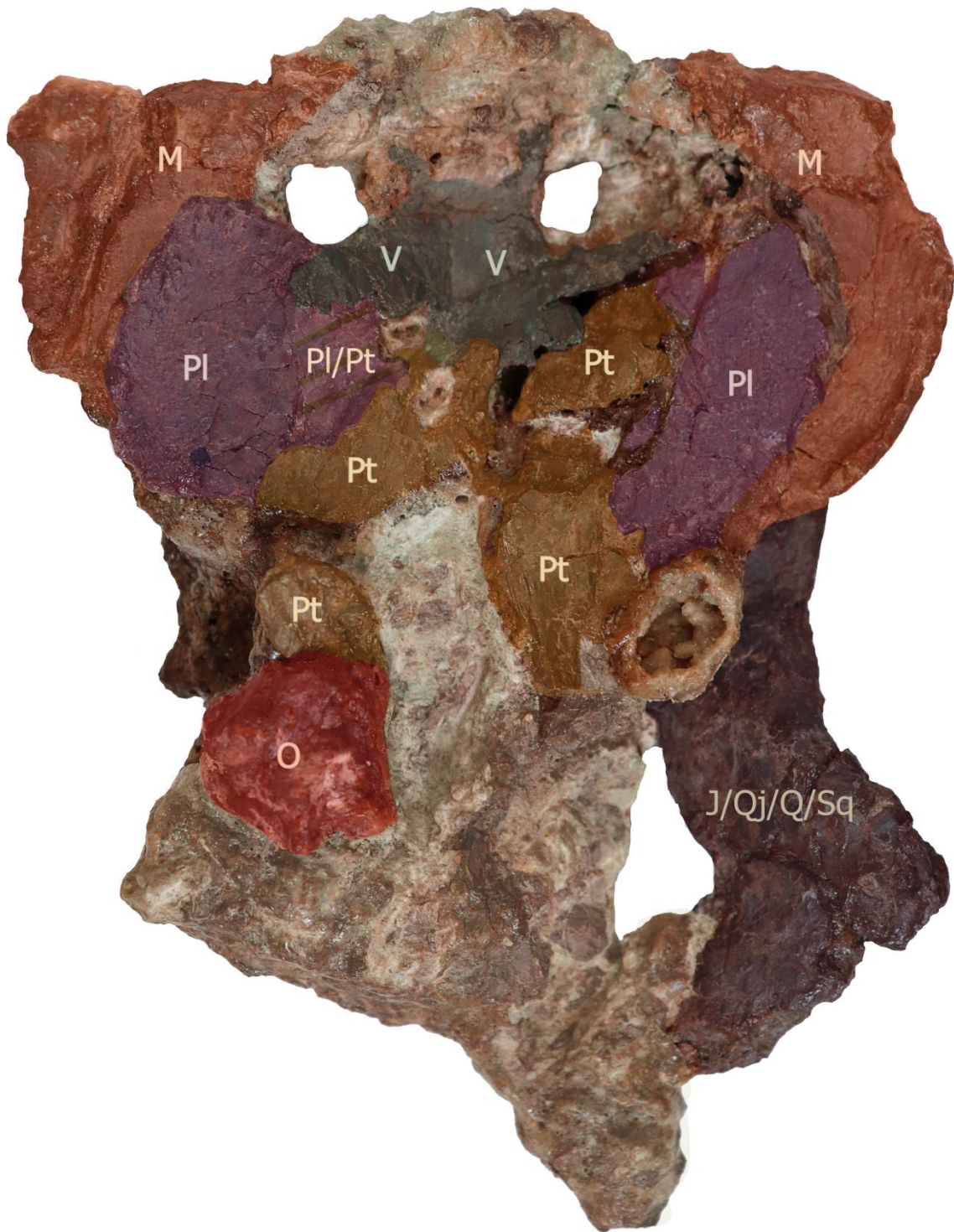
Fig. 25. Interpretation of bones in the ventral side of the Skull ML. A9182 – *Henodus sp*. from Rocha da Pena. Bones are indicated by colors. Abbreviations: J - juga; M- maxilla; Pl- palatine; Pt - pterygoid; O – occipital; Q - quadrate; Qj – quadratojugal; Sq- squamosal V-vomer.
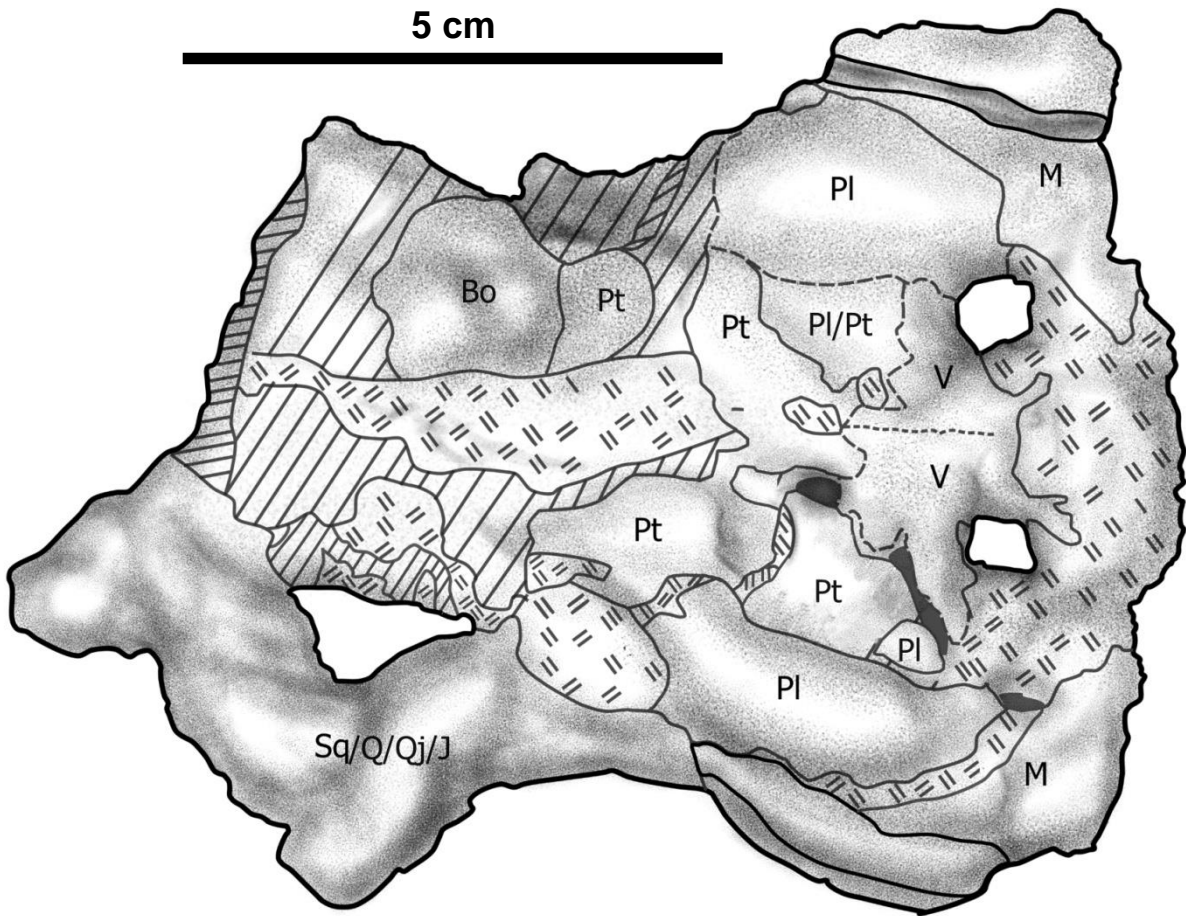
Fig. 26. Skull ML. A9182 – *Henodus sp* . from Rocha da Pena in ventral view and schematic interpretation of the skull. Abbreviations: Abbreviations: M- maxilla; Pl- palatine; Pt - pterygoid; Sq-squamosal; Bo – bassioccipital; V-vomer.

5 cm

Fig. 27. Skull ML. A9182 – *Henodus sp* . from Rocha da Pena in dorsal view.
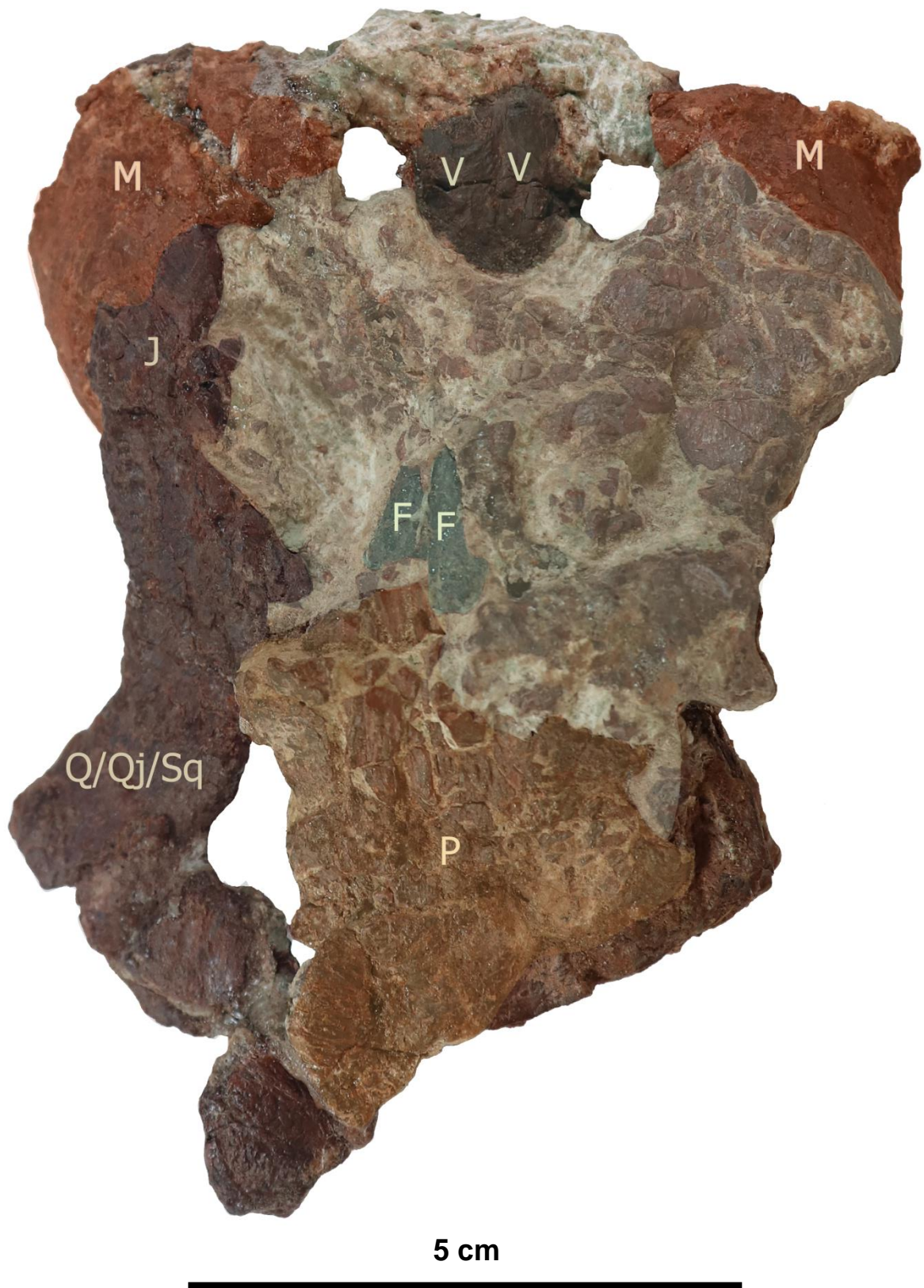
Fig. 28. Interpretation of bones in the dorsal side of the Skull ML. A9182 – *Henodus sp*. from Rocha da Pena. Bones indicated by colours. Abbreviations: F-frontal; J – jugal; M- maxilla; P - parietal; Q - quadrate; Qj – quadratojugal; Sq-squamosal; V-vomer.
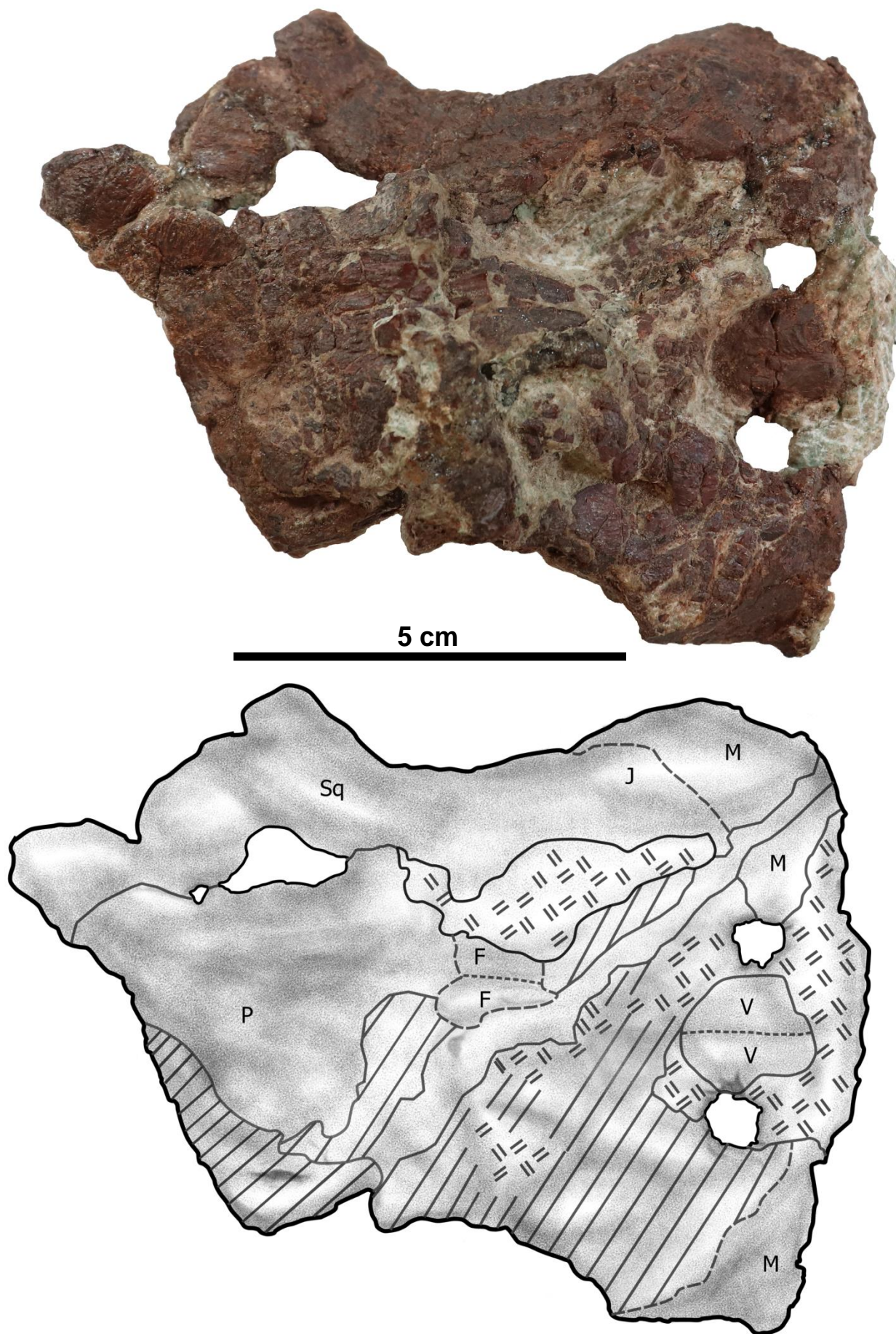
Fig. 29. Skull ML. A9182 – *Henodus sp* . from Rocha da Pena in dorsal view and schematic interpretation of the skull. Abbreviations: F-frontal; J – jugal; M- maxilla; P - parietal; Sq-squamosal;V-vomer.

ML. A9182   *H. chelypos*
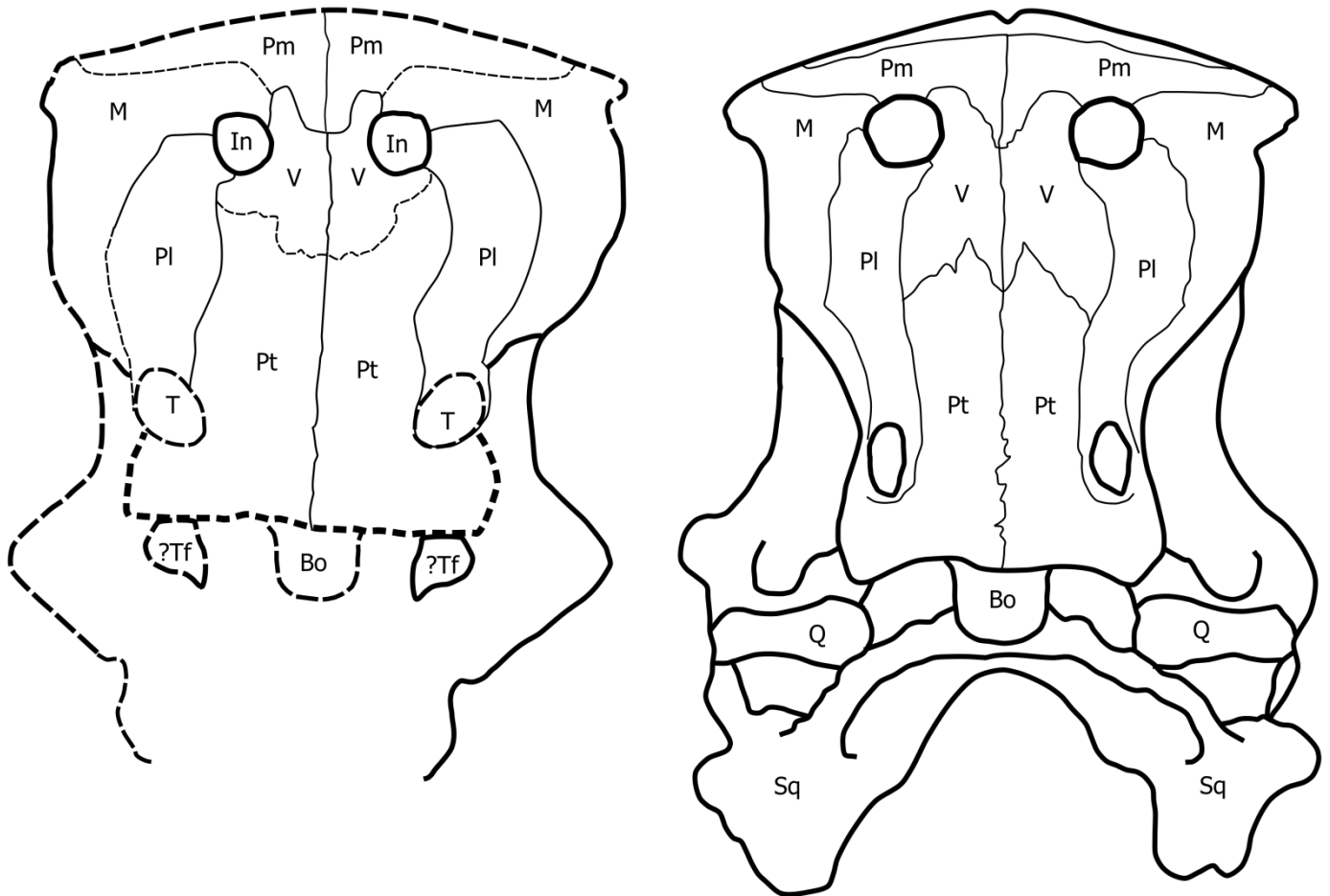
Fig. 30. Drawing interpretation of the skulls of the ML. A9182 and *Henodus chelyop* in ventral views. Continous line indicates unambiguous bone extensions. The dashed line indicates the hypothetical bone extensions. Dorsal view not included due to large uncertainty of skull table morphology of the ML. A9182 . *Henodus chelyops* drawing modified from de Miguel Chaves et al., 2018. Abbreviations: Bo – basioccipital In – internal nare; J - jugal; M- maxilla; Pm – premaxilla; Pl - palatine; Pt - pterygoid; T – temporal fenestrae; Q - quadrate; Sq- squamosal; V-vomer.

5.2 Phylogenetic results

Phylogenetic analysis after the matrix of Neenan et al. (2015) and modifications of de Miguel Chaves et al. (2018) with the ML. A9182 resulted in five most parsimonious trees, with a length of 135 steps (CI = 0.570; RI = 0.663; RC = 0.378). The topology of the consensus tree is consistent with results obtained by Neenan et al. (2015) and de Miguel Chaves et al. (2018).

The ML. A9182 is placed within Cyamodontida (Fig 31). However, any of the synapomorphies defining Cyamodontida (parietals with a distinct anterolateral process embraced by the postfrontal and the frontal (ch. 12; state 1); posterolateral margin of the postfrontals deeply concave and angulated (ch. 15; state 1); and posteroventral tubercle present at the distal tip of the paroccipital process (ch 48; state 1) is not possible to ascertain in ML. A9182. According to the performed analysis, ML. A9182 is part of Henodontidae and placed as the sister taxon of *Henodus chelyops* and *Parahenodus atancensis*. After the application of bootstrap the topology of Henodontidae changes, resulting in breakage of polytomy and placement of *P. atancensis outside* of *H.chelyop.* and ML. A9182. This separation is supported by low bootstrap (2), thus it is not considered in this work. The Henodontidae comprises the following synapomorphies: the absence of maxillary teeth but the presence of a longitudinal maxillary furrow (ch 35; state 4); one pair of palatine teeth (ch. 36; state 3); palatines at least partially separated by long pterygoids (ch. 60; state 0). De Miguel Chaves et al. (2018) also listed the presence of a contact between the jugals and the squamosals (ch. 56; state 1) among Henodontidae synapomorphies. However, according to the matrix of Neenan et al. (2015) (the same one was used by de Miguel Chaves et al. (2018)), this feature is also present in other placodont taxa in various clades within which the feature is not shared by all its representatives. Therefore the presence of a contact between the jugals and the squamosals should be considered as homoplasy and not as a synapomorphy.

Specimen ML. A9182 displays two of the Henodontidae synapomorphies: palatines at least partially separated by long pterygoids (ch. 60; state 0); absence of maxillary teeth but the presence of a longitudinal maxillary furrow (ch 35; state 4). One pair of palatine teeth (ch. 36; state 3) can not be assessed in the ML. A9182 with certainty. However, this feature might have been also present as the carbonate geode could be a recrystallized alveoli. All of the scored feature states in the phylogenetic analyses are consistent with conditions stated for *H. chelyops*.

The placement ML. A9182 within Henodontidae is supported by relatively high bootstrap (comparing to the majority of results for most of the placodont clades) which is 55. The obtained topology and position of ML. A9182 as a sister taxon to *Henodus* may support the identification of ML. A9182 as *Henodus*. However, these results should be treated with large caution as only 7 of the total 63 characters were possible to be scored. Therefore it is not excluded that the obtained results may be impacted by the substantial incompleteness of the feature scoring.

Fig. 31.Strict consensus tree obtained based on the cranial data matrix of Neenan et al. (2015) and modifications of de Miguel Chaves et al. (2018). Position of the Late Triassic skull from Algarve indicted as MLA. 9182 in bold. Bootstrap (top) and Bremer support values (bottom) are indicated.

5.3 Discussion - identification

SpecimenML. A9182 is identified as a placodont skull. The square-shaped and significantly dorsoventrally flattened skull is a rather rare feature within sauropsid taxa. Only few Triassic taxa with such a morphology were recovered including*Atopodentatus unicus* (Chun et al.,2016) and *Henodus chelyops* (von Huene, 1936). ML. A9182 displays a very strong resemblance to the cyamodontoid placodont *Henodus chelyops*.

The ML. A9182 shares with *H.chelyops*a number of feature including: (1) flat and broad skull, (2) hour-glass like the shape of the skull in dorsoventral view, (3) toothless maxillae (4) substituted by deep, longitudinally extending curved groove, (5) non-contacting elongated palatines separated by pterygoids and vomer, (6) short, broad and spatulate rostrum, (7) the elongated, slightly ventrally inclined slender later margin of the cranium with the terminating triangular process at the level of the central area of parietal. Due to the poor preservation of the roof table of ML. A9182, which in *Henodus* contains two autapomorphies (upper temporal fenestra vestigial or absent; parietal broad and fan-shaped), these conditions can not be assessed with certainty. In the ML. A9182 The preserved part of the parietal is broad and broadens posteriorly, resembling the condition of a fan-shaped parietal occurring in *Henodus*. The great number of shared features between ML. A9182 and *H. chelyops*, which altogether constitute the unique set of features among Triassic taxa, substantiate the assignation of ML. A9182 as a specimen to *Henodus*.

ML. A9182 displays few differences from the *H. chelyops.* However, it needs to be taken into account that taphonomic alterations could have lead to modification of the original state of some of those features. The ventral surface of ML. A9182 is flat with most of the bones extending at a similar horizontal level, whereas the skull of *H. chelyops* is dorsally curved. Taking into account the distinctly crushed skull table of the ML. A9182, it is possible that the skull has been compacted and its curvature could have been reduced. The ventrolateral margin of the orbit in ML. A9182 is elongated and extends in a horizontal plane comparing to the sub-circular orbit in *H. chelyops,* which is steeply inclined. The crashed skull table may suggest the original orbit morphology got possibly altered with compaction reducing the orbit inclination. However, albeit partially cracked, the preserved lateral margin of the orbit does not exhibit any signs of significant deformation inferring rather the original or only slightly altered condition of this morphology. Another difference distinguishing ML. A9182 from *H. chelyops* is the broader rostrum with more rounded margins, resulting in the more robust appearance of the anterior portion of the skull compared to *H. chelyops.* In *H. chelyops* the rostrum margins are rather constricted and straight conversely to convex margins in the ML. A9182. Comparing to *H. chelyops,* the middle part of the longitudinal extension of the maxilla in ML. A9182 has a much wider lateral extension and terminates laterally up till the maximal lateral extension of the lateral process. In *H. chelyops* the respective area of the maxilla laterally reaches only the base of the lateral process, while

the level of the maximum lateral extension of the process is reached by the anteriormost later part of the maxilla. Contrasting to *H. chelyops,* ML. A9182 possesses a relatively large opening extending medially to the lateral process, which does not occur in *H. chelyops*. The position and morphology of the opening indicate it could possibly represent the temporal fenestra. The relatively well-preserved smooth medial margin of the process does not exhibit any significant cracked surfaces implying the opening is part of an original morphology and not the result of a taphonomic alternation, at least within a close area to the process margin. However, it is not clear whether this opening remained originally uncovered and indeed represented the open temporal fenestra or if it was covered by parietal or other skull table bones, which are incompletely preserved in the ML. A9182. In *H. chelyops* the parietal covers this area directly contacting the medial margin of the process and completely covering the upper temporal fenestra or leaving the small vestigial opening (Rieppel, 2001). However, the skull of specimen III of *H. chelypos* possesses openings in the area respective to temporal fenestra (Huene, 1938) and the opening seen in the Ml. A9182. Nevertheless, Rieppel (2001) argued that those openings are the results of taphonomic alternations and not an original morphology as indicated by irregular contours and different sizes of the opening at both sides of the skull. Moreover, the depression of parietal within the respective area to the opening is seen in both the ML. A9182 and specimen III of *H. chelyops* occur at three skulls skull of *H. chelyops* (specimens II, IV, VI). That may suggest that this area of the skull table was more prone to taphonomic alternations and destruction. Rieppel (2001) suggested that it might be the result of the reduced ossification of the parietal at its lateral margins. Another difference between the ML. A9182 and *H. chelyops* concern the morphology of the vomer. In *H. chelyops* the lateral margin of vomer contacts laterally the medial borders of palatine and internal nare, whereas in ML. A9182 the preserved part of the vomer extends laterally almost up till the lateral margin of an internal nare. In ML. A9182 the better preserved left anterior fragment of palatine contact only the posterolateral margin of an internal nare, whereas in *H. chelyops* anterior part of palatine participates in the whole extension of a posterior margin of an internal nare. However, it should be noted that this part of ML. A9182 skull got significantly taphonomically affected, with fragments of bones missing or being deformed. In ML. A9182 maxillae expand anteriorly significantly beyond the level of the anterior margin of internal nares. In *H.chelyops* the maxillae anterior margin is only slightly beyond the level of anterior margin of internal nares. This area however is still in large part covered by sediment and together with the lack of premaxillae, the precise assessment of this feature is hindered.

Based on the presented comparison it is problematic to assess with certainty whether the ML. A9182 represents the *H. chelyops* or possibly a closely related new taxon. Despite many general similarities, the ML. A9182 shows few differences. Concerning the orbit morphology and occurrence of the fenestra, it is highly uncertain if they may constitute autapomorphies or are the result of taphonomic alternations and/or incomplete preservation. The occurrence of the open temporal fossa

would strongly suggest the taxonomic distinctiveness. As a basal Henodontid, *Parahenodus* had an open temporal fenestra, although reduced in size compared to other cyamondontid placodonts, the occurrence of such a feature in the ML. A9182 would not be surprising. It could indicate the transitional state of this feature between *Parahenodus,* with still preserved elongated rostrum and open temporal fenestrae, and *Henodus,* with rectangular cranium morphology and lacking or having vestigial temporal fenestrae. However, because in *H. chelyop* this area of the skull table was probably more prone to alternations (Rieppel, 2001), I consider the original occurrence of an open upper temporal fenestra in the ML. A9182 as unlikely. Nevertheless, the smooth surface of the bone at the lateral margin of the opening may indicate the occurrence of a reduced opening, as seen in the specimen II of *H. chelyops.*The more robust and wide rostrum morphology of ML. A9182, which is not significantly impacted by taphonomy provides another distinction from German material. However intraspecific variation should also be considered. The significant intraspecific cranial geometry variability was noted in some species. It depends mainly on the ontogenetic stage but also polymorphism features including sexual dimorphism and geographical distribution. The large snout shape variability within sauropsids was observed for example in Testudine turtles *Trionyx ferox* (Dalrymple, 1977) and *Trachemys dorbigni* (Portela et al., 2020) and eusuchian *Allodaposuchus precedens* (Martin et al., 2016). Therefore the observed difference in snout shape morphology between the ML. A9182 and *H.chelyops* should be treated with caution while considering it as an autapomorphy. The vomer and different spatial relations of palatine with vomer and internal nare may stand for taxonomic distinctiveness of the ML. A9182. However, the taphonomic alternations hinder the usage of this feature discrepancy for a precise novel taxon separation.

The large distance between the area of modern southern Portugal and southern Germany during the Late Triassic and location in two different domains namely Western Tethys and Germanic Basin respectively, may help to explain the difference of morphology between the placodont material from those places, either considering it as an intra or interspecific variation. The geographic separation could have possibly lead to speciation and emergence of a new Henodontid genus or a new species of *Henodus* in the western margin of Laurasia.

Concluding, the definitive taxonomic identification can not be performed but three scenarios can be suggested, depending on the interpretation of the conditions of morphological preservation of the ML. A9182 features:

1) The ML. A9182 represents a new Henodontid taxon, possibly a new genus constituting the transitional form between *P. atancensis* and *H.chelyops*.
2) The ML. A9182 represents a new species of *Henodus*.
3) The ML. A9182 represents *H. chelyops* but displays modified conditions of few features implying a larger degree of intraspecific variation of *H. chelyops*.

Due to the prevailing number of similarities to the *H. chelyops* and large uncertainty of assessment of the most distinctive features presented by the ML. A9182, the ML. A9182 is tentatively considered as *Henodus* sp.

5.4 Discussion - chronological, paleobiogeographic and paleoenvironmental implications

The fact that the ML. A9182 is coeval to *H. chelyops* remains unknown as the Rocha da Pena locality lacks precise dating. Based on the occurrence of *Metoposaurus* the age of the site is presumed to range between Carnian - middle Norian, which is consistent with the age of *H.chelyops* which was recovered from Lower Carnian deposits. Therefore specimens recovered in Rocha de Pena can be of a similar age to the *H. chelyops* from Germany (early Carnian) or the stratigraphic range of *Henodus* was wider and extended till the younger age (possibly up to middle Norian).

Together with the isolated postcranial material from Rocha da Pena and São Bartolomeu de Messines (previously also described in an unpublished thesis by Hugo Campos), ML. A9182 constitutes only the second recorded occurrence of *Henodus,* which so far has been exclusively known from Goldersbach near Tübingen-Lustnau situated in southwestern Germany. These finds extend the paleogeographic range of that genus outside of the Germanic Basin and enlarge it up till the western margin of Laurasia (Fig 32). Nevertheless, the occurrence of *Henodus* in the Iberian Peninsula is not that surprising owing to the occurrence of another henodontid placodont *P. atancensis,* discovered in presumably shallow marine Carnian to Norian deposits of central Spain. As the record of Henodontidae is extremely scarce and the precise age of their remains is uncertain, it is hard to infer with any reasonable confidence the Henodontidae paleobiogeographic history. The currently available data may imply the western Tethys as a place of Henodontid diversification and dispersion as within this area both basal *P. atancensis* and derived *Henodus* were found. Nonetheless, more material is needed to confirm and substantiate this hypothesis.

During Late Triassic, both Algarve and southern German regions were situated at low latitudes (ca. 20° N) within the tropic zone. They were both located at the continental margin in proximity to the Tethys ocean. Lower Carnian Grabfeld formation, from which *H. chelyops* was recovered, contain sediments (shales, nodular gypsum, salt, and pedogenic deposits) deposited the succession of sabkha, playa and salina environments under the arid climate, with short-lasting marine influence (Shukla et al., 2010). The sedimentological records of Algarve succession indicate similar environmental conditions with an arid climate, formation of evaporites and deposition of interlayered mudstones and carbonates. Thus taking into account the geographic position and geological setting it can be presumed that the habitat inhabited by *Henodus* was in both localities similar, namely warm shallow water, possibly: lagoon, coastal area or inland water body in proximity to the sea.
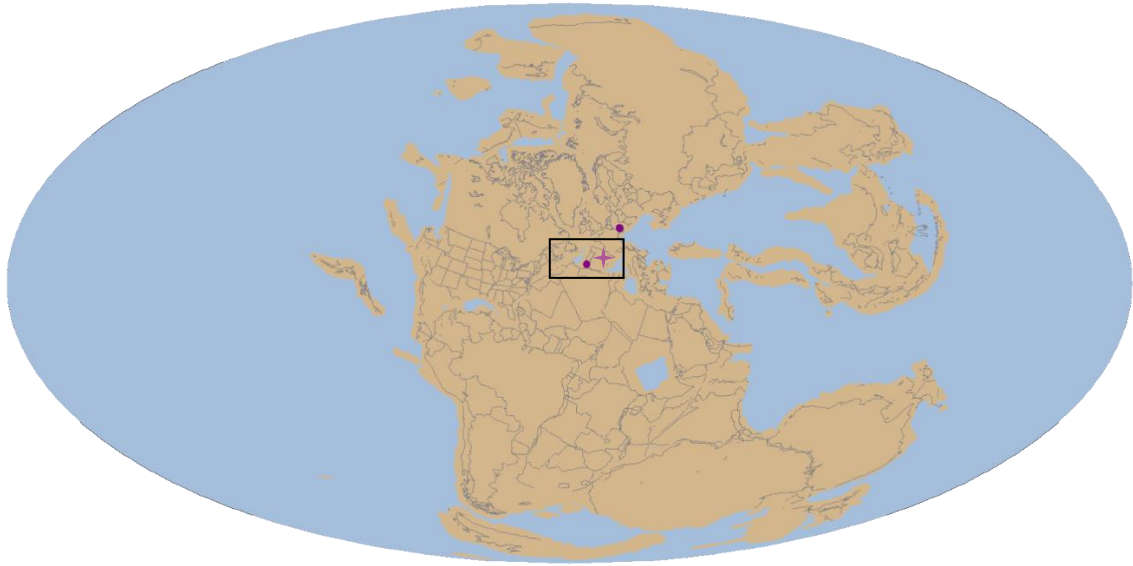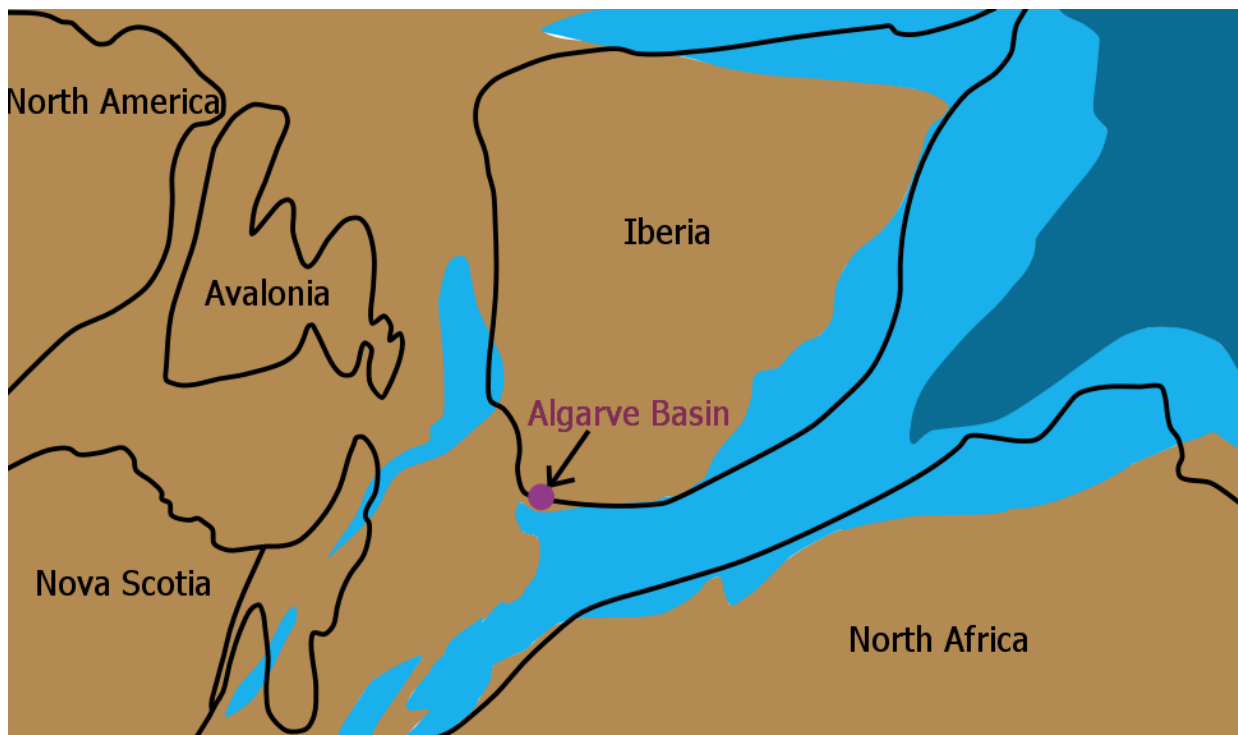
Fig 32.Paleogeographic setting of Henodontidae fossils. A.Palaeogeographic map of the Late Triassic illustrating the distribution of *Henodus* (purple dots) and *Parahenodus* (asterisk). Paleomap generated using Fossilworks based upon data from the Paleobiology Database, Alroy 2013. B. In the area of the black rectangle which is presented in the schematic illustration of paleogeography of Iberia during the Upper Triassic (adapted from Pereira et al. 2016a, b). Occurrence of *Henodus* in the deposits of Algarve Basin (purple dot) indicated.

5.5. Description of isolated remains from Layer 9 ('*Henodus* layer')

Chondrichthyes Huxley, 1880

Elasmobranchii Bonaparte, 1838

Euselachii Hay, 1902

Hybodontoidea Owen, 1846

FCT-UNL 620 - hybodont fin spine and fragment of an osteoderm (Fig 33)

Complete dorsal fin spine embedded in the rock and associated with placodont osteoderm. Only the lateral surface is fully exposed. The middle part of the spine is covered by strongly carbonated sediment. The spine is elongated, 3,4 cm long, mediolaterally flattened, oval in cross-section and slightly recurved distally. It narrows gradually towards the apex. The lateral surface of the spine is covered with numerous parallel, longitudinal ridges extending apicobasal creating an ornamentation pattern composed of distinct ridges and grooves. The spaces between the ridges are the widest in the basal part of the spine and decrease gradually towards its apex. In the apical area of the spine, millimeter-sized denticles at the posterolateral part of the spine are partially exposed. The distinct longitudinal groove and ridge ornamentation at the lateral surfaces of the recurved fin spine and the occurrence of series of denticles on its posterior surface are thought to be characteristic features of hybodont sharks (e.g. Maisey, 1978, 1987).

Hybodontiformes was a cosmopolitan clade existing since Carboniferous till Cretaceous, occupying both marine and freshwater environments (e.g. Benton, 2015). The group proliferated in the Triassic and is known from many European marine and freshwater deposits (e.g. Rees and Underwood, 2002; Fischer, 2008; Diedrich 2008; Sulej et al., 2012). Triassic hybodontids were also found in the marine deposits of Iberian Penisula. That includes records from Ladinian of Iberian Range (Pla et al., 2013) and Middle to Upper Triassic finds including Carnian *Lonchidion derenzii* from the southwest part of the Betic Range, in southern Spain (Manzanares et al., 2016;2018). The herein presented spine constitutes the first record of hybodonts in the Triassic of Portugal.

One incomplete and poorly preserved osteoderm is associated with a hybodont fin spine. It is 4 mm thick and 22 mm wide at the largest extension. It has irregular borders but overall is hexagonal. The surface of the osteoderm is smooth and does not display any ornamentation. Its size, hexagonal like shape, and surface morphology is similar to material attributed to Cyamontodid placodonts (Rieppel, 2001). Most of the other coeval taxa possessing osteoderms eg. multiple archosaurs are characterized by osteoderms with distinct grooves and ridges ornamentation, which is not present in FCT-UNL 620. Similar osteoderms to FCT-UNL 620 were also collected from Middle and Late Triassic localities in central Spain, which were attributed to indeterminate cyamodontoid placodonts

and osteoderms of Psephosauriscus carapace (de Miguel Chaves et al., 2020). Due to the occurrence of *Henodus* remains within the same layer, it is possible that the FCT-UNL 620 belonged to that taxon. Henodus' carapaces recovered in Germany include quite similar osteoderms to FCT-UNL 620 at their lateral margin regions. However, due to the rather poor state of preservation of FCT-UNL 620 osteoderm and distinct homogeneity of Cyamontodoid placodonts osteoderm morphology, the detailed taxonomic assignation is not possible.
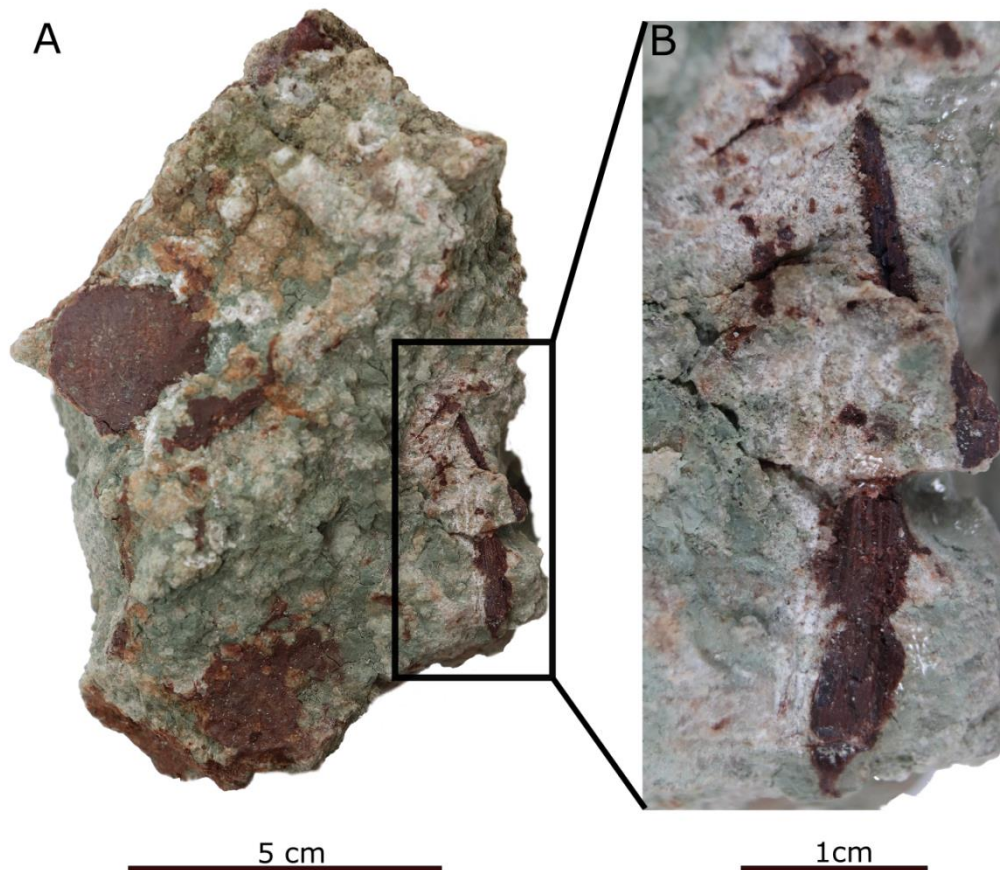
Fig. 33. Photos of FCT-UNL – 620. A. Carbonated mudstone block with placodont osteoderm and hydodont fin spinefrom Rocha da Pena. B. Hybodont fin spine.

FCT-UNL 621 – 625(Fig.34)

The majority of the remains recovered from the 'Henodus layer' are fragments of ribs and osteoderms. The FCT-UNL 621- 623 are fragments of ribs varying in size between 1,9 centimeters to 5,6 centimeters in length. The FCT-UNL 621 and FCT-UNL 623 are fragments of rib shafts and are distinctly dorsoventrally flattened. The FCT-UNL 621 is also slightly recurved. The FCT-UNL 623 comprises the rib head and fragment of the shaft. The rib head is massive and recurved. Due to the poor state of preservation and fragmentary nature of the described specimens, taxonomic identification is problematic.

The FCT-UNL 624 and The FCT-UNL 625 are fragments of the osteoderms. The preserved parts are quite irregular. The FCT-UNL 624 has an overall smooth surface irregularly covered with smaller than one millimeter-sized pits. Whereas The FCT-UNL 625 surfaces are covered in irregular millimeter-sized ridges and groves. Due to the poor state of preservation and fragmentary nature of the described specimens, taxonomic identification is problematic. The shape of the FCT-UNL 624 fragment and surface morphology, as well as the small-sized ridge and grove pattern of FCT-UNL 625, resemble the material attributed to indeterminate cyamodontoid placodonts (Rieppel, 2002; de Miguel Chaves et al., 2020).
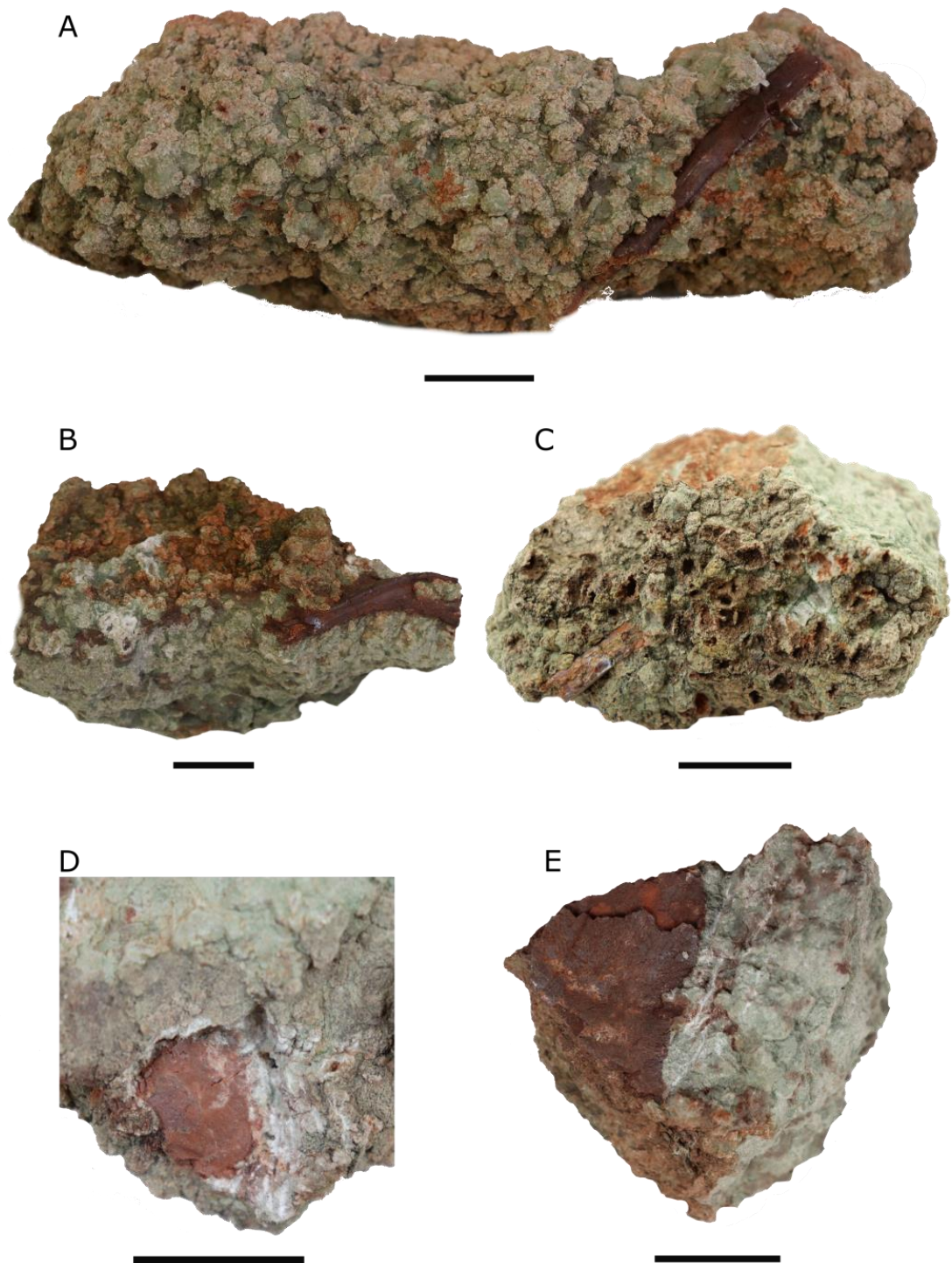
Fig. 34.Isolated reptile remains (FCT-UNL 621 – 625) from the layer 9, from Rocha da Pena. A,B,C. Fragments of ribs. D,E. Fragments of osteoderms resembling material attributed to cyamodontoid placodonts. All scale bars 2cm.

FCT-UNL 626– vertebra (Fig. 35)

Small (1,4 cm long; 1,1 wide and 0,8 thick), elongated vertebral centrum. It is polygonal in the cranial view and rectangular in dorsal view. The posterior articulation surface of the vertebra is concave. The anterior one is partially destroyed, which hinders the assessment of the original condition, nevertheless, the amphicoelous condition is presumed. The articulation surface with the neural arch is preserved. The dorsal surface of the centrum is concave, abruptly deepening in the central area of the articulation surface resulting in the occurrence of the small oval depression. The dorsolateral margins of the centrum are defined by lateral processes extending throughout the entire length of the centrum's margin, broadening posteriorly. They are pronounced and wide, especially in the posterior area of the centrum.
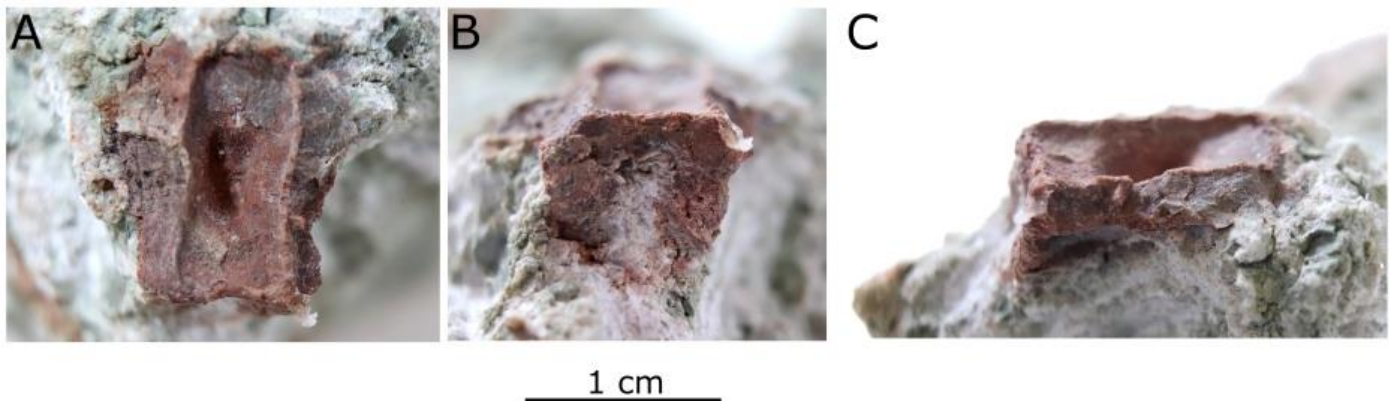
Fig. 35. Reptile vertebrate centrum. (FCT-UNL 626)from Rocha da Pena in (A) dorsal ,(B) axial, (C) lateral views.

Actinopterygian scales (Fig. 36).

Within the recovered blocks of the layer 9, four actinopterygian scales morphotypes were observed. Morphotype one (Fig. 36A) is a ganoid scale with a rhomboidal to almost rectangular shape and short lateral process resembling the 'peg and socket' articulation system (Heckert,2004; Antczak and Bodzioch, 2018). Scales of this type often have a distinctly cracked surface. Morphotype two (Fig. 36B) is a ganoid scale characterised by the smooth surface, sigmoidal to rhomboidal shape and smoothened edges. It is thicker compared to scales of morphotype one and morphotype three. Morphotype three (Fig. 36C) is characterised by oval to elongated scale shapes and longitudinal ridge and groove pattern. Morphotype four is represented only by one incomplete scale (Fig. 36D). It is more massive and thick compared to other scale types. It has preserved reflective, iridescent, original enameloid. The scale outline is irregular, which can be the result of taphonomic processes. It is likely that the scale had an originally sigmoidal-like shape and was similar to morphotype 2.

The common convergence of fish scales morphology between the taxa (Ginter, 2012), as well as large morphological variability of scales depending on the position at the body (Giordano et al., 2016), hinders precise assignations of the gathered material. Nevertheless, isolated scales are often attributed to the high taxonomic level (eg. Norden et al., 2015; Heckert, 2004; 2012). Relatively thick scales with similar features to morphotype one and morphotype two, having rhomboidal shape, smooth surface, 'peg and socket' articulation, are often attributed to Redfieldiidae (eg. Heckert, 2004; Heckert et al., 2012). Scales similar to the morphotype three are in some works assigned to Palaeoniscidae, mainly based on distinct groove and ridge ornamentation (eg. Heckert, 2004; Heckert et al., 2012; Landon et al., 2016).
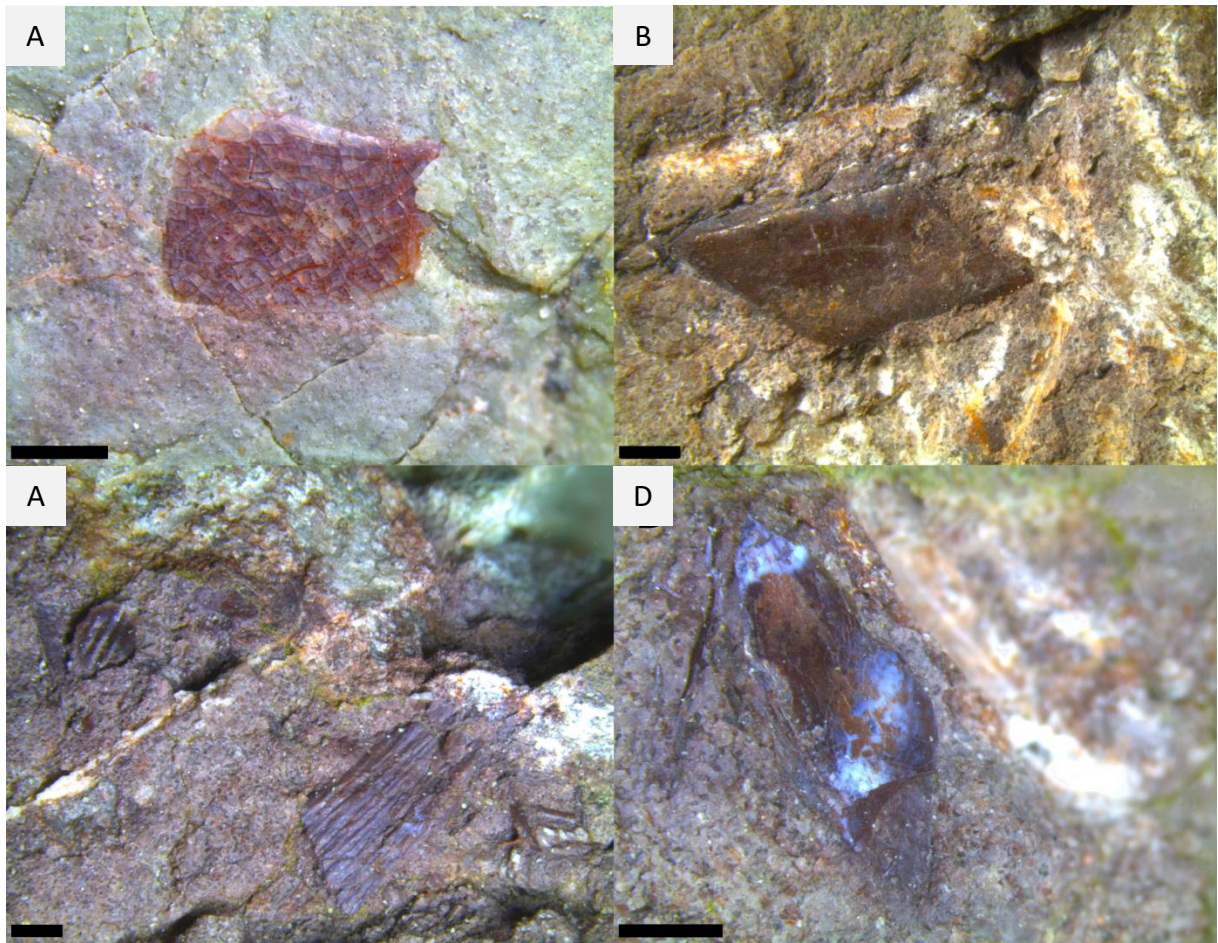
Fig.36. Photographs of Actinopterygian scales recovered from layer 9 at Rocha da Pena. A. Morphotype 1 - cf. Redfieldiidae B. Morphotype 2 - cf. Redfieldiidae. C. Morphotype 3 - cf. Palaeoniscidae. D. Morphotype 4 - Actinopterygii indet. Scale bars - 1mm.

5.6 Taphonomy

Almost all of the collected specimens are isolated and fragmentary, rather poorly preserved remains. Bones exhibit various inclinations within the layer varying from horizontal to sub-vertical positions. The orientation of bones could not have been investigated since a large number of the collected samples comes from the isolated blocks of layer 9, collected from the surface (34 out of 42 specimens). Many of them still preserved the bedding planes, which enabled the observation of bone inclinations. The analyzed carbonated mudstone blocks are comprised of mixed fragmentary remains of various taxa including identifiable specimens belonging to placodont, actinopterygian fishes, and hybodont shark.

A large degree of fragmentation, the occurrence of only isolated remains and close co-occurrence of fossils belonging to different taxa, suggest some rate of the redeposition of those skeletal elements (Rogers, 2008). The exact rate of the transportation of those remains unknown, as a larger sample is needed to assess the prevailing taphonomic features. The preliminary observations suggest a distinct rate of abrasion and fragmentation possibly connected with a distinct rate of transportation. However, such preservation features might be also connected with a long exposition of the remains at the bottom of the standing water body, resulting in the long-lasting physical and geochemical weathering processes, which not necessarily had to be coupled with a large transportation rate (Rogers, 2008).

The carbonated mudstone layer within which the specimens were found, could have been possibly secondary carbonated, as indicated by the occurrence of carbonate nodules and unequal content and dispersion of carbonate within the mudstone. Thus the poor bone preservation might be also the result of the early diagenetic processes which affected the whole fossil-bearing layer.

The occurrence of evaporitic gypsum desert roses and desiccation cracks at the top of the layer suggests either the existence of a shallow and ephemeral water body or marginal position within the water body, near the shore. The recovered identified remains belong solely to the aquatic taxa, with a lack of representation of any terrestrial species. Notable is also the lack of any invertebrate fossils. It might have been caused by intensive diagenesis resulting in the dissolution of the calcitic or aragonitic shells of mollusk and other invertebrates. Owing to the commonly occurring sequence of skeletal material destruction which involves initial weathering of calcium carbonate elements and phosphate elements at the end (Brett and Baird, 1986), it is possible that due to diagenetic processes only bone material has been preserved. The early diagenetic processes are thought to be responsible for a significant depletion of aragonite shell material due to its dissolution, especially in low energy and/or high organic content environmental settings (eg. Cherns and Wright, 2009). If considering the possible re-deposition of skeletal remains, the physical sorting of the fossils by the action of water flow can be also considered. The hydrodynamic sorting of the skeletal remains coupled with a low abundance of

invertebrate fossils has been observed for example in the marginal setting of Middle Triassic deposits in Winterswijk (Heijne et al., 2019). As indicated by the large abundance of evaporites and green color of the sediment which is sometimes associated with brackish conditions (Tucker, 2001), the depositional environment of Layer 9 could have been characterised by increased salinity or hypersaline conditions. Such circumstances cause environmental stress, often resulting in reduced diversity and abundance of invertebrates (e.g. Rogers, 2008; Klompmaker and Fraaije 2011). Such conditions coupled with probable low preservation potential could explain the lack of invertebrate fossils and restricted diversity of the fauna. The Goldersbach site, where *Henodus* remains were found is also characterised by a very low content of invertebrate remains, almost solely composed of crustaceans (Huene, 1936). The paleoenvironment was construed as possibly brackish. That may suggest comparable environmental conditions of the paleoenvironment in the Goldersbach site and at part of the section of the Rocha da Pena site.

Those observations, the occurrence of *Henodus*, which was considered to inhabit shallow marine or brackish environments, and the previously presented geological stetting, suggest the investigated layer might have been deposited in a marginal environment including coastal lagoon or sabkha flat setting in proximity to the sea. Thus, the recovered fauna could live in brackish/saline shallow lagoon or ephemeral lacustrine/saline environment formed within the coastal sabkha plain (Fig 37). However, as the animal remains were possibly re-deposited, the original environment inhabited by this fauna remains unsure. Presented observations and preliminary conclusions should be taken with caution as it can be affected by a small sampling.

Based on the obtained data, the genesis of the accumulation can not be established. However, there are a few possible explanations which can be taken into account:

1) The existence of ephermal restricted water body, its subsequent evaporation, local habitat loss resulting in the death of animals and accumulation of their remains.
2) The shallow water habitat, deposition of animal remains, and their subsequent re-deposition and accumulation in proximity to the shore in the result of tidal water circulation or as the effect of storm accumulation, which would be consistent with the redeposition indication.
3) The shallow water habitat, time-averaged deposition of animal remains, and their subsequent weathering and small-scale redeposition.
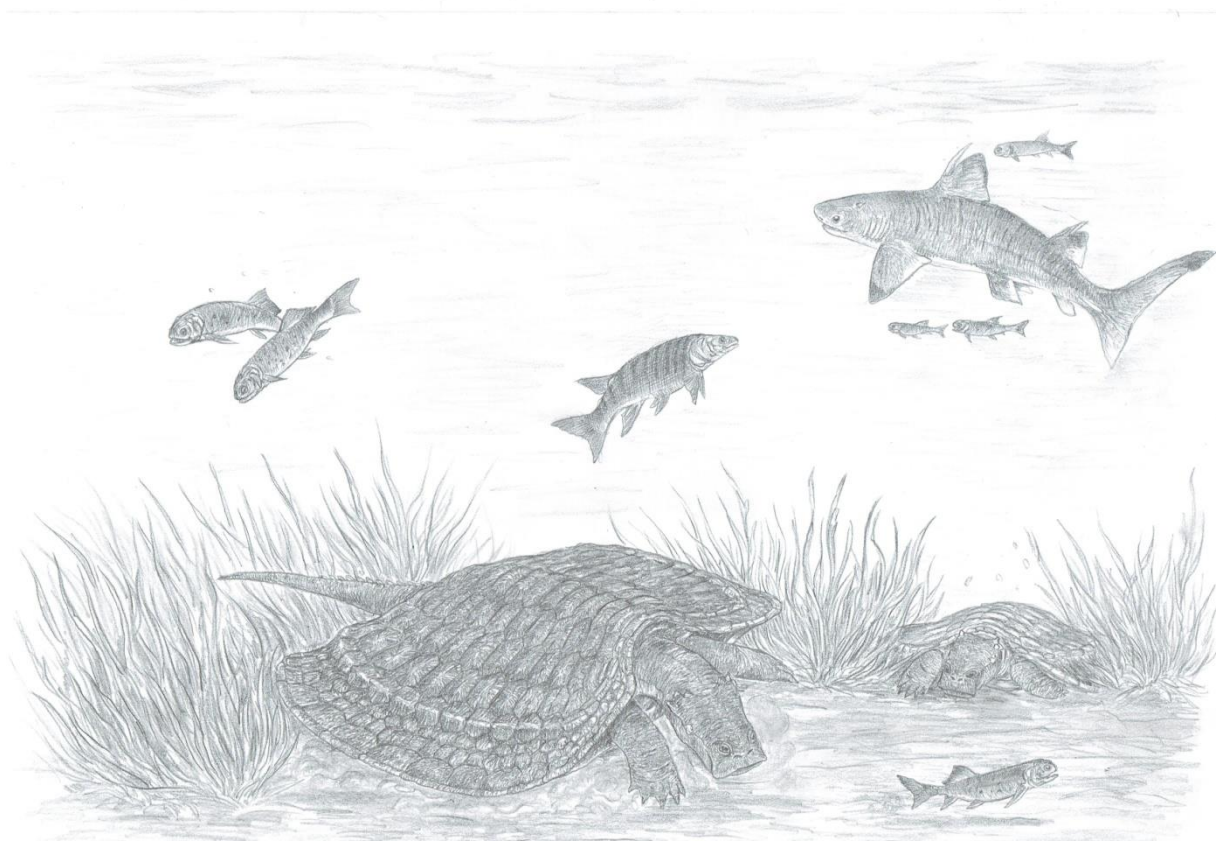
Fig. 37.Hypothetical life reconstruction of the Late Triassic ecosystem at Rocha da Pena, based on the recovered remains from Layer 9. Drawing by Jakub Kowalski.

5.7. Description of isolated remain from the *Metoposaurus* bonebed.

FCT-UNL 628 – osteoderm.(Fig. 38)

The osteoderm was found within debris at the base of the *M. algarvensis* bonebed. It is irregular, polygonal with slightly undulating edges. At the dorsal surface, the very low and subtle ridge extends longitudinally throughout most of the preserved part of the medial extent of the osteoderm. The dorsal surface within the central area of the osteoderm is perforated by very small foramina. Distally the surface sculpture becomes dominated by radial ornamentation composed of minute irregular ridges and grooves. In the transverse section, the medial part of the osteoderm is very slightly upraised. The assignation to Archosauria is can be rather excluded, as most of the Late Triassic archosaurs possed osteoderms with pronounced ridges and ornamentation. Osteoderms of similar shape and morphology to FCT-UNL 628 are known in representatives of Cyamodontid placodonts (Rieppel, 2002b). The FCT-UNL 628 display a strong resemblance to osteoderms observed at the carapaces of *Psephoderma* (Rieppel 2002b) and *Sinocyamodus*(Wang et al.,2018), which is manifested in a similar hexagonal-like shape, occurrence of a keel extending longitudinally through the medial area of an osteoderm and very subtle grove and ridge ornamentation patter near the osteoderm margins. Due to the occurrence of remains assigned to *Henodus* (skull and characteristic transversely elongated osteoderms described by Hugo Campus in the unpublished thesis), it is possible, that the FCT-UNL 628 osteoderm belonged to that taxon. In completely preserved carapaces of *H. chelyops*, relatively thin, irregular, and polygonal osteoderms with a smooth surface and subtle longitudinal medial ridge, similar to the presented specimen, are located at the top of of the C-shaped ridges, stretching near the lateral margins of the carapace.

Fig.. 38.Placodont osteoderm (FCT-UNL 628) from *Metoposaurus* bonebad.

6. Scientific input of the thesis and open unresolved questions

The performed research enabled the:

(1) Sedimentological bed by bed description of previously undescribed layers within Triassic outcrops of Rocha da Pena

(2) Paleoenvironment interpretation based on a sedimentological study taking into account bed by bed analysis, providing new supporting evidence for previous paleoenvironmental interpretations, which were mainly based on macro-scale geological analysis of Algarve Basin deposits.

(3) The performed fieldwork revealed the previously not investigated fossiliferous layer.

(4) Description of novel vertebrate fossil material resulting in confirmation of occurrence of Henodontid placodont in the Upper Triassic of Algarve and first hybodontid shark record in the Triassic of Portugal

Unresolved questions:

(1) The nature of some sedimentological structures and detailed paleoenvironment interpretation remains unresolved. Although the interpretation and probable scenarios are provided, there is missing evidence to strongly confirm the depositional setting of mudstone, carbonated mudstone, siltstone complex and uppermost section including the thick silty-sandstone layer The thin section or high-resolution geochemical studies are needed for a substantiation of the proposed interpretations.

(2) The studied section constitutes probably the upper or uppermost part of the AB2 unit of Gres de Silves Formation, as it is suggested by closely outcropping Lower Jurassic dolomite strata of AB3 unit overlying Triassic deposits. However, the exact position of the studied section within the AB2 remains unresolved and requires a wider range of stratigraphic studies.

(3) The described skull ML. A9182 is assigned to Henodontidae and tentatively assigned to *Henodus*. sp. However due to many ambiguities in the interpretation of skull bones morphology in ML. A9182, mainly due to its poor preservation, the detailed taxonomic position of the Algarve placodont remains unresolved.

(4) The age of locality remains unresolved. The performed work did not provide new material of index fossils, which could help in resolving this question. The co-occurrence of *Metoposaurus,* probable basal representative of phytosaurs and *Henodus* suggest rather a Carnian age. However, the large stratigraphic range of Metoposaurus and quite uncertain possible stratigraphic range of *Henodus* due to its very restricted representation in the fossil record hinder the definitive answer.

7. Conclusions

The performed fieldwork and observations resulted in the provision of paleoenvironment interpretation and description of novel vertebrate material from Rocha da Pena. Although the gathered evidence is inconclusive for paleoenvironment interpretation, the most possible scenario is suggested. The lowermost strata within the studies sections, composed of blocky marbly mudstones represent the early stage paleosoil sediments deposited in a playa environment under an arid climate. The mudstone, carbonated mudstone, siltstone complex was likely deposited within a marginal environment, possibly a coastal area of a lagoon. Those deposits are overlaid by mudstones, siltstones laminated siltstones possibly deposited under coastal tidal conditions. The uppermost layers represented by silty-sandstones with Hummocky and Swaley cross-stratification and Flasser bedding may indicate a shallow marine depositional environment, however, more data is needed to confirm this interpretation. These observations suggest the transgressive episode and successive increase of depositional environment proximity to the sea at the area of Algarve during the Late Triassic.

The novel vertebrate material recovered from a single carbonated mudstone revealed a new fossiliferous layer, possibly a bonebed. The placodont material composed of osteoderms is assigned to cyamontodoid placodont. The ML. A9182 skull is identified as belonging to *Henodus* sp. based on a set of seven autapomorphies. However, due to a few features distinguishing the ML. A9182 from *H.chelyops*, it is possible that ML. A9182 represents a new taxon, possibly new species of *Henodus* or a novel genus within Henodontidae. Nevertheless, taphonomic conditions hinder the unambiguous separation of the ML. A9182 as a new taxon. The occurrence of *Henodus* in Algarve extends the paleogeographic distribution of that genus up to the western Tethys as the previous record has only been known from Germanic Basin deposits in southern Germany. This find also confirms the Upper Triassic age of the Rocha da Pena deposits. As the German material of *Henodus* is from Lower Carnian, the age of Rocha da Pena can be coeval or the stratigraphic range of *Henodus* was larger and extended possibly up till middle Norian. The remaining fossil material is composed of fish scales attributed to actinopterygians and fin spine assigned to hybodontid shark. The recovered hybodontid fin spine constitutes the first Triassic record of hybodonts in Portugal. The recovered material has signs of redeposition, however larger sampling is needed to confirm this observation. Based on the geological setting and the occurrence of *Henodus*, the environment inhabited by described fauna is construed as a shallow water environment within coastal/nearshore or a shallow lagoon setting.

7. Bibliography

Ahlberg, A., Arndorff, L. Guy-Ohlson, D., 2002. Onshore climate change during the Late Triassic marine inundation on the Central European Basin. Terra Nova 14:241–248

Azerêdo AC, Duarte LV, Henriques MH, Manuppella G., 2003. Da dinâmica continental no Triásico aos Mares do Jurássico Inferior e Médio. Cadernos de Geologia de Portugal. Instituto Geológico e Mineiro, Lisboa, pp 1–43

Bahr, A., Kolber, G., Kaboth-Bahr, S., Reinhardt, L., Friedrich, O. and Pross, J., 2020. Mega-monsoon variability during the late Triassic: Re-assessing the role of orbital forcing in the deposition of playa sediments in the Germanic Basin. Sedimentology, 67: 951-970.

Benton MJ, Zhang Q, Hu S, Chen Z-Q, Wen W, et al., 2013. Exceptional vertebrate biotas from the Triassic of China, and the expansion of marine ecosystems after the Permo-Triassic mass extinction. Earth Sci Rev 125: 199– 243

Benton, M. J., 2015. Vertebrate Paleontology,4th Edition. Blackwell Science Ltd., Oxford, 468 pp

Benton, M. J., Bernardi, M. Kisnella, C., 2018. The Carnian Pluvial Episode and the origin of dinosaurs. Journal of the Geological Society

Benton, M.J., and A.J. Newell., 2014. Impacts of global warming on Permo-Triassic terrestrial ecosystems.Gondwana Research25 (4): 1308–1337.

Boggs, Sam. 2001. *Principles of Sedimentology and Stratigraphy.* Upper Saddle River, N.J.: Prentice Hall.

Brayard, A., Krumenacker, L.J., Botting, J.P., Jenks, J.F., Bylund, K.G., Fara, E., Vennin, E., Olivier, N., Goudemand, N., Saucède, T., Charbonnier, S., Romano, C., Doguzhaeva, L., Thuy, B., Hautmann, M., Stephen, D.A., Thomazo, C., Escarguel, G., 2017. Unexpected Early Triassic marine ecosystem and the rise of the Modern evolutionary fauna. Sci. Adv. 3

Brett, C. E., Baird G. C., 1986. Comparative taphonomy; a key to paleoenvironmental interpretation based on fossil preservation. *PALAIOS* ; 1 (3): 207–227.

Breda, A. and Preto, N., 2011. Anatomy of an Upper Triassic continental to marginal-marine system: the mixed siliciclastic–carbonate Travenanzes Formation (Dolomites, Northern Italy). Sedimentology, 58: 1613-1647.

Brusatte, S. L., Butler, R. J., Mateus, O., & Steyer, J. S., 2015. A new species of Metoposaurus from the Late Triassic of Portugal and comments on the systematics and biogeography of metoposaurid temnospondyls. Journal of Vertebrate Paleontology, 35(3), e912988.

Charig, A, J., 1984. Competition between therapsids and archosaurs during the Triassic period: A review and synthesis of current theories. In M.W.J. Ferguson, ed., The structure, Development and Evolution of Reptiles, pp. 597-628. Zoological Society of London Symposia 52. London: Academic Press

Chen, Z.Q., and M.J. Benton., 2012. The timing and pattern of biotic recovery following the end-Permian mass extinction. Nature   Geoscience5 (6):375–383.

Cherns, L. and Wright, V.P., 2009. Quantifying the impacts of early diagenetic aragonite dissolution on the fossil record. Palaios, 24, 711–756.

Chun, L., O. Rieppel, C. Long, and N. C. Fraser., 2016. The earliest her-bivorous marine reptile and its remarkable jaw apparatus. ScienceAdvances 2:e1501659. doi: 10.1126/sciadv.1501659.

Dalrymple, G. H., 1977. Intraspecific Variation in the Cranial Feeding Mechanism of Turtles of the Genus Trionyx (Reptilia, Testudines, Trionychidae). Journal of Herpetology, 11(3), 255.

Davis R. A., Dalrymple R. W., 2012. Principles of Tidal Sedimentology.Springer: Dordrecht.

de Miguel De Miguel Chaves, C., Ortega, F., & Pérez-García, A., 2018. A new placodont from the Upper Triassic of Spain provides new insights on the acquisition of the specialized skull of Henodontidae. Papers in Palaeontology.

de Miguel De Miguel Chaves C, Scheyer TM, Ortega F, Pérez-García A., 2020. The placodonts (Sauropterygia) from the Middle Triassic of Canales de Molina (Central Spain), and an update on the knowledge about this clade in the Iberian record. Hist Biol. 32(1):34–48.

Diedrich CG., 2011. The shallow marine placodont Cyamodus of the central European Germanic Basin: its evolution, paleobiogeography and paleoecology Hist Biol, 1 – 19, doi:10.1080/08912963.2011.575938.

Diedrich CG., 2010. Palaeoecology of *Placodus gigas* (Reptilia) and other placodontids – Middle Triassic macroalgae feeders in the GermanicBasin of central Europe – and evidence for convergent evolution withSirenia. Palaeogeogr Palaeoclimatol Palaeoecol. 285(3 – 4):287 – 306.

Diedrich, C. and Gradinaru, E., 2013, Distribution of basal Middle Triassicfossil reptile placodonts in the Germanic Basin and northern Tethys: New Mexico Museum of Natural History and Science Bulletin, 61

Dupraz, C., Reid, R. P., and Visscher, P. T., 2011. Microbialites, mod-ern, in: Encyclopaedia of Geobiology, edited by: Reitner, V., andThiel, J., Springer, Heidelberg, 617–635.

Giordano, P. G., Arratia, G. and Schultze, H. P., 2016: Scale morphol-ogy and specialized dorsal scales of a new teleosteomorph fish from the Aptian of West Gondwana. Fossil Record, vol. 19, p. 61–81.

Greene, A.R., Scoates, J.S., Weis, D., Katvala, E.C., Israel, S., and Nixon, G.T., 2010. The architecture of oceanic plateaus revealed by the volcanic stratigraphy of the accreted Wrangellia oceanic plateau: Geosphere, v. 6, p. 47–73.

Greene, J. S. Scoates, D. Weis, E. C. Katvala, S. Israel, G. T. Nixon., 2010. The architecture of oceanic plateaus revealed by the volcanic stratigraphy of the accreted Wrangellia oceanic plateau. Geosphere 6, 47–73

Heckert, A. B., 2004. Late Triassic microvertebrates from the lower Chinle Group (Otischalkian-Adamanian: Carnian), southwestern U.S.A. New Mexico Museum of Natural History and Science Bulletin, 27: 1–23

Heckert, A., Mitchell, J., Schneider, V. & Olsen, P., 2012. Diversenew microvertebrate assemblage from the Upper Triassic Cumnock Formation, Sanford Subbasin, North Carolina,USA. Journal of Paleontology, 86: 368–390.

Heijne, J., Klein, N. & Sander, P.M., 2019. The uniquely diverse taphonomy of the marine reptile skeletons (Sauropterygia) from the Lower Muschelkalk (Anisian) of Winterswijk, The Netherlands. *PalZ* 93**,** 69–92.

Huene, F. V., 1936. Henodus chelyops, ein neuer Placodontier. Palaeontographica, A 84: 99-147.

Huene, F. V., 1938. Der dritte Henodus. Ergänzungen zur Kenntnis des Placodontiers Henodus chelyops Huene. Palaeontographica, A 89: 105-115.

Klappa, C.F., 1980. Rhizoliths in terrestrial carbonates: classification, recognition, genesis and significance.Sedimentology, 27, 613–629.

Klein, N. and Scheyer, T. M., 2013. European origin of placodont marine reptiles and the evolution of crushing dentition in Placodontia. Nature Communications, 4 (1621), 1–7.

Klompmaker, A.A., and R. Fraaije. 2011. The oldest (Middle Triassic, Anisian) lobsters from The Netherlands: taxonomy, taphonomy, paleoenvironment, and paleoecology. Palaeontologica Electronica 14: 1–16

Lee, M.S.Y. 2013. Turtle origins: insights from phylogenetic retrofitting and molecular scaffolds. Journal of Evolutionary Biology 26 (12).

Lopes, F. M. V., 2006. Geologia e génese do relevo da Rocha da Pena (Algarve, Portugal) e o seu enquadramento educativo. Dissertação para a obtenção do grau de mestre Em Biologia e Geologia – Especialização em Educação, Universidade Do Algarve Faculdade De Ciências Do Mar E Do Ambiente.

Lucas SG, Tanner LH., 2018. The Missing Mass Extinction at the Triassic- Jurassic Boundary; The Late Triassic World, Topics in Geobiology 46 pp 721-785

Lucas, S. G., L. F. Rinehart, K. Krainer, J. A. Spielmann, and A. B.Heckert. 2010. Taphonomy of the Lamy amphibian quarry: a Late Triassic bonebed in New Mexico, U.S.A. Palaeogeography, Palaeoclimatology, Palaeoecology 298:388–398.

Manuppella, G., 1988. Litostratigrafia e tectónica da Bacia Algarvia. Geonovas, Lisboa, vol. 10, 67-71

Maisey JG. 1987. Cranial Anatomy of the Lower Jurassic Shark Hybodus reticulatus (Chondrichthyes: Elasmobranchii), with Comments on Hybodontid Systematics. American Museum Novitates 2878: 1–39.

Maisey, J. G., 1978, Growth and form of spines in hybodont sharks: Palaeontology, v. 21, no. 3, p. 657-666.

Manzanares, E., Pla, C., Ferrón, H. G., & Botella, H., 2018. Middle-Late Triassic chondrichthyans remains from the Betic Range (Spain). Journal of Iberian Geology, 44(1), 129–138.

Manzanares, E., Pla, C., Martınez-Perez, C., Ferron, H., & Botella, H., 2016. Lonchidion derenzii, sp. nv., a new lonchidiid shark (Chondrichthyes, Hybodontiforms) from the Upper Triassic of Spain, with remarks on Lonchidiid enameloid. Journal of Vertebrate Paleontology

Martin, J. E., Delfino, M., Garcia, G., Godefroit, P., Berton, S., & Valentin, X. (2015). New specimens of Allodaposuchus precedensfrom France: intraspecific variability and the diversity of European Late Cretaceous eusuchians. Zoological Journal of the Linnean Society, 176(3), 607–631.

Marzoli, A.,Renne, P. R., Piccirillo, E. M., Ernesto, M. i De MIN, A. 1999. Extensive 200 milion year old continental flood basalts of the Central Magmatic Province . Science 284: 616 - 618.

Mateus, O., Butler, R. J., Brusatte, S. L., Whiteside, J. H., & Steyer, J. S.,2014. The first phytosaur (Diapsida, Archosauriformes) from the Late Triassic of the Iberian Peninsula. Journal of Vertebrate Paleontology, 34(4): 970-975.

Milroy, P., Wright, V.P. and Simms, M.J., 2019. Dryland continental mudstones: Deciphering environmental changes in problematic mudstones from the Upper Triassic (Carnian to Norian) Mercia Mudstone Group, south-west Britain. Sedimentology, 66: 2557-2589.

Muller, R., Nystuen, J.P. and Wright, V.P., 2004. Pedogenicmud aggregates and paleosol development in ancient dryland river systems: criteria for interpreting alluvial mudrock origin and floodplain dynamics. J. Sed. Res., 74,537–551.

Neenan JM, Klein N, Scheyer TM., 2013. European origin for sauropterygian marine reptiles and the evolution of placo-dont crushing dentition. Nature Communications 4: 1621

Nichols G., 2012. Sedimentology and stratigraphy, 2nd edition. Blackwell Publishing, Oxford.

Nordén, K.K., Duffin, C.J., Benton, M.J., 2015. A marine vertebrate fauna from the Late Triassic of Somerset, and a review of British placodonts. Proceedings of the Geologists' Association 126, 564–581

Olsen, P.E., Shubin, N.H. i Anders, M.H., 1987. New Early Jurassic tetrapod assemblages constrain Triassic-Jurassic tetrapod extinction event. Science 237:1025–1029

Ortí, F., Pérez-López, A., & Salvany, J. M., 2017. Triassic evaporites of Iberia: Sedimentological and palaeogeographical implications for the western Neotethys evolution during the Middle Triassic–Earliest Jurassic. Palaeogeography, Palaeoclimatology, Palaeoecology, 471, 157–180.

Palain, C. 1968. Preuves paléontologiques de l'existence de Keuper au Portugal dans la province de l'Algarve. C. CR Académie des Sciences de Paris, 267: 694-696.

Palain, C.,1976. Une série détrique terrigène. Les «Grès de SiIves»: Trias et Lias inférieur du Portugal. Memória dos Serviços Geológicos de Portugal, Nova Série, 25: 377 pp.

Pereira, M.,F., Ribeiro, C., Gama, C., Drost, K., Chichorro, M., Vilallonga, F., Hofmann, M.,Linnemann, U., 2017.Provenance of upper Triassic sandstone, southwest Iberia(Alentejo and Algarve basins): tracing variability in the sources. International Journalof Earth Sciences 106, 43–57.

Pla, C., A. Marquez-Aliaga, and H. Botella. 2013. The chondrichthyan fauna from the Middle Triassic (Ladinian) of the Iberian Range (Spain). Journal of Vertebrate Paleontology 33:770–785.

Portela, P.R., Oliveira, R.J., Machado, F.P; Drehmer, C. J., Valente, A. L. S., Dornelles, J. E. F., 2020. Morphology and intraspecific variation in the skull and mandible of the slider turtle Trachemys dorbigni (Testudines, Emydidae). Zoomorphology 139, 373–384

Pratsch, J. C.,1958. Stratigraphisch-Tektonische untersuchungen um Mesozoikum vom Algarve (Südportugal). Beihefte zur Geolog, 30: 123 pp.

Preto N., Bernardi M., Dal Corso J., Gianolla P., Kustatscher E., Roghi G. & Rigo M.,2019. The Carnian Pluvial Episode in Italy: History of the research and perspectives. Bollettino della Società Paleontologica Italiana, 58: 35-49.

Rees, J. & Underwood, C. J., 2002. The status of the shark genus Lissodus Brough, 1935, and the position of nominal Lissodus species within Hybodontidae (Selachii): Journal of Vertebrate Palaeontology, 22: 471–479.

Reif W.,E, Stein, F., 1999. Morphology and function of the dentition of Henodus chelyops (Huene, 1936) (Placodontia, Triassic). Neues Jahrbuch für Geologie und Paläontologie, Monatshefte 1999: 65–80.

Renesto, S., 2005. A new specimen of Tanystropheus (Reptilia Protorosauria) from the Middle Triassic of Switzerland and the ecology of the genus. Rivista Italiana di Paleontologia e Stratigrafia, 111:2039-4942. https://doi.org/10.13130/2039-4942/6327

Renesto, S.., Dalla Vecchia F.M., 2018. The Late Triassic World: Earth in a Time of Transition; Late Triassic Marine Reptiles. Topics in Geobiology 46: 59–91; 263–313

Retallack, G.J.,1988. Field recognition of paleosols. In: Paleosols and Weathering Through Geologic Time:Principles and Applications (Eds J. Reinhardt and W.R.Sigles) Geol. Soc. Am. Spec. Pap., 216, 109–118.

Riding R ., 2011. Microbialites, stromatolites, and thrombolites. In: Reitner J, Thiel V (eds) Encyclopedia of geobiology. Springer, Dordrecht, pp 635–654.

Rieppel O., 1995. The genus Placodus: systematics, morphology,paleobiogeography, and paleobiology. Fieldiana Geol, N.S.31(1472):1 – 44.

Rieppel, O., 2000. Sauropterygia. I. Placodontia, Pachypleurosauria, Nothosauroidea, Pistosauroidea. Handbuch der Paläoherpetologie 12A: 1–134

Rieppel, O., 2001. The cranial anatomy of Placochelys placodonta Jaekel, 1902, and a review of the Cyamodontoidea (Reptilia, Placodonta). Fieldiana, Geology, 45,1 –101

Rieppel, O., 2002b. The dermal armor of the cyamodontoid placodonts(Reptilia, Sauropterygia): morphology and systematic value.Fieldiana Geol, N.S. 46(1517):1 – 41.

Rieppel, O. 2002a. Feeding mechanics in Triassic stem–group sauropterygians: the anatomy of a successful invasion of Mesozoic seas. Zoological Journal of the Linnean Society, 135, 33–63.

Rocha, R. B.,1976. Estudo estratigráfico e paleontológico do Jurássico do Algarve ocidental. Ciências Terra (UNL) 2:1–178

Rogers, R. R., & Kidwell, S. M., 2007. A conceptual framework for the genesis and analysis of vertebrate skeletal concentrations. In Rogers, R. R., Eberth, D. A., & Fiorillo, A. R. (Eds.), Bonebeds: Genesis, analysis, and paleobiological significance (pp. 1-63). Chicago, IL: University of Chicago Press.

Romer, A.S., 1966. Vertebrate paleontology, 3rd edn. University Chicago Press, Chicago

Russell, D., & D. Russell., 1977. Premiers résultats d'une prospection paléontologique dans le Trias de l'Algarve (Portugal). Ciências da Terra, 3: 167-178.

Scheyer TM, Neenan JM, Bodogan T, Furrer H, Obrist C, Plamondon M., 2017. A new, exceptionally preserved juvenile specimen of Eusaurosphargis dalsassoi (Diapsida) and implications for Mesozoic marine diapsid phylogeny. Scientific Reports 7: 4406.

Scheyer, T. M., Neenan, J. M., Renesto, S., Saller, F., Hagdorn, H., Furrer, H., Rieppel, O. and Tintori, A., 2012. Revised paleoecology of placodonts – with a comment on 'The shallow marine placodont Cyamodus of the central European Germanic Basin: its evolution, paleobiogeography and paleoecology' by C.G. Diedrich (Historical Biology, iFirst article, 2011, 1–19, https://doi.org/ 10.1080/08912963.2011.575938). Historical Biology, 24, 257–267

Scheyer, T.M., Romano, C., Jenks, J., and Bucher, H., 2014. Early Triassic marine biotic recovery: the predators' perspective. PLoS ONE 9 (3): e88987.

Schoch, R. R., & Sues, H., 2019. The origin of the turtle body plan: evidence from fossils and embryos. Palaeontology. doi:10.1111/pala.12460

Scotese, C.R., 2014. Atlas of Phanerozoic Rainfall Maps (Mollweide Projection),Volumes 16, PALEOMAP ProjectPaleoAtlas for ArcGIS, PALEOMAP Project, Evanston, IL. (2) Atlas of Phanerozoic Rainfall (Mollweide Projection), Volumes 1-6, PALEOMAP Project Atlas for ArcGIS, PALEOMAP Project, Evanston, IL.

Sellwood, B. W., and P. J. Valdes., 2006. Mesozoic climates: general circulation models and the rock record. Sedimentary Geology 190:269–287.

Shukla, U. K., Bachmann, G. H., & Singh, I. B., 2010. Facies architecture of the Stuttgart Formation (Schilfsandstein, Upper Triassic), central Germany, and its comparison with modern Ganga system, India. Palaeogeography, Palaeoclimatology, Palaeoecology, 297(1), 110–128.

Steyer, J. S., Mateus, O., Butler, R. J., Brusatte, S. L., & Whiteside, J. H., 2011. A new metoposaurid (temnospondyl) bonebed from the Late Triassic of Portugal. Journal of Vertebrate Paleontology, Program and Abstracts 2011: 200A.

Sues, H,D., Fraser, N.C., 2010. Triassic life on land: the great transition. Columbia University Press, New York.

Sulej, T., Niedźwiedzki, G. & Bronowicz, R., 2012. A new Late Triassic vertebrate fauna from Poland with turtles, aetosaurs and coelophysoid dinosaurs. Journal of Vertebrate Paleontology, 32: 1033–1041.

Szulc, J., Racki, G., Jewuła, K. & Środoń, J., 2015b. How many Upper Triassic bone-bearing levels are there in Upper Silesia (southern Poland) A critical overview of stratigraphyand facies. Annales Societatis Geologorum Poloniae, 85:587–626.

Talbot M.R. and Allen PA. 1996. Lakes. In: Reading H.G. (ed.), Sedimentary Environments: Processes, Facies and Stratigraphy. Blackwell Science, Oxford, pp. 83-124.

Tanner LH, Lucas SG, Chapman MG., 2004. Assessing the record and causes of Late Triassic extinctions. Earth Sci Rev 65:103–139   Tanner LH, Lucas SG, Chapman MG (2004). "Assessing the record and causes of Late Triassic extinctions". Earth-Science Reviews. 65 (1–2): 103–139.

Terrinha, P., Rocha, R., Rey, J., Cachão, M., Moura, D., Roque, C., Martins, L., Valadares, V., Cabral, J., Azevedo, M. R., Clavijo, E., Dias, R. P., Matias, H., Madeira, J., Silva, C. M., Munhá, J., Rebelo, L., Ribeiro, C., Vicente, J., Noiva, J., Youbi, N., Bensalah, M. K. & Barbero, L., 2006. A Bacia do Algarve: Estratigrafia, paleogeografia e tectónica. In Dias, R., Araújo, A., Terrinha, P. & Kullberg, J. (Eds.), Geologia de Portugal no contexto da Ibéria (pp. 247-316). Évora, PT: Universidade de Évora.

Trindade, M.J., Rocha, F., and Dias, M.I., 2010. Geochemistry and mineralogy of clays from the Algarve Basin, Portugal: a multivariateapproach to palaeoenvironmental investigations. Current Analytical Chemistry, 6, 43–52

Tucker, M. E., 2001. Sedimentary Petrology, 3rd edition, Oxford: Blackwell Science.

Wang, W., Li, C., Wu, X.-C., 2018. An adult specimen of Sinocyamodus xinpuensis (Sauropterygia: Placodontia) from Guanling, Guizhou, China. Zool. J. Lin. Soc. 185(3), 910–924.

Wang, W., Li, C., Scheyer, T. M., & Zhao, L. (2019). A new species of Cyamodus (Placodontia, Sauropterygia) from the early Late Triassicof south-west China.Journal of Systematic Palaeontology, 17,1457–1476.

Ward, P. D., 2006. Out of Thin Air: Dinosaurs, Birds and Earth's Ancient Atmosphere. Washington, DC: Joseph Henry Press.

Werneburg, I. and Böhme, M. 2017. The Paleontological Collection Tübingen. In Beck, L.A. and

Joger, U. (eds.), Paleontological Collections of Germany, Austria, and Switzerland. Springer, Berlin.

Wilson, K.M., Pollard, D., Hay, W. W., Thompson, S. L. I Wold, C. N., 1994. General circulationmodel simulations of Triassic climates: Preliminary results. In G. de V. Klein, ed., Pangea,: Paleoclimate, Tectonics Sedimentation during Accretion, Zenith, and Breakup of a Supercontinent, pp. 91-116. Geological Society of America Special Paper 288.

Witzmann, F., & Gassner, T.,2008. Metoposaurid and mastodonsaurid stereospondyls from the Triassic–Jurassic boundary of Portugal. Alcheringa, 32(1): 37-51

Zhao, L.J. Li, C.Liu, J. He, T. (2008). "A new armored placodont from the Middle Triassic of Yunnan Province, Southwestern China". *Vertebrata PalAsiatica*. **46** (3): 171–177.

Zieliński, T. 2014. Sedymentologia. Osady rzek i jezior. Wydawnictwo Naukowe UAM, Poznań, 594 pp

Appendix

Character scores for matrix from Neenan et al. (2015) and de Miguel Chaves et al. (2018) supplemented with scores from the Ml. A9182 skull.

Palatodonta

?00?00?010?000000????????0?????01000??0???????????00?011100??1?

Paraplacodus

 000000?0????0??00?0?0?00?0?0??00010010??01??0?????000010111??01

Placodus gigas

100000000[01]010000110000000000000011[01]110000100000000000112111110

Placodus inexpectatus

 1000?0?0?1000?0112????0????????0110110?????????????0?0011211??11

Cyamous rostratus

?000001111011012?0110111011001[01]02021000000201[01]0110011?0?211110?

Cyamous hildegardis

2?00?????1???1???????01????????02[01][01][12]0[01]???0?0?????011200211110?

Cyamous kuhnschnyderi

20000011111111011?111?11?111101002[01]2200000020110110011200?11110?

Macroplacus

20??110101000[01]0112111?0?0110010??12201110010?1???????201?1?110?

Placochelys

2111001001[01]0011111111001021011 11??1200111011001001111120121?110?

Protenodontosaurus

20011000010001020211?00?[01]2101110113 2001100[12]00000110???01?1?110?

Psephoderma

211011100[12]0000021111?00?011011?1??22011110[12]1001000111101 21?1100

Psephochelys

20101111011000011211?000001001?1??22001110?10?10??11110021?110?

Glyphoderma

2?10001001100111111????0????0???1??????????????1???1??100?1???00

Sinocyamodus

2?00?01001?1001201???00???10???0201201100??10????0?12002111100

Parahenodus

???????1?1??01120????00???1???????43?1????2?01?1?????201?1?0???

Henodus

20210101?1010?1???11000?0?11?1????43?1?000?100011010120111?0100

ML. A9182

??2?????????????????????????????4???1000?????????????????0???